Essays on Modeling Human Behavior During Epidemics: Simulation, Statistical, and Optimization Approaches

Kian Babaei Shalmani

Dissertation submitted to the faculty of the Virginia Polytechnic Institute and State University in partial fulfillment of the requirements for the degree of

Doctor of Philosophy

In

Industrial and Systems Engineering

Navid Ghaffarzadegan, Committee Chair

Deborah Dickerson

Lauren Childs

Ran Xu

February 18, 2026

Blacksburg, Virginia

Copyright 2026, Kian Babaei Shalmani

Keywords: Mobility, Epidemic modeling, Delay, COVID-19, Risk perception, Human response, Epidemics, System dynamics, Policy analysis, Human behavior, Vaccination

Essays on Modeling Human Behavior During Epidemics: Simulation, Statistical, and Optimization Approaches

Kian Babaei Shalmani

Abstract

Human behavior is at the core of epidemics. Public risk perception shapes compliance with non-pharmaceutical interventions, mobility and contact patterns, and vaccine uptake; in turn, these behaviors alter transmission dynamics and future perceptions. A central challenge in integrating behavior into epidemiological analysis is that perception and response are not instantaneous. Information diffuses through societies with delays, and behavioral adjustment often occurs gradually and asymmetrically responding differently when risk is rising than when it is falling. Ignoring these delay structures can bias empirical inference about behavioral responsiveness and can misstate the effects of policies evaluated using models that treat behavior as exogenous or contemporaneous.

This dissertation advances the modeling and estimation of behavioral feedback in epidemics by focusing on how delayed risk perception links epidemic indicators to behavioral change and policy outcomes. The first essay develops and validates a delay-aware empirical framework for estimating how mobility responds to epidemic risk. Using synthetic experiments, it shows that assuming immediate response (or relying on ad hoc fixed lags) can yield biased estimates of both the magnitude and timing of behavioral response. The essay introduces a structured approach to representing perception delays using distributed-lag formulations motivated by information diffusion and provides practical methods for estimating delay parameters alongside behavioral sensitivity.

The second essay extends the framework by allowing delay structures to be asymmetric across phases of the epidemic, recognizing that behavioral responses to increasing risk may differ from responses to declining risk. Through additional synthetic tests and application to U.S. state-level COVID-19 mobility data, the essay demonstrates that the assumed delay structure materially affects inference about responsiveness and can change conclusions about how quickly behavior adjusts to worsening versus improving conditions.

The third essay connects behavioral estimation to policy design by examining optimal vaccination strategies under endogenous, delayed behavioral feedback. It compares a conventional SEIRV framework with constant contact rates to a behavioral SEIRbV framework in which perceived risk reduces contacts with a perception delay. In both a homogeneous setting and an age-stratified allocation setting, the analysis shows that accounting for behavioral feedback can shift suppression thresholds and the relative performance of vaccination strategies, highlighting the marginal importance of operational levers such as earlier starts and faster rollout alongside prioritization rules.

Taken together, the three essays show that delays in risk perception are a first-order feature of epidemic systems. By providing methods to estimate delay-aware behavioral responses and demonstrating how behavioral feedback reshapes vaccination policy evaluation, this dissertation contributes tools and evidence to improve inference, forecasting, and the design of effective interventions in epidemic settings.

Essays on Modeling Human Behavior During Epidemics: Simulation, Statistical, and Optimization Approaches

Kian Babaei Shalmani

General Audience Abstract

During disease outbreaks like COVID-19, people change how they behave: they might stay home more, wear masks, or choose to get vaccinated. These behavioral responses can significantly affect how a disease spreads and how effective government policies are. This dissertation uses mathematical models and real-world data to better understand these behaviors and improve predictions about disease dynamics.

The first study looks at how people's movement patterns changed during the COVID-19 pandemic. Using mobile phone data from across the United States, we found that there is a significant delay between when people start staying home and when this behavior actually shows up in the data. Accounting for this delay leads to more accurate estimates of how much people reduced their movement.

The second study examines how people perceive risk during epidemics using a simulation-based experiment. Participants made decisions in a simulated epidemic scenario, and the results showed that people respond to risks in uneven ways—they tend to react more slowly to rising threats than they relax when threats decrease. Understanding this asymmetry is important for designing public health communication strategies.

The third study focuses on vaccination decisions. Using a model where individuals weigh the perceived cost of vaccination against the risk of infection, we explore how optimal vaccination policies should account for people’s behavioral responses. The results show that ignoring these responses can lead to suboptimal policy designs and worse public health outcomes.

Dedication and Acknowledgments

I dedicate this dissertation to my mother, whose countless sacrifices and unwavering belief in my potential have been the foundation of everything I have achieved. To my father, whose steadfast support and encouragement gave me the strength to pursue this journey. This work is as much yours as it is mine.

I would like to express my deepest gratitude to my advisor, Dr. Navid Ghaffarzadegan, whose mentorship, intellectual guidance, and genuine investment in my growth have shaped both this dissertation and my development as a researcher. Your ability to challenge and inspire in equal measure has been invaluable.

I am also grateful to my committee members for their time, expertise, and thoughtful contributions to this work. To Dr. Deborah Dickerson, thank you for your insightful feedback and for broadening the analytical perspectives of this research. To Dr. Lauren Childs, your careful attention to methodological rigor strengthened this work considerably. To Dr. Ran Xu, your constructive suggestions helped sharpen the focus and clarity of my arguments.

Finally, I thank my friends and colleagues who walked alongside me during this journey. Your camaraderie, encouragement, and shared moments of laughter made even the most challenging times bearable.

Table of Contents

List of Figures

List of Tables

1. Introduction to the dissertation

Human behavior is at the core of epidemics. Government lockdown decisions and public compliance with those, individual mask-wearing, social distancing, and vaccination choices influence the spread of infectious disease, and shape epidemic patterns. This was commonly observed during the recent COVID-19 pandemic (Chernozhukov et al., 2021). Scholars have increasingly called for integrating this interplay between human actions and infectious disease dynamics into epidemiological models, pointing out that without such integration especially over longer time horizons epidemic projections and policy suggestions can be unreliable (Bauch & Galvani, 2013; Funk et al., 2010; Rahmandad et al., 2022a). Inaccurate forecasts that may come from models oversimplifying human behavior can lead to misguided policy decisions and ultimately cost lives (Rahmandad et al., 2021).

But how can we better incorporate human behavior in epidemic models? Human behavior and its relationship with disease spread is nuanced and complex (Wei & Zhuang, 2023). Merely inserting a behavioral term into a model oversimplifies the feedback loops that connect individual choices and epidemic outcomes (LeJeune et al., 2025). For instance, the adoption of non-pharmaceutical interventions (NPIs) by governments or the public reduces transmission, which in turn alters perceived risk and drives future decisions about NPIs (Rahmandad et al., 2022b; Saad-Roy & Traulsen, 2023). Compounding these feedbacks are inherent delays—time lags in how quickly risk perception develops, how swiftly people respond to changes in cases or deaths, and how sensitive they are to those shifts (Lim et al., 2023; Mahmud et al., 2024). From system dynamics and control theory, we know that delays between cause and effects can have major impacts on the emerging dynamics (Sterman, 2000).

Thus, essential to incorporating human behavior is an effective modeling and estimation of information diffusion in societies which creates delays between risk indicators (such as the state of an epidemic and the associated risks), human perception of risks, and human behavior (such as mask wearing or social distancing). Overlooking these delays can mask important dynamics that ultimately shape an epidemic's trajectory (G. Zhang et al., 2025).

Another pressing policy question is how best to distribute vaccines when supply and distribution capacity are limited, given that human risk perception and response can dynamically change (Fitzpatrick & Galvani, 2021; Lipsitch & Dean, 2020). On one hand, prioritizing certain population groups over others may have substantial impacts on transmission and mortality (Childs et al., 2022). On the other hand, more vaccination brings down risk indicators (such as daily death and cases) which can lead to complacency in human response, creating more risks of infection. Although existing studies have begun to account for behavioral feedback in vaccination strategies, less is known about how these feedback loops might shift optimal priority recommendations (Rahmandad, 2022). For example, while early vaccination of at-risk groups may reduce deaths, it could also relax overall risk perceptions, leading to a behavioral "rebound"

of increased interactions that may sustain transmission. Alternatively, prioritizing high-contact groups first could leverage the natural caution of more responsive groups, limiting deaths until they, too, are vaccinated. The interplay between these mechanisms is complex, and it is not immediately evident whether or how such dynamics alter overall policy recommendations (Rahmandad, 2022). I operationalize this question by comparing a conventional SEIRV framework with constant contact rates to a behavioral SEIRbV framework in which perceived risk (proxied by recent mortality) endogenously reduces contacts with a perception delay. I examine how optimal vaccination coverage and rollout speed shift in a homogeneous-population setting (Study 1) and then extend the analysis to an age-stratified setting that allocates daily doses between younger, high-contact and older, high-risk groups (Study 2). The results show that accounting for behavioral feedback can meaningfully change both coverage/capacity thresholds and the ranking of vaccination policies: the behavioral model typically requires higher coverage and capacity to suppress the epidemic and places a stronger premium on starting earlier, while in the age-stratified model vaccination speed often matters more than switching between young-first and old-first allocation rules.

This dissertation examines the issues outlined above. The overarching goal of this dissertation is **to enhance our understanding of behavioral responses in epidemic settings, from the complex interplay between human choices and disease progression to the role of delays and asymmetries in shaping outcomes.** By refining how models incorporate behavioral feedback loops, we can move more confidently toward real-world applications and develop more robust policy analyses. Ultimately, a richer grasp of these feedbacks and delays can better inform interventions ranging from NPIs to vaccination strategies and help save lives.

1.1. Dissertation Structure

This dissertation is structured around three essays, each employing a different approach within the field of epidemiological modeling: theoretical modeling of delays, regression analysis, and system dynamics, differential-equation based modeling. Figure 2.1 illustrates both the organization of the dissertation, and the methods adopted in each essay.

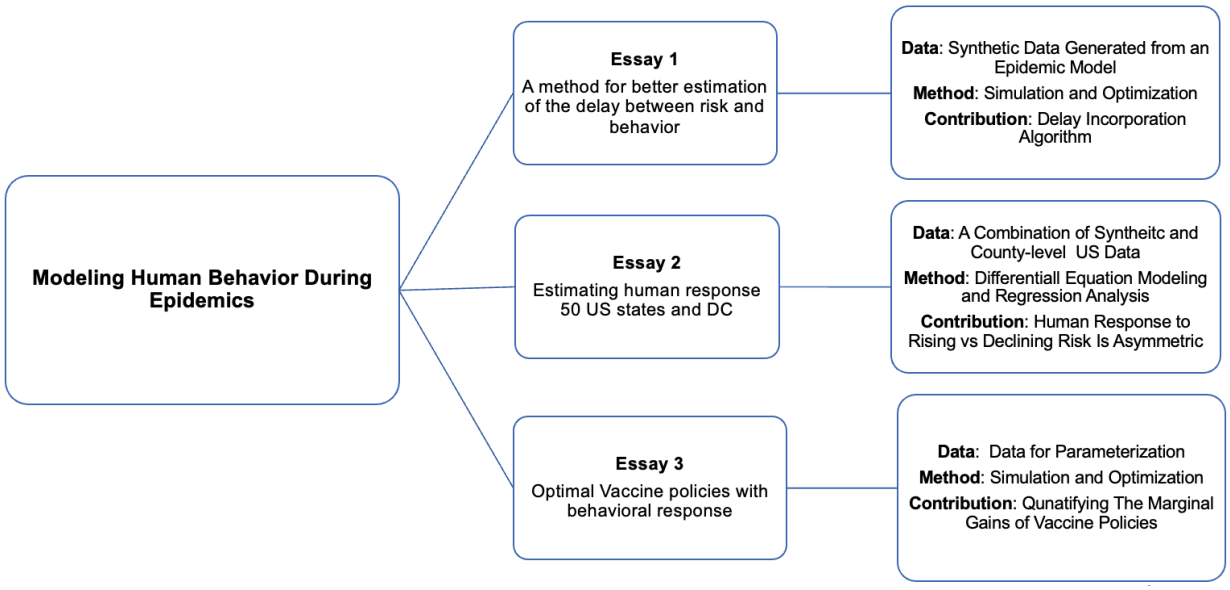

Figure 2.1. Dissertation structure and contributions

The first essay investigates whether disregarding delays in human response leads to biased estimations. Building on these findings, the second essay explores the importance of accurately specifying delay structures, with particular attention to asymmetric delays. The third essay shifts the focus to policy analysis by examining optimal vaccine policies.

In the following paragraphs, I summarize each essay, highlighting its core contributions and broader impact on epidemiological modeling.

Essay 1: Examinations of public responses to pandemic risk, often measured by changes in mobility patterns, have shown mixed results across different waves of the COVID-19 pandemic. Many existing studies estimate the effect of disease incidence or policy interventions on mobility by focusing primarily on immediate associations. However, this paper demonstrates that various system delays including the time required for information to diffuse and for both the public and government to perceive and act on risks can significantly bias these estimates. We introduce a method that employs the Erlang distribution to capture such lagged effects, thereby reducing bias in empirical estimations. Using a synthetic dataset, we illustrate how this approach recovers ground-truth values across a range of delay periods and structures. Finally, we propose an algorithm that researchers and policymakers can use to systematically incorporate delays into their models, leading to more accurate assessments of how pandemic risk influences public mobility.

Essay 2: Many critical social processes ranging from how public opinion responds to economic shocks to how risk perceptions shape behaviors during a pandemic involve the assimilation of information that ultimately informs individual and collective actions. Although these perception

delays are well documented, empirically estimating them remains challenging. In this paper, we examine the issue in the context of human responses to disease dynamics, where changes in public risk perception, driven by information diffusion, can exhibit significant and asymmetric delays depending on whether risk is rising or falling. Despite these complexities, most models rely on simplistic assumptions about the lag between cause (risk) and effect (human response). Using synthetic data (where the ground truth is known), we demonstrate that incorrect delay specifications or the assumption of symmetry can bias and mislead empirical estimates. To address these shortcomings, we explore alternative methods for identifying appropriate delay structures. We then apply these asymmetric delay models to statewide U.S. COVID-19 mobility data, highlighting how different estimation techniques can affect measured sensitivity to mortality. Finally, we compare our proposed methods to more flexible statistical approaches namely Autoregressive Distributed Lags (ARDLs) and evaluate their performance in projecting mobility out of sample.

Essay 3: Many of today's public health challenges stem from policy decisions made in the past, underscoring the need for rigorous, evidence-based approaches. Among the most critical policy decisions are those related to vaccination, particularly regarding prioritization and the pace of distribution. Although behavioral responses play a pivotal role in shaping epidemiological outcomes, they are frequently overlooked or treated as external factors. Only a limited number of studies integrate behavioral dynamics directly into their models. This paper addresses that gap by employing a behavioral epidemic model to determine optimal vaccination strategies under conditions that account for endogenous, risk-driven changes in contact behavior. Specifically, it compares a standard SEIRV model (constant contact rates) with a behavioral SEIRbV model (contact rates respond to perceived mortality risk with a perception delay) and treats vaccination policy as a simulation-based optimization problem. The analysis quantifies how behavioral feedback shifts coverage and capacity thresholds for epidemic control, as well as the marginal gains of optimal policies relative to less effective alternatives, including whether improving rollout speed yields larger benefits than changing age-based prioritization rules. The findings demonstrate that policy leverage lies in rapid responsiveness rather than in optimal distribution schemes.

1.2. Contributions and Impact

By introducing delays into mobility modeling, this dissertation makes significant contributions to the fields of epidemiological modeling and operations research. In doing so, it helps unravel the intertwined relationship between human behavior and infectious diseases within epidemic research. Through a rigorous combination of synthetic data analysis and real-world data experiments, the dissertation develops a robust framework for delay modeling, thoroughly tests and validates it in a synthetic environment, and then applies these insights to U.S. data. Building

on this foundation, it further explores optimal policy design, illuminating how delays shape public health decision-making.

Essay 1 introduces a novel approach to mobility estimation by addressing the bias created when delay and its structure are overlooked. Through the proposed delay incorporation algorithm, a step-by-step procedure is provided to systematically add delay to various regression-based models.

Essay 2 further demonstrates the importance of accurately specifying perception delays whether in length, shape, or symmetry when modeling how changes in reality translate into behavioral or policy responses. Through synthetic experiments and U.S. COVID-19 mobility data, the study shows that mis-specified delays can yield significantly biased estimates, obscuring insights into how quickly individuals respond to increasing versus decreasing risks.

Essay 3 provides a detailed analysis of vaccination policies, examining how delayed behavioral responses affect optimal policy decisions. It specifically addresses whether incorporating behavioral feedback alters recommended strategies and quantifies the marginal gains of these optimal approaches compared to less effective alternatives. Building on the completed third paper, it further shows that behavioral feedback can raise the coverage/capacity thresholds needed for suppression and increase the marginal value of earlier, faster rollout—often outweighing the benefits of switching between young-first and old-first allocation rules across a wide range of conditions.

1.3. Limitations

Despite its contributions, this dissertation has several limitations that should be acknowledged and we review at the end of each chapter. An overview of the limitation follows. The first essay explores how changes in mobility are modeled by focusing solely on the impact of COVID-19–related deaths, which necessarily simplifies the complex set of signals shaping public behavior. For example, among the limitations are the assumption that deaths are the primary driver of mobility responses, the reliance on a synthetic environment for validation rather than direct real-world application, and structural constraints inherent in the simulation framework. In addition, the analysis omits other influential external factors—such as vaccination campaigns, media coverage, and policy mandates—and assumes a symmetric delay response, implying that behavioral adaptation occurs similarly during periods of increasing and decreasing risk.

Essays 2 and 3 address many of these limitations, while also introducing new boundaries that shape the scope of the dissertation. Essay 2 extends the mobility framework by incorporating COVID-19 case counts alongside deaths, enabling a more comprehensive characterization of public risk perception and response. It further strengthens external validity by applying the model to U.S. mobility data and relaxes the assumption of symmetric delays by allowing for asymmetric response structures, recognizing that behavioral reactions may differ between rising and declining risk. Essay 3 focuses on vaccination as a key external driver affecting both disease

dynamics and behavior, partially addressing the omission of intervention effects in earlier work. Rather than attempting to exhaustively compare all possible vaccination strategies, it emphasizes the marginal gains of alternative policies relative to less effective baselines.

As a result, while the dissertation advances understanding of behavioral delays and their policy implications, its findings should be interpreted within the context of the modeling assumptions and the specific behavioral and policy dimensions considered. Future research could extend this framework by incorporating additional behavioral signals, institutional responses, and heterogeneous population dynamics to further improve realism and generalizability. Such extensions would help assess the robustness of the conclusions across different diseases, policy environments, and social contexts. I invite researchers to further examine the findings and extend the models to better capture policy implications of social and behavioral dynamics in epidemics.

1.4. References

Bauch, C. T., & Galvani, A. P. (2013). Social Factors in Epidemiology. *Science*, *342*(6154), 47-49. https://doi.org/10.1126/science.1244492

Chernozhukov, V., Kasahara, H., & Schrimpf, P. (2021). Causal impact of masks, policies, behavior on early covid-19 pandemic in the US. *Journal of econometrics*, *220*(1), 23-62.

Childs, L., Dick, D. W., Feng, Z., Heffernan, J. M., Li, J., & Röst, G. (2022). Modeling waning and boosting of COVID-19 in Canada with vaccination. *Epidemics*, *39*, 100583.

Fitzpatrick, M. C., & Galvani, A. P. (2021). Optimizing age-specific vaccination. *Science*, *371*(6532), 890-891.

Funk, S., Salathé, M., & Jansen, V. A. A. (2010). Modelling the influence of human behaviour on the spread of infectious diseases: a review. *Journal of The Royal Society Interface*, *7*(50), 1247-1256. https://doi.org/10.1098/rsif.2010.0142

LeJeune, L., Ghaffarzadegan, N., Childs, L. M., & Saucedo, O. (2025). Formulating human risk response in epidemic models: exogenous vs endogenous approaches. *European Journal of Operational Research*.

Lim, T. Y., Xu, R., Ruktanonchai, N., Saucedo, O., Childs, L. M., Jalali, M. S., Rahmandad, H., & Ghaffarzadegan, N. (2023). Why Similar Policies Resulted In Different COVID-19 Outcomes: How Responsiveness And Culture Influenced Mortality Rates: Study examines why similar policies resulted in different COVID-19 outcomes in using data from more than 100 countries. *Health Affairs*, *42*(12), 1637-1646.

Lipsitch, M., & Dean, N. E. (2020). Understanding COVID-19 vaccine efficacy. *Science*, *370*(6518), 763-765.

Mahmud, M. S., Eshun, S., Espinoza, B., & Kadelka, C. (2024). Adaptive human behavior and delays in information availability autonomously modulate epidemic waves. *medRxiv*, 2024.2011. 2023.24317838.

Qiu, Z., Espinoza, B., Vasconcelos, V. V., Chen, C., Constantino, S. M., Crabtree, S. A., Yang, L., Vullikanti, A., Chen, J., & Weibull, J. (2022). Understanding the coevolution of mask wearing and epidemics: A network perspective. *Proceedings of the National Academy of Sciences*, *119*(26), e2123355119.

Rahmandad, H. (2022). Behavioral responses to risk promote vaccinating high-contact individuals first. *System Dynamics Review*, *38*(3), 246-263.

Rahmandad, H., Lim, T. Y., & Sterman, J. (2021). Behavioral dynamics of COVID-19: estimating underreporting, multiple waves, and adherence fatigue across 92 nations. *System Dynamics Review*, *37*(1), 5-31.

Rahmandad, H., & Sterman, J. (2022). Quantifying the COVID-19 endgame: Is a new normal within reach? *System Dynamics Review*, *38*(4), 329-353.

Rahmandad, H., Xu, R., & Ghaffarzadegan, N. (2022a). Enhancing long-term forecasting: Learning from COVID-19 models. *PLoS Comput Biol*, *18*(5), e1010100. https://doi.org/10.1371/journal.pcbi.1010100

Rahmandad, H., Xu, R., & Ghaffarzadegan, N. (2022b). A missing behavioural feedback in COVID-19 models is the key to several puzzles. *BMJ Glob Health*, *7*(10). https://doi.org/10.1136/bmjgh-2022-010463

Saad-Roy, C. M., & Traulsen, A. (2023). Dynamics in a behavioral–epidemiological model for individual adherence to a nonpharmaceutical intervention. *Proceedings of the National Academy of Sciences*, *120*(44), e2311584120.

Sterman, J. D. (2000). Business Dynamics: Systems thinking and modeling for a complex world. *MacGraw-Hill Company*.

Wei, Z., & Zhuang, J. (2023). On the adoption of nonpharmaceutical interventions during the pandemic: An evolutionary game model. *Risk Analysis*, *43*(11), 2298-2311.

2. Essay 1: Debiasing Mobility Estimation by Modeling Delay Structures

2.1. Abstract

While we expect the public to respond to pandemic risk by changing their mobility patterns, mixed evidence exists on the magnitude of the effect during different waves of the COVID-19 pandemic. Studies that estimate the effect of the disease or related policies on public mobilities mostly rely on statistical analysis that investigates immediate association between the two. In this paper, we show that finding the effect is non-trivial due to various system delays inherent in information diffusion and the time it takes for the public and government to perceive risk and act upon it. Our analysis shows that without accounting for the delay period and the delay structure, the empirical estimations of the effects might be biased. We then offer a method to debias the estimations using Erlang distribution to represent lagged effects. We validate the method in a synthetic dataset showing that the ground truth values can be uncovered in the presence of various delay periods and structures. We then propose an algorithm that can be employed by modelers to include delays in their estimations.

Keywords: Mobility, Epidemic modeling, Delay, COVID-19

2.2. Introduction

Understanding patterns of human response and the effects of pandemic risks on human behavior are of significant importance. The recent pandemic experience showed that the public responded to evolving risks of the disease by changing their daily routines, interactions, and mobility, and such responses affect the trajectory of the disease. However, modeling change in human response is complicated due to various factors such as difficulties of precise modeling of human risk perception, and representation of information uncertainties, and the processes and system delays associated with information diffusion which affects public risk perception and action. The US National Science Foundation recently called for studies that incorporate changes in human behavior during a pandemic as a grand challenge towards developing more useful epidemic models.

An important public response to a pandemic is through change in mobility (Arthur et al., 2017). As observed during the recent outbreak, people limited their outside interactions by staying at home or decreasing unnecessary mobility and the use of public transportation. Governments also implemented lockdown policies that directly impact public mobility (Oraby et al., 2021). Such responses are realized with a lag that corresponds to the time it takes to perceive the risks and act by staying home or altering the frequency and mode of transportation. Recent studies provide valuable frameworks for linking changes in mobility to various factors, including government policies and disease cases. The majority of these studies concentrate on the impact of mobility on disease transmission (Shakeel et al., 2021). However, only a few examine the reverse relationship—how the state of the pandemic influences public mobility. This latter effect is relatively complex and involves various factors, such as government policies and media reports, which are often influenced by the current state of the disease with a certain degree of delay. In

addition, such information delay is not necessarily a constant lag affecting all players but has a specific distribution where some people are influenced earlier than others. Whether or not shifting the data by a fixed period, a commonly used approach, resolves the issue is an empirical question.

In this study, we provide evidence that careful attention should be paid in considering delays in a causal effect between pandemic risks and human responses. We propose a novel approach to enhance the accuracy of estimating the impact of epidemic risk on mobility. Our methodology involves quantifying and estimating delays between the occurrence of risk and the subsequent response. To achieve this, we utilize synthetic data generated through a simulation model, where we set the ground truth for the effect of pandemic deaths on mobility and the associated delay. We show that the simplistic approach of a constant shift in data to incorporate a fixed delay fails to recover the effect. This study offers a method that helps recover the delay structure and period which leads to an unbiased estimation of the public's mobility response to the disease.

2.3. Background

Human mobility patterns are significantly disrupted during pandemics (Warren & Skillman, 2020). Changes in these patterns are either because of government-enforced NPIs (Nonpharmaceutical interventions) or the public's natural fear-induced response to the disease's risk (Abouk & Heydari, 2021; Perra, 2021). Although the effect of disease on mobility patterns is widely accepted, its quantification and estimation are challenging (Funk et al., 2015). The importance of accurately estimating mobility lies in its intertwined relationship with the spread of the disease (Rahmandad et al., 2022b); attempts at estimating mobility without considering its dynamics will potentially end in misleading results.

What makes mobility estimation tricky is the complex nature of mobility and human behavior as a whole (Ferguson, 2007). To start, measuring change in mobility has proven a daunting task to researchers until recently, leaving few trustworthy high-quality datasets for researchers to work with (Funk et al., 2010; Verelst et al., 2016). Additionally, inconsistencies in human behavior are another hurdle in the estimation process; for instance, in the case of COVID-19, modelers failed to replicate mobility change consistently over longer periods of time due to differences in mobility responses during different waves of the disease (Rahmandad et al., 2022a). This is important as it indicates that there is a missing piece in mobility estimation.

As mobility patterns are not constant even outside the extreme events such as global pandemics, it is important to have a better understanding of factors influencing these patterns over time (Gonzalez et al., 2008). A set of studies looks at quantifying mobility before and after a specific period of time with the goal of providing an informed view of different patterns in mobility change. By looking at changes in mobility in a setting similar to a steady state, one can create a baseline for normal patterns of mobility to then compare with the disruptions caused by the

disease (Ruktanonchai et al., 2021). The use of non-disease-related variables to model mobility in these types of studies and prevalent, for instance, factors such as age, gender, and race (Feehan & Mahmud, 2021). These studies often find connections from individuals' backgrounds to their mobility patterns, contributing to the process of mobility estimation as a whole. However, often these estimations do not hold in the long term (Guidotti et al., 2016). This is due to the static nature of these estimations which does not incorporate external effects in an endogenous manner. These complexities only grow when the extra effect of a disease is added.

Disease and mobility have a two-way interaction (Osi & Ghaffarzadegan, 2024). In mobility change research, most studies consider the effects of mobility on the disease, whereas one of the driving forces of mobility change is in fact, the state of disease (Pardo-Araujo et al., 2023). To understand mobility change, it is important to consider and study both sides of this interaction. Nevertheless, as the primary focus of our study is mobility estimation, we refer to the effects of the disease on mobility as the direct relation and the effects of mobility change on the disease as the reverse relation.

During a global pandemic, one driving research interest is in determining the governmental policies that can best curb the severity of the outbreak (Fang et al., 2020). As most of these policies include a form of mobility control, the reverse relation has been studied extensively. For instance, Huang and colleagues considered a combined effect of social distancing and vaccination policies on changes in the spread of COVID-19, arguing that stricter mobility restrictions would prevent the growth of the disease. Similarly, in a study conducted by Hsiang and colleagues, the reaction of different populations to anti-contagion policies has been modeled analyzing the best time to implement a restrictive policy during a pandemic (Hsiang et al., 2020; Huang et al., 2021). One questionable assumption of these studies is the consideration of mobility as a policy-bound desired value that does not change over time. However, the certain feature of mobility is its dynamism. Without studying the direct relation, mobility change cannot be explained.

Among few studies that consider the dynamic aspect of mobility change by considering the direct relation, we can point to an interesting work where the authors considered the added effects of increasing COVID-19 cases, extreme weather, and socio-economic factors to previously modeled mobility pattern structure (Liu et al., 2023). Nevertheless, even in considering the direct relation there is evidence of mixed results when mobility is estimated over extended times, specifically over several waves of the disease, leading to some questioning if it is possible to consistently predict and estimate mobility (Bergman & Fishman, 2023). While there might be several challenges that contribute to this shortcoming, including not having access to consistent high accuracy data of mobility change during the disease, limitation of testing and real time reporting, etc. Our first hypothesis is that not modeling delays is also an important contributing factor to this shortcoming that is often overlooked in models.

H1: Neglecting information delays in estimating mobility leads to biased estimations

Looking at different mathematical formulations in behavioral epidemic models, we see that while there are several approaches, such as compartmental modeling (Huang et al., 2021), econometrics (Hsiang et al., 2020), machine learning (Bao et al., 2020), network modelling (Chang et al., 2021) mobility estimation often boils down to being a function of a few other variables that in theory do have a delay response, but very few models actually implement the effects caused by delays. From these models, again, few considered the inherent delays in the direct relation. Nevertheless, there are valuable insights in looking at how delay was incorporated in these models. One recent study considered time lag effects of COVID-19 policies on transportation systems (Bian et al., 2021). Using a regression-based structure, the authors estimated the most likely delay between an enacted policy and its consequent effect on mobility change. Another study used delay differential equations to predict the growth rate of COVID-19 (Dubey et al., 2022). Also, another example of delay inclusion can be seen in a study by Xi and colleagues where the authors quantify time-lag effects of mobility on COVID-19 transmission using regression modelling (Xi et al., 2020). In all these three cases, the final equation that either estimates mobility or uses mobility to estimate changes in the disease contains a time lag, or in other words a fixed delay. This structure of delay simply shifts the data with a constant time lag assuming that all information is transferred in this fixed time period. This brings us to our second hypothesis:

H2: Using fixed delay approximation when the delay follows an alternative distribution leads to biased estimations

To test our two hypotheses, we first provide examine mathematical formulation of delays. Next, we test our first hypothesis by comparing two modelling settings with one approach not including the effect of delay and the other one with a fixed delay structure. This will conclude our Study I. In Study II, we test our second hypothesis by considering an alternative delay setting. We then compare and discuss the results of these modelling approaches in detail.

2.3.1. Using information delay to estimate risk perception

The concept of information delay is intuitive: it takes time for us to hear about a new event or news, such as a change in economy, a political turmoil, or an emergence of a new disease, from main sources, the media, or friends. It further takes time to perceive the implications of the new event on us, and to act upon them. Such delays are present in our daily lives and affect our responses. As such, it is often important to have an accurate representation of delays in our systems models.

There are two major questions that most dynamic modelers think about when dealing with information delays: the delay period, and the delay structure. The first concept is trivial, while its actual estimation might be complicated: It is about the time period that it takes for the receiver to adjust its perception with the source. For example, it takes time for people to perceive the real

risks of a pandemic. Maybe there will be some denial at first, and then as cases increase or there are more deaths people perceive the risks. On the second concept, the delay structure, a modeler needs to find a proper mathematical structure to represent the lag in information: is the receiver directly connected to the source, or the information goes through layers of filters before getting to its final destination. As such, it is important to note that simply including a delay factor in our modelling is not sufficient as it does not provide much insight.

The cornerstone of the structure of information delay is adaptive expectations. This refers to the gradual adjustment of beliefs toward actual values. For example, our perception of the capabilities of our new boss is a lagged state that adjusts itself to her capabilities as we receive more information about her. Each new observation slightly alters our previous perception, which itself was constructed based on previous observations. In its simplest format, the rate of adjusting is proportional to the gap between our perception of a value and its most up to date informed value (i.e., error), and the process of adjusting continues as long as there is an error. In that sense our perception is being adjusted proportional to the error, as presented in Equation 2.2.1.

$$\frac{d\hat{X}}{dt} = \frac{X - \hat{X}}{D} \qquad (2.2.1)$$

where X is the actual value, $\hat{X}$ is the perceived value (lagged), and D is the average delay period. This delay structure is referred to as the first-order delay. As the equation shows, the highest rate of change for a step increase in X is immediately after X changes, that is first-order delays are highly sensitive to the latest piece of information. On the other extreme, in some systems it takes longer for a chain of information to start influencing perception. The most intuitive structure which resembles a conveyer is the fixed-order delay, represented in Equation 2.2.2.

$$\hat{X}_t = X_{t-D} \qquad (2.2.2)$$

In many cases, a fixed delay is not representative of the reality. For example, during a pandemic, the public's risk perception adjusts itself to the actual level of risk over time as some people are slower and some are quicker in perceiving the new information, and information goes through various filters. A great example for this is the origination of COVID-19 in Wuhan, China. Dr. Li Wenliang was the first person who noticed a pattern in patients that resembled a potential outbreak of severe acute respiratory syndrome (SARS). There was in fact an initial delay between the infection of patient zero and the time this observation was made. After expressing his initial concerns, he was contacted by local officials to stop "spreading rumors." This created another delay as the public was not properly informed of the outbreak, because of the interventions. It was only after ten days that a declaration of an outbreak was made, and even then, the public's risk perception was not yet adapted to the severity of the disease. As it is illustrated in the example, there are multiple stages of delay until information reaches the public and creates behavioral change. An alternative delay structure, therefore, would be an n-th order delay which can be derived by cascading multiple first-order delays. This delay structure will be further discussed in study II.

The idea of delay structures and their mathematical expression including fixed delay and n-th order delay are based on the mathematical fundamentals of system dynamics works in delays (Forrester, 1961; Sterman, 2000).

2.4. Study I

We discussed the potential benefits of considering delay in the public's response to perceived risks, and in turn, changes in their behavior. Our hypothesis is that by modeling this delay structure, a more accurate mobility estimation can be achieved. Nevertheless, simply adding a delay term is unlikely to add value to our estimation, and in some cases may even worsen the model's performance. In other words, considering the right structure for including delay is what makes the difference.

In the first study, we assume a fixed delay structure in the causal relationship between the disease and mobility. We use a behavioral epidemic model to generate synthetic data and simulate potential scenarios for the progression of disease and public's mobility change. We first construct a regression model that explains mobility based on disease data without considering delays. Next, using the fixed delay assumption, we build a second regression model that uses lagged disease information as its independent variable. By comparing the results of these two regression models, we get a better understanding of the potential benefits of including a delay structure in mobility estimation. Furthermore, we discuss the limitations in a fixed delay assumption and if another delay inclusion structure could provide a more accurate result.

2.4.1. Methods

2.4.1.1. Synthetic data generation

The synthetic model used in our study is inspired by the SEIRb model which is a compartmental epidemic model with a behavioral feedback loop (LeJeune et al., 2025; Xu et al., 2021). In the original model, there is no direct measure of mobility. Instead, behavioral change is seen through changes in contact rates of individuals. Mobility is added in our modified version as an intermediary variable with values between 1 (normal mobility) and 0 (no mobility) that is then multiplied by normal contact rate to create the same concept of contact rate in the original model. Figure 3.1 represents the stock-flow diagram of our modified SEIRb model in more detail. Equations (1)-(4) are a depiction of the underlying assumption that govern the main structure of our epidemic model, where S is the susceptible, E is the exposed, I is the infected, R is recovered, D is the dead, and N represents the population.

$$\frac{dS}{dt} = -\beta . c' \frac{SI}{N} \qquad (1)$$

$$\frac{dE}{dt} = \beta . c' \frac{SI}{N} - \frac{E}{\lambda_e} \qquad (2)$$

$$\frac{dI}{dt} = \frac{E}{\lambda_e} - \frac{I}{\lambda_i} \qquad (3)$$

$$\frac{dR}{dt} = (1 - i)\frac{I}{\lambda_i} \qquad (4)$$

$$\frac{dD}{dt} = i\ \frac{I}{\lambda_i} \qquad (5)$$

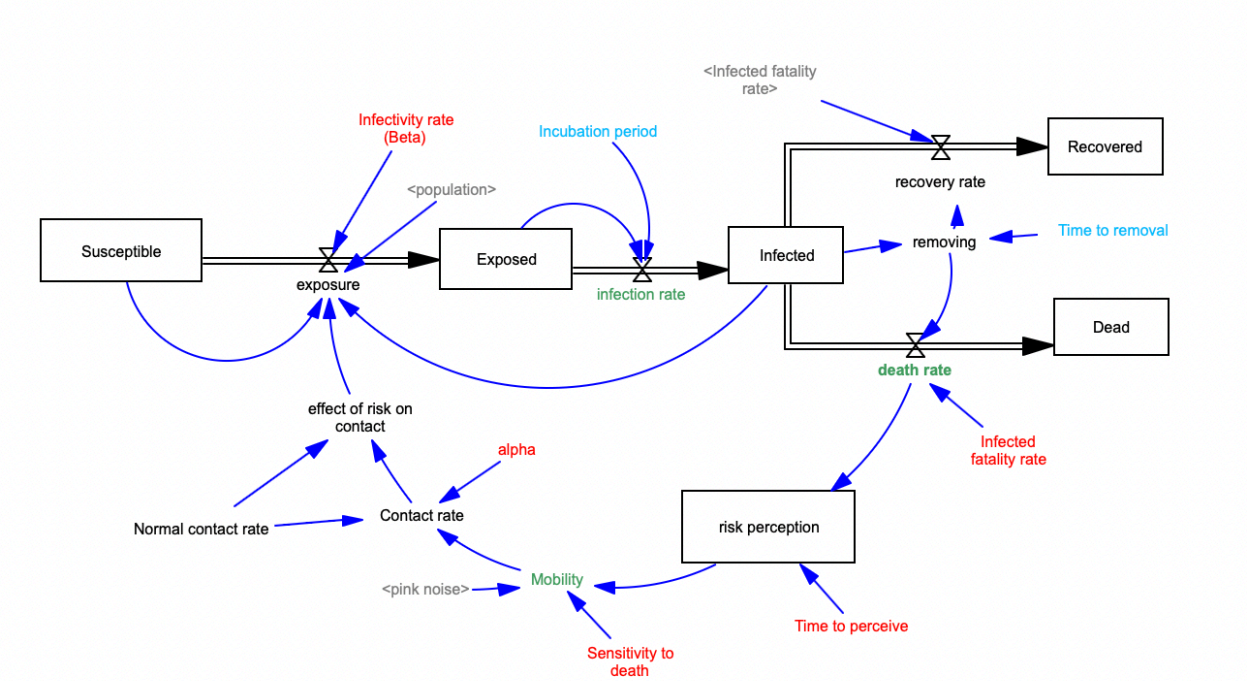

Figure 2.1. Simplified stock flow diagram of the behavioral epidemic model containing mobility.

In the above equations, β is the infectivity rate, c' is the effect on risk on contact, λ_e is the average incubation period, λ_i is the average infection period from the onset of symptoms to either death or recovery, and i is the infected fatality rate.

The behavioral feedback in the model works through affecting the exposure rate. With lower perceived risk, the total contacts are reduced and consequently, less people are exposed to the disease, and vice versa. The driver of such behavioral response is seen within mobility change. Equation (6) shows how mobility is formulated in the model.

$$Mobility\ (M)\ = \exp\left(-\mathrm{k}.\hat{f}.\epsilon\right) \qquad (6)$$

Where k represents the public's sensitivity to death, $\hat{f}$ refers to the perceived risk of past death values, and ϵ is the noise term. Each of these terms are further explained in detail.

k is a measure of the public's change in mobility in response to changes in death. In simpler terms, k is change in (log of) mobility for 1 death per million population.

$\hat{f}$ or the past deaths term represents public's perceived risk of the disease. This idea is built into the model by considering the disease fatality over time, or in other words, aggregating past deaths. The value of $\hat{f}$ is derived by multiple exponential smoothing of past death values. In the case of a single exponential smoothing, as in Figure 3.1, change in $\hat{d}$ can be represented as:

$$\frac{d\hat{f}}{dt} = \frac{\hat{f} - f}{\lambda_p} \qquad (7)$$

Where f is the actual daily death value, and λ_p is the time it takes to perceive the changes in deaths and its related risk. The separation of actual death and perceived death is made to emphasize on the concept of delay. The public's risk adjustment is not instant, it takes time. In the synthetic model, delay setting is represented by two terms: first, delay length which is the same as time to perceive (λ_p), and second, delay order which is the number of exponential smoothing done on past death values, or in terms of the stock-flow diagram, the number of stocks that come in between death rate and mobility, each applying an exponential smoothing.

ϵ or the error term is considered to allow a more realistic depiction of changes in mobility patterns. The structure of this term can be further explained as an autocorrelated noise reflecting intrinsic stochastic factors that cause real-world mobility data to deviate from expected values, namely changes due to weather patterns and holiday seasons (Xu et al., 2021). This noise is calculated through an exponential smoothing of white noise, with a mean of 1, standard deviation of 0.2, and a correlation time of 30 days. The correlation time indicates the effect of past values on the current value, using an exponential decay distribution with its time constant being the correlation time. (refer to the topic of correlated noise in(Sterman, 2000)).

Mobility change is then transformed into changes in contact rates. Later on, this effect on exposure influences the unfolding of the disease, including disease fatality. The important consideration for mobility and contact change is that smaller changes in mobility lead to larger changes in contacts as mobility considers the changes in individuals and their decision to stay home whereas contact looks at the connections of two or more individuals. For instance, if one colleague shows up to work and one does not, the mobility change between the two is 50 percent; however, the contacts have reduced by 100 percent, as there is no contact created with just one individual. The following two equations describe contact rate changes mathematically:

$$c = \mathrm{M}^{\alpha}.c_0 \qquad (8)$$

$$c' = \frac{c}{c_0} \qquad (9)$$

Where c is the contact rate, and c_0 is the normal contact rate. α represents the discussed exponential relationship between mobility change and contact change.

Given these settings, multiple scenarios can be simulated, each representing a possible realization of the stochastic epidemic model. Figure 3.2 is an example visualization of three possible scenarios of changes in mobility over the time span of 1000 days. These scenarios are generated using the incorporated stochasticity through the pink noise error term.

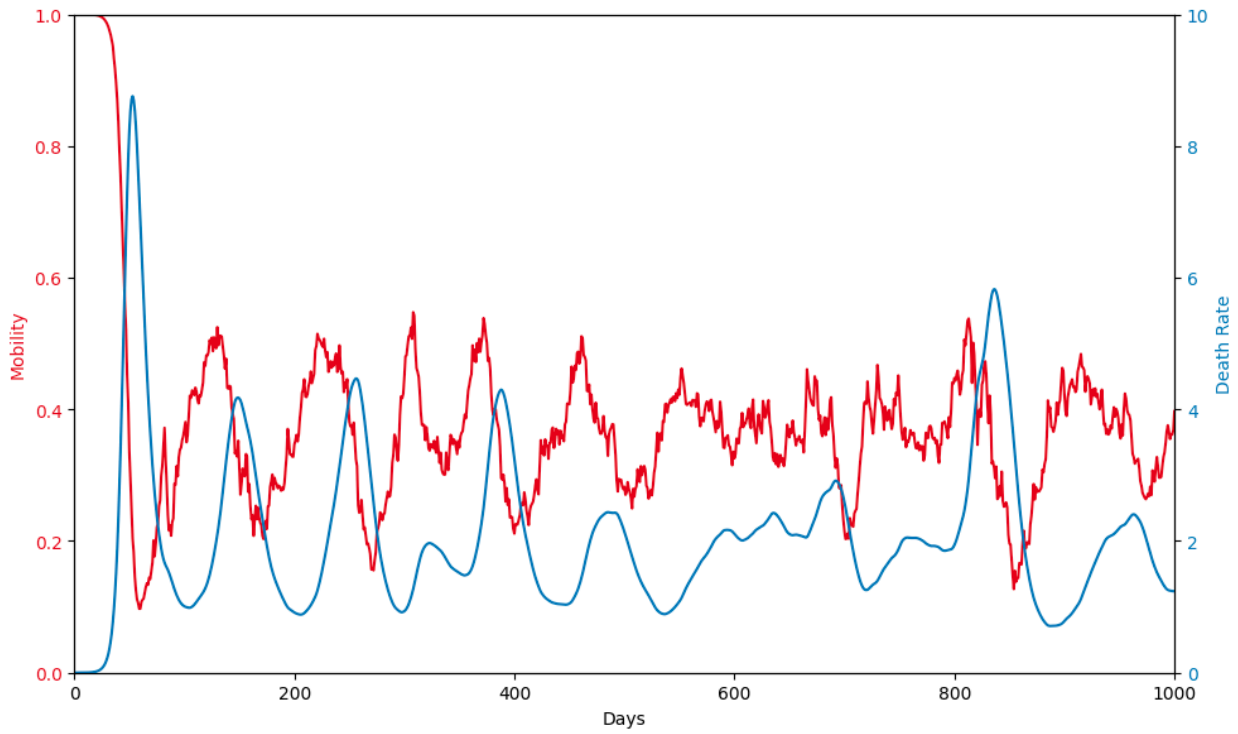

Figure 2.2. An example of simulation results of changes in mobility and death rate over a time span of 1000 days.

2.4.1.2. Process

We develop two distinct regression models that aim to use disease information, specifically deaths, to explain mobility change. In both regression models, mobility and death rate outputs from the synthetic model are the only data used. The difference in the two models, however, is in the consideration of delay. The first model uses yesterday's death rate to explain today's mobility. On the other hand, the second model allows looking further back into time, arguing that death from n days ago is the best independent variable for estimating today's mobility. It is

important to mention that n is a variable that can take the value of 1, creating a regression model identical to the first model. The idea is that by allowing n to be a variable rather than a fixed constant, the added value of delay can be tested.

Below, the mathematical settings behind these two regression models are shown.

Regression model 1: $\log(Mobility_t) = \beta_0 + \beta_1 Death\ rate_{t-1} + \epsilon$

Regression model 2: $\log(Mobility_t) = \beta_0 + \beta_1 Death\ rate_{t-n} + \epsilon$

The reason for selecting a logarithmic structure for our regression models comes back to our assumption in the synthetic model. Based on Equation (6) we have:

$$Log(Mobility) = \left(-\mathrm{k}.\hat{f}.\epsilon\right) \qquad (10)$$

Which represents the general structure that our regression models are trying to construct.

A recursive process is required to find the best value for n in the second regression model. The approach used in this study compares the explanatory power or R squared values of each given value for n. To elaborate, for each selection of n, death data are shifted forward in time such that mobility at time t corresponds to death at time t-n. Next, the regression model is run and the results, namely the R squared value and coefficient are stored. This process is repeated until all possible values of n have been tested. At this stage, one value of n has produced the highest R squared value; this value of n is then selected to be the best estimate of delay length.

Additionally, the coefficient that corresponds to the highest R squared regression setting contains meaningful information. Because of the structure of our regression model, the coefficient β_1 can be a good estimate of the sensitivity to death (k) as it expresses mobility change given change in death rate, the same concept as sensitivity.

3000 datasets are simulated each representing a stochastic scenario with changing delay structures including delay lengths of 30, 60, and 90 days. We want to test the ability of each model to:

1) Explain mobility change
2) Recover the effect size or sensitivity to death (k)
3) Recover delay structure, in this case delay length or time to perceive risk

To explain mobility change we look at the R squared values of each regression model. For recovering the effect size, we look at the coefficient of each regression model. Lastly, for recovering delay length we consider n to be the best estimate for delay length. We test this estimation by looking at the percentage error compared to the ground truth values. It is worth mentioning that the first regression structure does not consider a delay structure, thus the delay length estimate is only applicable in the second regression model.

2.4.2. Results

2.4.2.1. Regression model performance: how well is mobility change explained

After completing the simulation of 3000 stochastic scenarios and plugging in these values into the two structured regression models, we were able to get insightful results from each of the models. To begin with, we looked at how well the regression models were able to fit the data. To do so, R squared values were assessed. Figure 3.3 is a boxplot comparison of the two regression models, showcasing the distribution of r squared values over different simulations in each model.

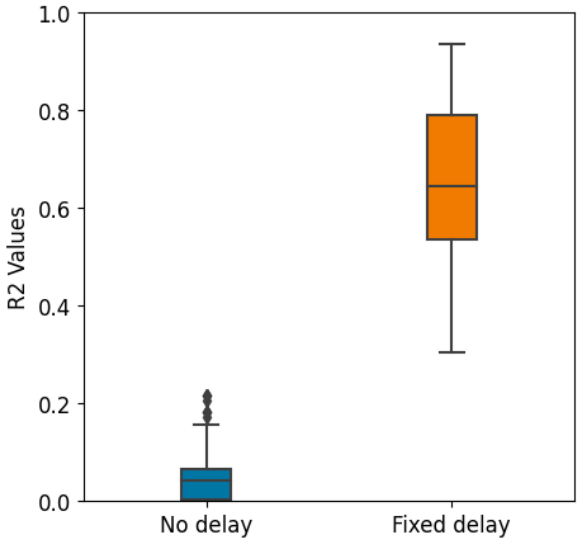

Figure 2.3. Comparison of R squared values of the regression model 1 and 2

We can clearly see that the inclusion of delay is significant in better explaining mobility change. The regression model without a delay structure has an average R squared value of 0.04 which indicates a poor fit of the model to the data. On the other hand, the fixed delay model that searches for the best shift to data which represents the time it takes for the public to perceive risk and react, does a much better job of fitting the data with an average R squared value of 0.66. While far from an ideal model, it is a great indication that the addition of the concept of delay is indeed a necessity for a good fit.

2.4.2.2. Effect size (sensitivity to death) recovery

In the second observation, we focus on the retrieval of the effect size. This effect represents people's reaction to an increase or decrease in the disease perceived risk caused by its fatality. In

the synthetic model, the initial value set for the public's response is -0.5, representing a decrease in mobility with an increase in the perceived risk.

Looking at both regression models, we can argue that the coefficient β_1 can be a good estimate as it represents mobility change given a unit of change in deaths. Figure 3.4 provides a comparison of the estimates that each regression model has of this value.

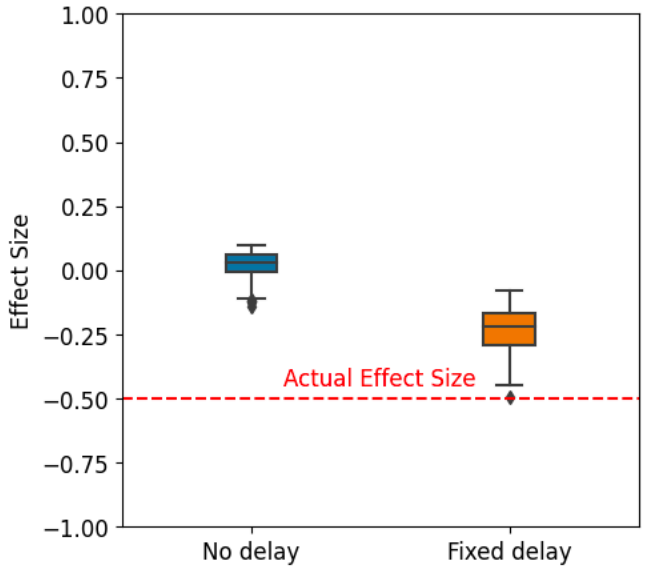

Figure 2.4. Comparison of the estimated effect size (sensitivity to death) for regression model 1 and 2

We can see that the first model, the model with no delay consideration, does not recover the effect size at all. With an average close to zero, what it conveys is that there is a response from the public to the change in risk perceived from the disease. Based on the settings of our synthetic model, we know that this is not the case.

The second model, which considers a fixed delay structure, does indeed assign higher importance to the public's sensitivity to death, with an average value of -0.23. While this value is far from the ground truth of -0.5, it does indicate that the model is able to understand the direction of the public's reaction correctly by correctly assigning a negative value to this effect. Furthermore, it again is an indication of the added value of including delay in our regression model.

2.4.2.3. Delay structure recovery

In our final observation, we look at the models' capability in recovering the structure of delay we designed in our synthetic setting. As the first regression model does not consider a delay structure within its formulation, estimating the delay structure would not be applicable to it. However, in the regression model structure, the concept of delay is included through a shift of n

days. Through an iterative process the optimal shift value is estimated and then compared with the concept of the time to perceive delay in the synthetic model. The underlying value for this variable is set as 30, 60, and 90 in different simulations to test the regression model's robustness in estimation. Figure 3.5 shows the percentage error of this estimation over 3000 simulation runs.

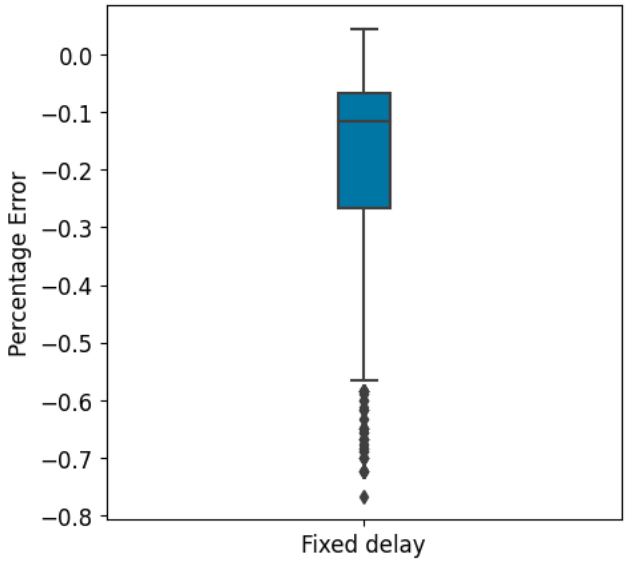

Figure 2.5. Percentage error in delay length or public's time to perceive risk in second regression model.

The first notable observation from the results is the asymmetry of the errors. The model consistently underestimates the delay value. Furthermore, the distribution is quite dispersed estimating a wide range of possible values, which is undesirable. Overall, the average percentage error in delay length estimation is -0.19 which is not particularly high, indicating that the delay inclusion is indeed able to recover the concept, however there might be additional nuances that are missing in this simple fixed delay structure.

From all these three observations, we consistently see the added value of including delay in our regression model. Nevertheless, the results are not ideal. This motivates us to pursue a second study in which we look further into possible structures for delay structure and to test if we would achieve a significant improvement in our regression model's overall performance by making additional changes in our delay incorporation structure.

2.5. Study II

Following study I's insights, which clearly indicated the necessity of incorporating the effect of delay in mobility estimation, we ask ourselves if there is a better way of considering the delay structure in our model.

There are indeed limitations to a fixed delay structure incorporation which we discussed in study I. One issue is the assumption that there is no distribution of the delayed reaction over time, indicating that a change in people's perception only occurs after a specific time. Similar to an on-off switch, people's awareness of risks is modeled to be complete after a certain time, and zero before that specific time.

Our new hypothesis is that by allowing a gradual setting for delayed risk response in which people gradually change their perceived risk, a better model for estimating mobility change can be achieved.

To test this hypothesis, we first explore the mathematics of such delay structure. Next, we apply this mathematics to our regression model. Finally, we design tests to assess our new model, and its added value compared to the fixed delay regression structure.

2.5.1. N-th order delay structure

In Section 2.3 we discussed that an alternative delay structure could be an n-th order delay which can be derived by cascading multiple first-order delays. Conceptually, this is equivalent to thinking that the source of information is perceived through a first order delay by the first recipient who then conveys the new information to the second receiver, and then the third receiver and so on. In dynamic modeling such higher order delays can be mathematically represented as Equation 2.2.3

For an nth-order delay we can show that:

$$\frac{dS_i}{dt} = \begin{cases} (\hat{X}_0 - S_i)/(l/n) & for\ i = 1 \\ \dfrac{S_{i-1} - S_i}{(\frac{l}{n})} & for\ i \in (2, \dots, n) \end{cases} \qquad (4.1.1)$$

Where S_i is the i-th stage in which a first-order delay process occurs. The output of each stage is then used as input for the next stage. The output of the nth stage S_n would be the final perceived value.

As the order of delay increases, the above calculation becomes computationally extensive and complex. An alternative approach to calculating higher-order delays is using the Erlang distribution. The Erlang distribution turns equation 4.1.1 to a weighted sum of all past pieces of information, as presented in equation 4.1.2.

$$\hat{X}_t \sim W_1.X_t + W_2.X_{t-1} + \cdots + W_i.X_{t-i+1} + \cdots$$

$$W_i = \frac{i^{o-1} e^{-i/(\frac{l}{o})}}{\left(\frac{l}{o}\right)^o (o-1)!} \qquad (4.1.2)$$

By using Equation 2.2.4 one can accurately estimate Equation 2.2.3, that is the perceived information with a delay length of l and order of o. This is particularly useful in computer programs for numerically estimating delays. In our case, as we will later discuss, our main contribution stems from utilizing the Erlang distribution in regression models to represent delay structures. Using a weighted average structure with weights that follow an Erlang distribution for delay sets a strong mathematical formation for analyzing and assessing the effects of different amounts and orders of delay. Having this mathematical structure of delay allows its incorporation into a regression model that can further explain the delayed effects of disease on mobility change.

2.5.2. Methods

2.5.2.1. Synthetic data generation

The model that we use for data generation is the same model we used for Study I. We use the exact same setting in the model and work with the same stochastic synthetic datasets.

2.5.2.2. Process

Similar to study I, we want to use a regression modelling approach that incorporates the effect of delay in mobility estimation. Conveniently, the n-th order delay structure can be simplified using an Erlang series which we derived in Equation 4.1.2. By incorporating this setting into our regression model, we obtain the following:

$$\text{Regression model 3: } \log(Mobility_t) = \beta_0 + \beta_1(W_1.Death\ rate_{t-1} + W_2.Death\ rate_{t-2} + \cdots + W_i.Death\ rate_{t-i}) + \epsilon$$

Where W_i represent the weight assigned to death rates from i days ago. These weights follow an Erlang distribution as expressed in Equation 4.1.2

The first question that arises with this structure is to what extent do we have to look back in time to build our regression model. In other words, what would be a good value for i. The initial assumption is that the longer we look back the better our estimation would be. However, this comes at a cost. The cost being, most importantly, missing data. To elaborate, for each observation in our dataset, we require the past i observations to build our regression model. Therefore, the first i observations would have missing values. In our synthetic setting, we assume that the disease begins on day 1 and it is safe to consider the days before as disease free. Nevertheless, choosing a higher i could still alter our regression results. On the other hand, choosing a small i can also adversely affect our model's performance, as it may fail to capture the full disease dynamics, particularly the waves, in a small dataset. Thus, choosing the correct i is indeed an important first step.

One approach is to choose the minimum ii required to achieve the desired level of mobility change explanation. To achieve this, we use noise-free synthetic datasets with alternating delay orders and delay lengths. For each dataset, we run regression models with increasing i values. The first regression model that reaches an R Squared value of 0.99 or higher determines our desired i value. The goal is to derive a meaningful relationship between i, the delay length, and the delay order.

With the structure of our regression model completed, we can apply our approach to stochastic synthetic data. Initially, we work with 30000 simulation runs which include varying delay lengths of 30, 60, and 90 days, and also, delay orders of 1 to 10. The first goal is to recover the underlying values of the delay structure without prior knowledge of their values. We break down this goal into smaller steps, with the first step being the recovery of delay order with known delay lengths. To do so, we plug in the known delay length values into our Erlang weight calculation. We use $\hat{o}$ as our estimate for delay order. By assigning different values to $\hat{o}$ for a given stochastic dataset, we can find the best estimate by analyzing the model with the highest R squared value.

The next step is to work with datasets with an unknown delay structure. In this setting, we follow a similar procedure, this time by doing a grid search for the best estimates of delay order and delay length. To elaborate, for each dataset, we iteratively increase the values of delay order and delay length, generating a regression model for delay orders ranging from 1 to 10 and delay lengths of 1 to 120 days. We store R squared values of each regression at each iteration. Finally, by analyzing at the model that produced the r squared we can derive the best estimates for delay length and delay order.

Similar to study I, an important concept that we are interested in is the public's sensitivity to death or the effect size of death on mobility. β_1 which is the coefficient of our regression model can be seen as a collective measure of people's reaction to past changes in death. We use β_1 as our estimate of sensitivity to death, denoted as k.

To further test the capability of our model in recovering this relationship, we design a set of experiments with varying underlying effects of death on mobility change in our synthetic model. In the first experiment, we consider a placebo effect, in which there is no meaningful relationship between death and mobility. Mobility change is solely based on the noise function. In this scenario, we test our effect size estimate to determine whether the regression model can correctly identify the lack of a meaningful relationship or if it fails due to overfitting. In the second and third scenario, we use the original setting in our synthetic model, but we change the underlying value of the sensitivity to death k. in the second scenarios, the original value which is -0.5 is used and in the third scenario, we double this value to be -1. We again test to see if our regression model is capable of recovering these underlying values.

Finally, we analyze the added value of incorporating the delay structure in Regression Model 3 over the previous models.

2.5.3. Results

2.5.3.1. Including past observations in the regression model

To complete our regression model, we first need to determine the number of past death observations to include. By plotting the minimum number of inclusions that is denoted as i based on the delay structure, we can gain a better understanding of their relationship. Figure 3.6 visualizes this relationship.

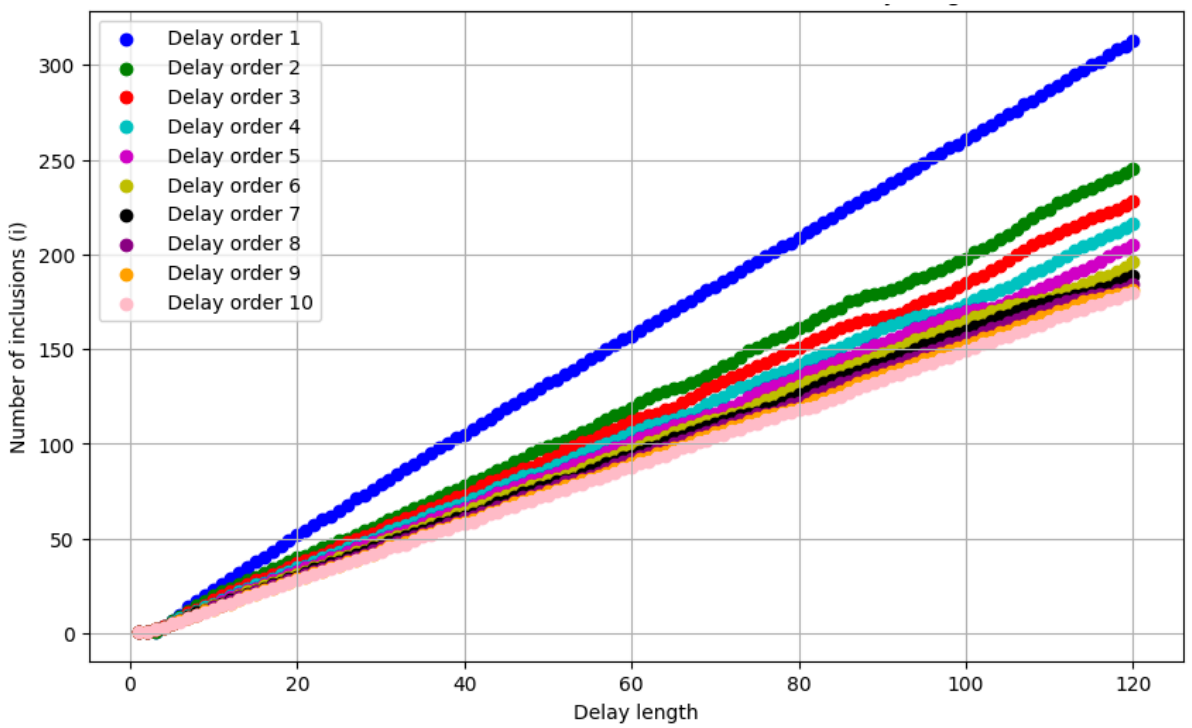

Figure 2.6. minimum number of inclusions to reach a 0.99 R squared for each delay length and order.

We observe that as delay length increases, we will be needing more past death inclusions. This does align with our expectations, as people take longer to adjust their risk perception of the disease. On the other hand, we see that an increase in delay order leads to a decrease in the value of i. This decrease seems to slowdown in higher orders and reach its minimum value at delay order of infinity which is the same setting as a fixed delay structure. In this case, we will need the past l days which is the delay length to capture all the necessary information in disease change.

Based on the above observations, we constructed the following structure for formulating i based on disease structure:

$$i = \beta_1 l + \beta_2 (\frac{l}{\sqrt{o}})$$

Using regression on our simulated datasets, we calculate the best coefficients.

$$i = l(1 + \frac{1.54}{\sqrt{o}})$$

this final formula has an R squared of more than 0.99, indicating a perfect fit of our i calculated through this formula to the one from the data.

2.5.3.2. Recovering the delay order

Next, we assess our regression model's ability to recover the underlying delay structure. We begin by structuring our regression model based on known delay lengths while treating the delay order as unknown. Figure 3.7 shows the average R squared values calculated across all simulated datasets with an underlying delay order of 1.

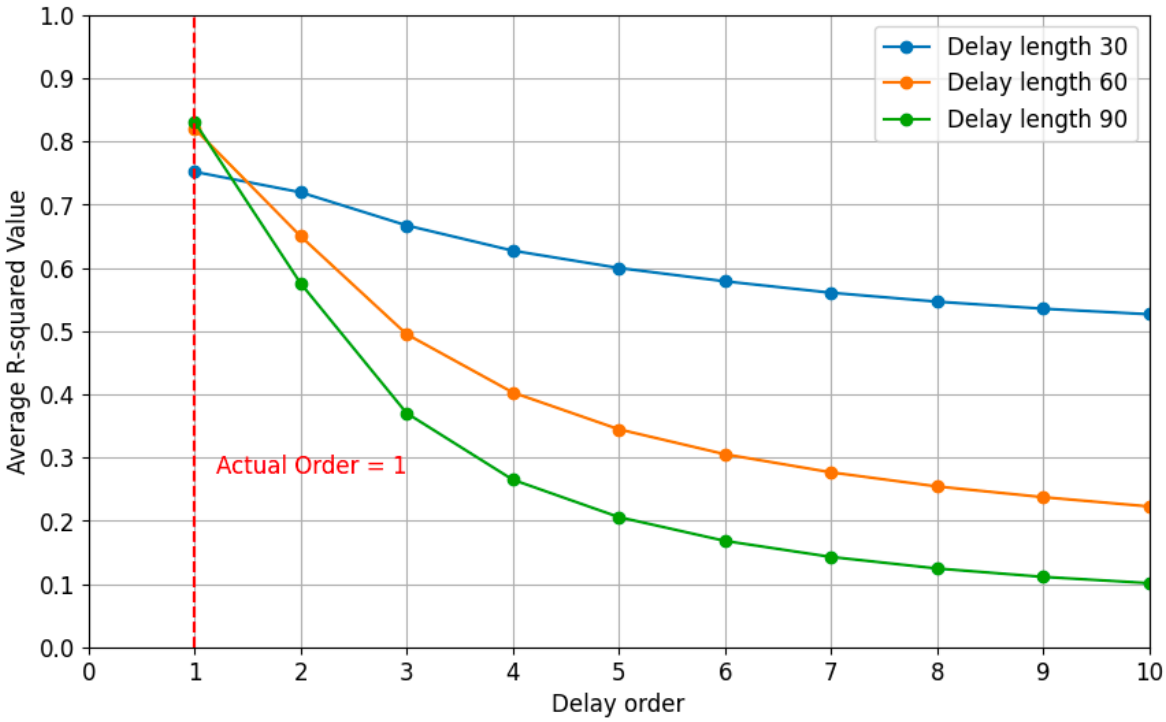

Figure 2.7. Average R squared values of regression models with varying delay order values of 1 to 10 for datasets with an underlying delay order value of 1

The model attempts to derive the best estimate for delay order by comparing the best fitting models. We can see that in all three cases of delay length of 30, 60, and 90 the best estimate is

indeed a delay order of one as it has the highest R squared value. In this case, the regression model was able to successfully recover the correct ground truth value of the delay order.

We experiment with all delay orders from 1 to 10 and in these cases, the regression models' best estimates match the ground truth values. This retrieval for delay orders 2, 3, and 4 is visualized in a panel plot in figure 3.8. The R squared charts for delay orders 6 to 10 are included in Appendix I.

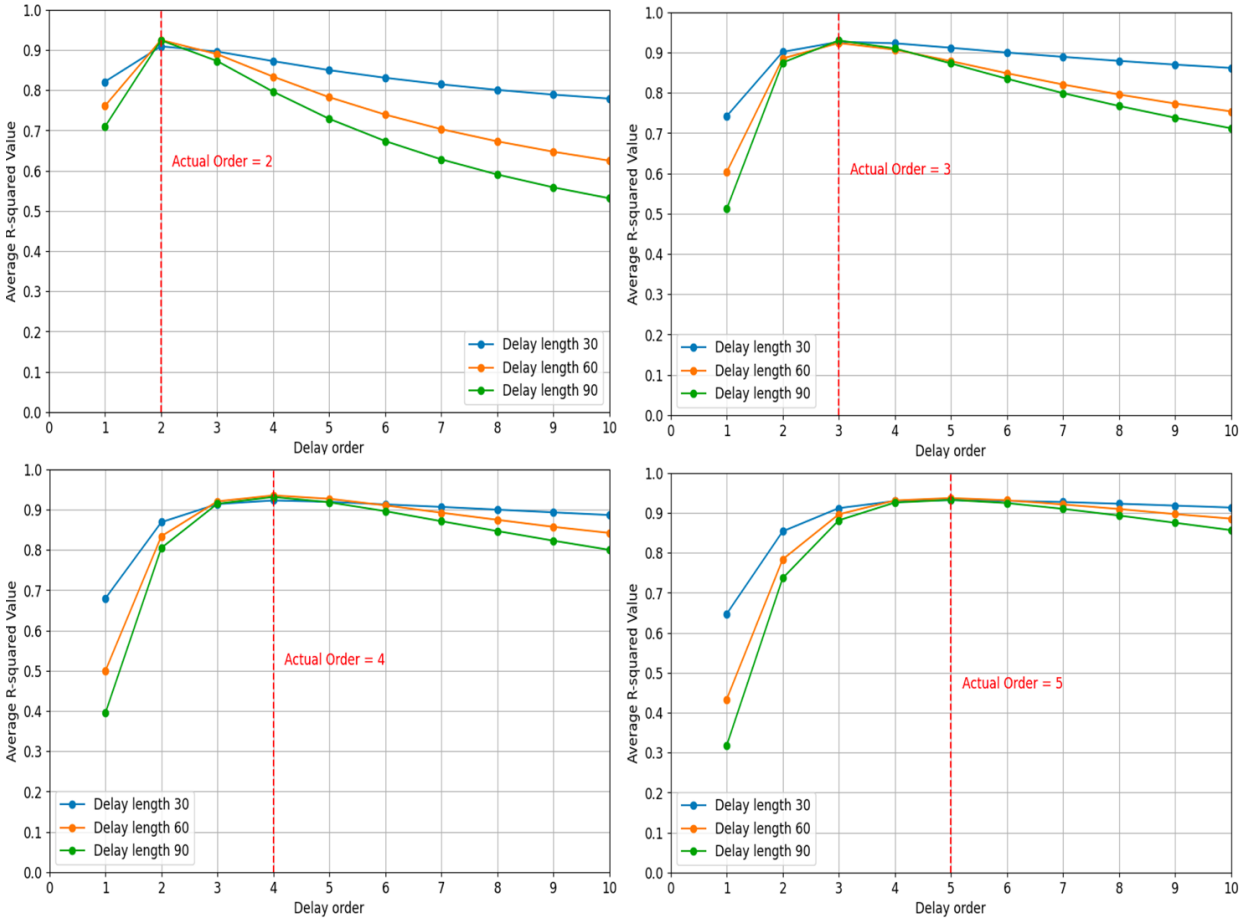

Figure 2.8. 4 plots of average R squared values of regression models with varying delay order values of 1 to 10 for datasets with an underlying delay order value of 2, 3, and 4

2.5.3.3. Recovering the full delay structure

The previous results were achieved with the assumption that underlying delay lengths are known in our regression setting and only the delay order is being estimated. However, in a more realistic setting, a dataset will not contain such information. Both the delay order and delay length are unknown and need to be estimated. In Figure 3.9 we depict the performance of our regression-

based process in recovering these values by showing their percentage errors using a boxplot. In both estimates, we observe an almost symmetrical distribution around zero, indicating that our process is producing an acceptable estimation range for actual delay structure. In both cases, we observed a minimal error in the model's estimation (MPE of -2.94% for delay order and 3.77% for delay length) demonstrating our model's capability to recover the ground truth delay values.

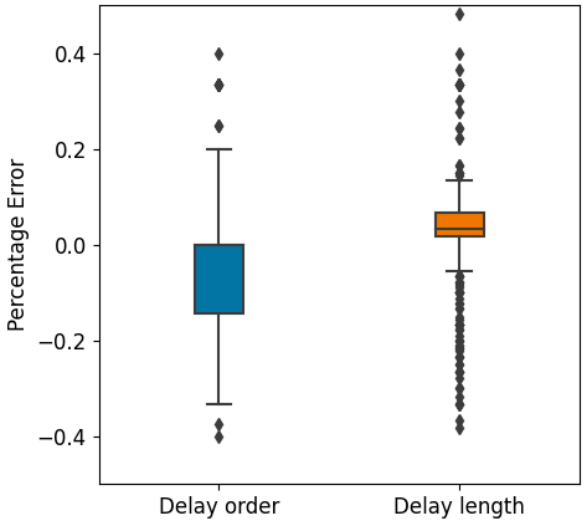

Figure 2.9. Percentage error values in delay structure recovery

2.5.3.4. Recovering the effect of past death on mobility change

To test our model's robustness in recovering the effect of past deaths on mobility, we designed three scenarios, each representing a different underlying structure: the placebo scenario, where changes in death have no meaningful effect on mobility, the base scenario in which sensitivity to death is set to -0.5, the third and final scenario in which we assigned a higher risk sensitivity with an underlying value of -1, double the amount in the base case. Figure 3.10 shows our model's estimation of sensitivity to death in each scenario. We see that in every single scenario, our model is able to estimate public's sensitivity to death within an acceptable range. In fact, the average values for our estimate in each scenario exactly match the ground truth values ($\hat{k}_1 = 0.00,\ \hat{k}_2 = 0.50,\ \hat{k}_3 = 1.00$). These results are more impressive knowing that these estimates are derived only by using mobility and death data, and without any information on delay structure underlying values.

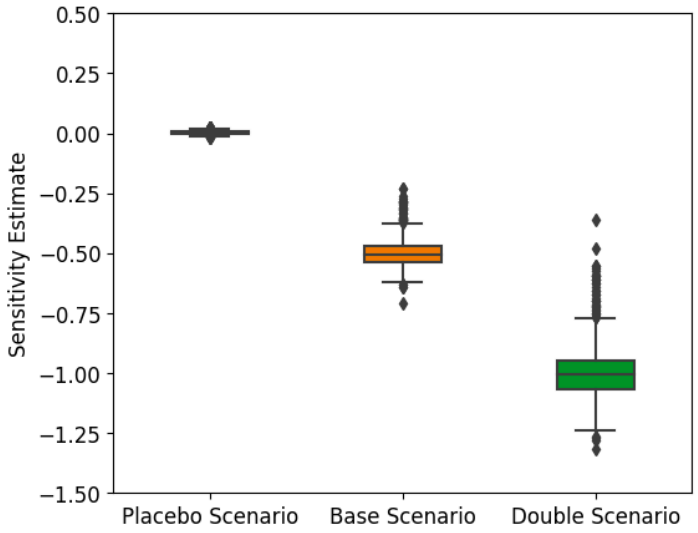

Figure 2.10. Model's performance in recovering sensitivity to death (k) in three scenarios

2.6. How to apply this process to another dataset: an algorithm

There are many processes where delays are a significant factor. In our case, we considered the delay in people's mobility change following changes in disease fatality rate and observed the added value of incorporating this delay into our modeling approach. Nevertheless, there are many other implications for adding delays to models, specifically those using a regression-based setting. In this section, we provide a step-by-step algorithm on how to add a n-th order delay structure to not only a disease dataset, but also other time series datasets that may include a delay factor.

This algorithm requires only two sets of variables as input, with one as the independent variable and the other as the dependent variable. As output, this algorithm provides the best estimate of the delay structure, specifically delay length and delay order. Using this estimate, one can test whether a delay factor is present by looking at the significance of the added delay structure.

Below are the detailed steps of this algorithm:

1) Select a range for possible delay orders (1, O) and delay length values (1, L)
2) Define your formulation for i based on the structure $i = \beta_1 l + \beta_2(\frac{l}{\sqrt{o}})$ (find the coefficients β_1 and β_2 by regression modeling)
3) Create $(\beta_1 + \beta_2)\, L$ new columns of delayed X values $(X_{t-1}, X_{t-2}, \dots, X_{t-(\beta_1+\beta_2)L})$
4) Start with delay order estimate $o = 1$ and delay length estimate $l = 1$

5) Build the regression model $Y = \beta_0 + \beta_1(W_1.X_{t-1} + W_2.X_{t-2} + \cdots + W_i.X_{t-i}) + \epsilon$ and store its R squared value. The weights are based on the following Erlang distribution:

$$W_i = \frac{i^{o-1}e^{-i/(\frac{l}{o})}}{\left(\frac{l}{o}\right)^{o}(o-1)!}$$

You will be including columns (X_{t-1} , X_{t-2} , … , X_{t-i}) in this regression.

6) If $l < L$ increase l by 1 and go to step 5

7) If $o < O$ increase o by 1, set $l = 1$, and go to step 5

8) Rank the models based on their R squared values. The model with the highest R squared value provides the best estimate for delay structure.

This algorithm is a step forward towards replicability of this and any other work using this approach.

2.7. Insights from Study I and II

In both studies, we observed that adding a delay structure to our model not only improved its performance but also enhanced its ability to recover the underlying structure and effects. At the end of Study I, we concluded that a fixed delay structure does improve the model's performance in explaining mobility change. However, this structure was unable to provide a consistent estimate for the effect of past deaths on mobility change. Also, the delay estimates were far from ideal. This motivated us to conduct Study II, where we used a more advanced delay structure in our regression model in hopes of achieving better overall performance. here, we compare the results of Study I and Study II and analyze these findings to argue if the added values of including an n-th order delay structure over a fixed delay structure are significant.

First, we begin by comparing the overall performance of these two delay structures. Figure 3.11 compares the average R squared values of these two models. It is clear that the n-th order delay structure incorporation consistently outperforms the fixed delay structure with the former averaging an R squared value of 0.93 and the latter averaging a value of 0.65.

Next, we examine how these two structures perform in recovering the delay structure. As the fixed delay structure does not consider delay order to be a variable, it does not provide an estimate for it. Thus, the comparison is solely based on delay length estimation. As shown in Figure 3.12, the model using the n-th order delay structure produces a more precise range of estimation with lower dispersion and higher symmetry around zero compared to the model using a fixed delay structure. The difference in mean percentage error is also significant, 3.77% for the n-th order setting and 19% for the fixed delay setting.

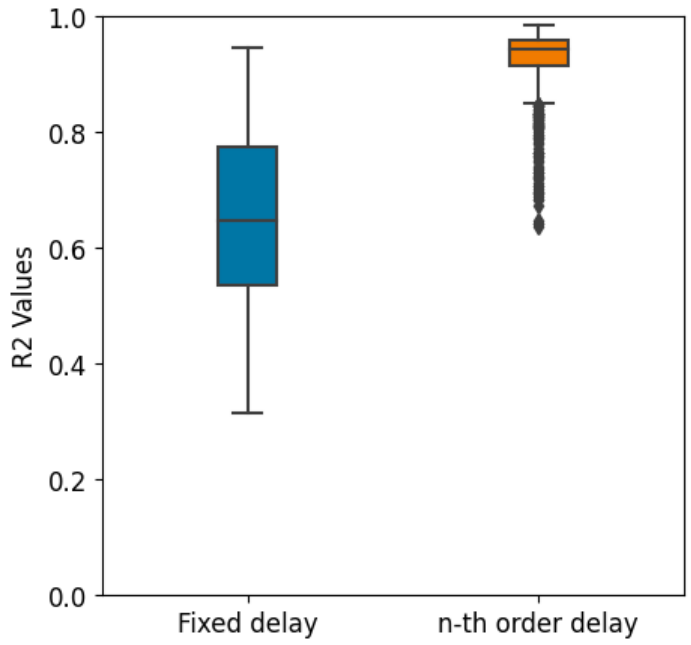

Figure 2.11. Difference in R squared values produced using a fixed delay structure and n-th order delay structure

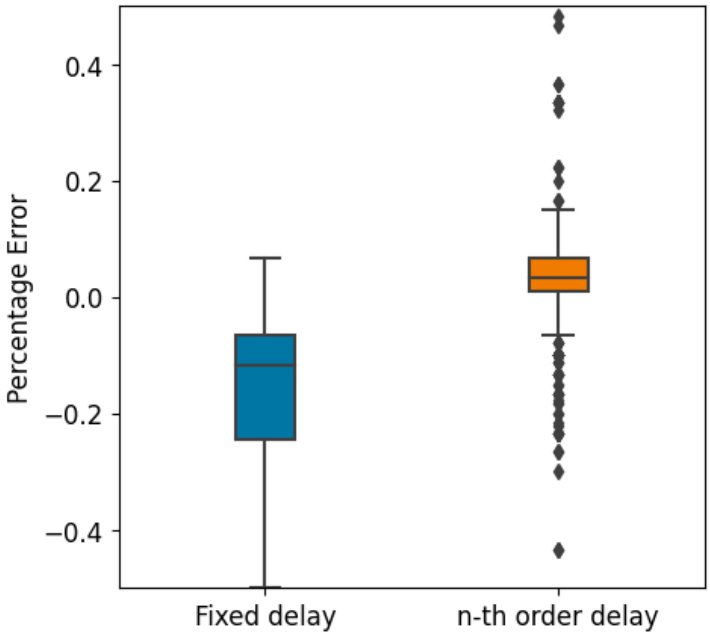

Figure 2.12. Comparison of percentage error in delay length estimation in the two modeling structures

Finally, we examine how these two models compare in recovering the effect of past deaths on mobility change, or people's sensitivity to death. Figure 3.13 showcases this difference in the base case scenario where the underlying sensitivity is -0.5

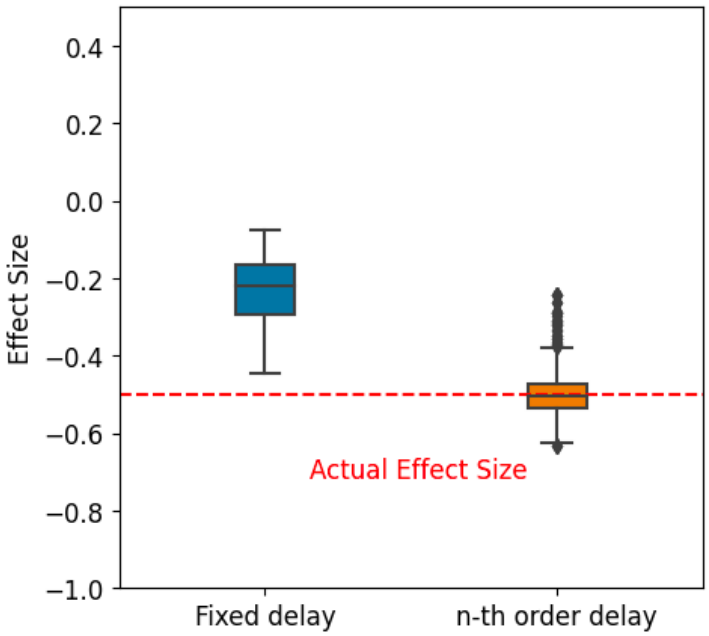

Figure 2.13. Comparison of sensitivity to death estimation in the two modelling structures

The n-th order delay structure perfectly captures the ground truth value of this effect with a highly accurate estimation range, whereas the fixed delay structure estimates the effect to have a mean of -0.23 which is far from the correct value.

In all three criteria, we observed that the n-th order delay structure incorporation dramatically improved our model's performance. Even though, this delay structure is more complex, its addition can be easily justified by looking at its effect of debiasing mobility estimation and recovering the effect of past deaths on mobility change.

2.8. Discussion and conclusion

Estimating people's behavior is complex. One factor that adds to this complexity is the delays in people's behavioral response which often goes unnoticed. In this study, we focused on the underlying delay effects on public's mobility change in response to changes in an infectious disease. We hypothesized that previous attempts at mobility estimation were biased due to missing the inherent delay structures in their modeling processes, and that incorporating a delay structure would help debias mobility estimation.

We designed three modeling approaches, one with no delay incorporation, one with a fixed delay incorporation, and one with an n-th order delay incorporation. Using a synthetic behavioral epidemic model, we tested different scenarios and underlying structures to generate datasets which were then used to validate each of our three approaches. It became evident that considering delays is vital to a well-performing model. Nevertheless, to achieve a model capable

of capturing the full effect of delay, a fixed delay structure is not sufficient. By allowing the model to look at previous information, we enable it to analyze different possible delay patterns and recover the correct underlying delay response. Considering an n-th order delay structure, creates an extra degree of freedom for the model to look for the best fitting delay order; whereas in a fixed delay setting, delay order is not being estimated and is considered to be infinity, an assumption that can be misleading.

In the case of modeling mobility change, there is more than just providing a better fit to the data. Understanding the drivers behind this change and in what ways they affect mobility is crucial for achieving a better estimate. We know that one key driver of mobility change during outbreaks is disease fatality. Incorporating an n-th order delay structure enabled us to recover the underlying connection between changes in mobility and death. This includes the recovery of the true effect of past death on mobility change or public's sensitivity to death, and also, the time it takes for this effect to take place, or in other words, the delay between changes in death and changes in public mobility patterns. While we were not able to correctly recover these values by using a fixed delay structure, an n-th order delay incorporation led to a highly accurate estimation of delay structure and sensitivity to death.

As many other processes follow a delayed response pattern within them, this study suggests that incorporating a similar delay setting in models can lead to less biased results by taking the effects of delay out of estimations. To help ease this inclusion, a step-by-step algorithm was developed that future research can use to improve their modeling approach and estimation. This application is not limited to infectious disease modeling, as it can be used in any time series data analysis that consists of a delay factor with some degree of calibration.

This study contributes to the literature on epidemic modeling and operations research as the proposed addition of delay consideration in modeling mobility is a step forward in answering the puzzle of the intertwined relationship between human behavior and infectious diseases in epidemic modeling research. Furthermore, the proposed algorithm follows a likelihood optimization process that can be applied to operations research studies. In more concrete examples, these implications can be traced back to the literature that we reviewed earlier. In the models that do include a delay, can benefit from rethinking the structure at use for delay incorporation. Based on our findings, switching to an n-th order delay structure can produce much better estimations. Also, this switch can be easily applied through our proposed algorithm. On the other hand, the models that do not consider the effects of delay at all, can greatly benefit from our study by simply following the proposed algorithm to incorporate the right delay structure, and analyzing if in fact, this incorporation is significant and meaningful in their estimations.

This study has several limitations that provides opportunities for future research. These can include:

1) Simplification of mobility change: In our regression setting, only past death rates are considered as factors affecting. This simplification does not fully capture the complex dynamics of mobility change in the real world. For instance, certain changes in human behavior during a pandemic are belief-based. This is seen in the case where groups disregard disease information due to their personal beliefs.

2) Real world applications: Currently, this approach has only been tested using data generated from a synthetic model. A great opportunity to expand this study is by applying this approach in real-world disease cases given that the recent pandemic provided us with the required data.

3) Synthetic model limitations: One key assumption made in using the synthetic model in our study was that its generated simulations closely resemble real world dynamics. However, we know that all models are wrong and some useful (George Box, 1976) The choice of using a synthetic model was mainly because of added flexibility in testing and validation. Nevertheless, we are aware of the limitations of this synthetic model and its effects on the generalizability of our findings.

4) External effects of vaccination: An important dynamic that not only influences the dynamics of mobility but also the disease as a whole is vaccination. Vaccinated groups do exhibit different mobility patterns due to their reduced perceived individual risks. Additionally, a higher vaccinated population will curb the disease as a whole disrupting the original links between mobility change and the spread of the disease.

5) Assumption of symmetrical delay response: In our study, we assumed that population responds to the risk of a disease in a symmetrical manner. Meaning that we would expect the same delay for fear-induced mobility restriction and for the return of mobility to its normal patterns in the absence of this risk. This assumption might not be a correct reflection of true mobility dynamics.

Overall, this study provides a novel approach to mobility estimation by considering the biasing effects of overlooking delay and its proper structure. Using the suggested delay incorporation algorithm, the process of adding delay to diverse regression-based models is made possible through a step-by-step procedure. We hope that by incorporating the effects of delay while using the correct setting, future research can benefit from its added values in estimation processes.

2.9. Appendix I

In section 4.3, a visualization of delay recovery on a dataset with an underlying delay order of 1 was showcased. We discussed that this process can be applied to all ground truth values of delay order, from 1 to 10. Here, the successful estimation of delay orders with underlying values of 6 to 10 are visualized.

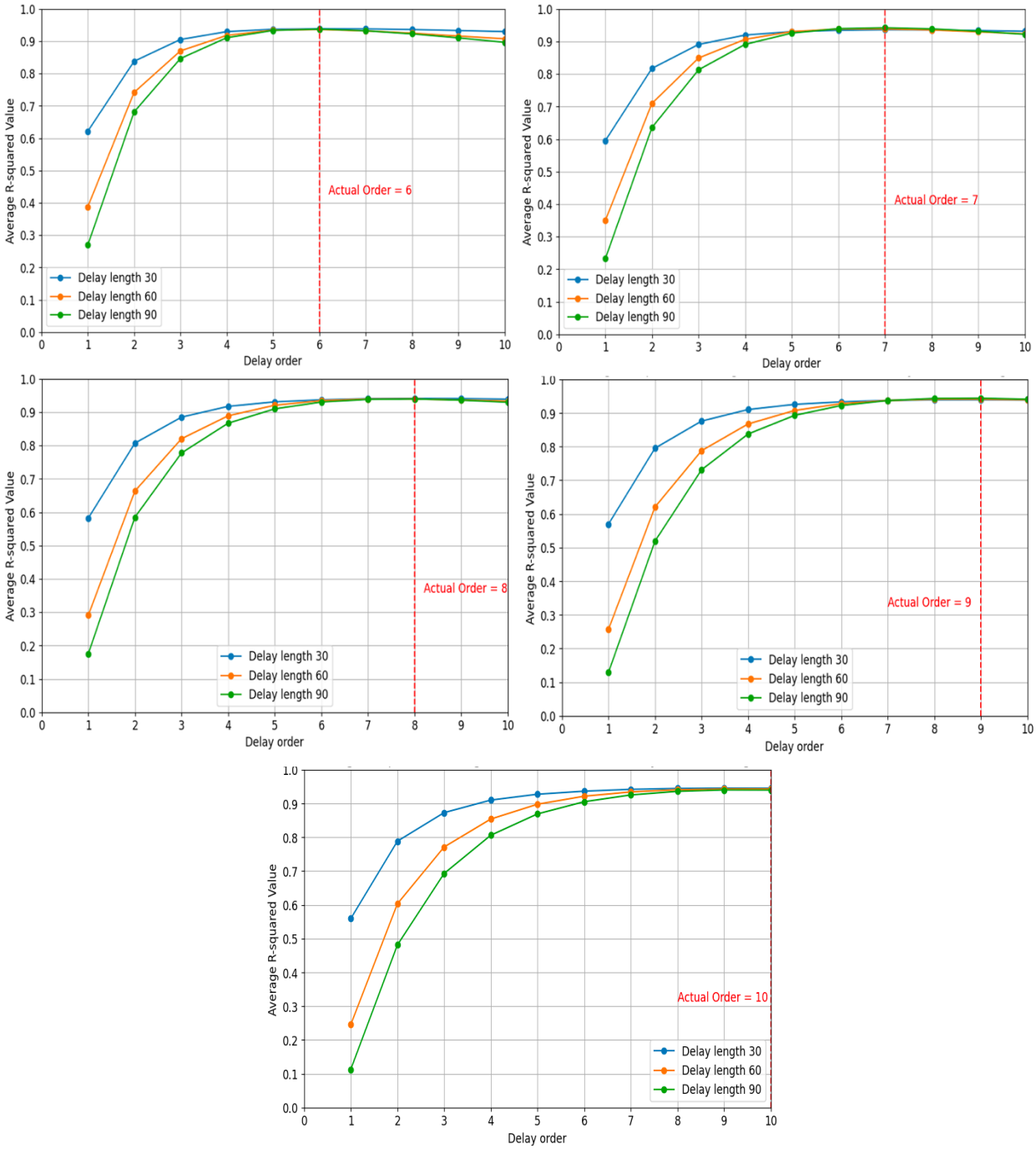

2.10. References

Abouk, R., & Heydari, B. (2021). The immediate effect of COVID-19 policies on social-distancing behavior in the United States. *Public health reports*, *136*(2), 245-252.

Arthur, R. F., Gurley, E. S., Salje, H., Bloomfield, L. S. P., & Jones, J. H. (2017). Contact structure, mobility, environmental impact and behaviour: the importance of social

forces to infectious disease dynamics and disease ecology [Review]. *Philosophical Transactions of the Royal Society B-Biological Sciences*, *372*(1719), 9, Article 20160454. https://doi.org/10.1098/rstb.2016.0454

Bao, H., Zhou, X., Zhang, Y., Li, Y., & Xie, Y. (2020). Covid-gan: Estimating human mobility responses to covid-19 pandemic through spatio-temporal conditional generative adversarial networks. Proceedings of the 28th international conference on advances in geographic information systems,

Bergman, N. K., & Fishman, R. (2023). Correlations of mobility and Covid-19 transmission in global data. *Plos One*, *18*(7), e0279484.

Bian, Z., Zuo, F., Gao, J., Chen, Y., Venkata, S. S. C. P., Bernardes, S. D., Ozbay, K., Ban, X. J., & Wang, J. (2021). Time lag effects of COVID-19 policies on transportation systems: A comparative study of New York City and Seattle. *Transportation Research Part A: Policy and Practice*, *145*, 269-283.

Chang, S., Pierson, E., Koh, P. W., Gerardin, J., Redbird, B., Grusky, D., & Leskovec, J. (2021). Mobility network models of COVID-19 explain inequities and inform reopening. *Nature*, *589*(7840), 82-87.

Dubey, P., Chen, Y., Gajardo, Á., Bhattacharjee, S., Carroll, C., Zhou, Y., Chen, H., & Müller, H.-G. (2022). Learning delay dynamics for multivariate stochastic processes, with application to the prediction of the growth rate of COVID-19 cases in the United States. *Journal of Mathematical Analysis and Applications*, *514*(2), 125677.

Fang, Y., Nie, Y., & Penny, M. (2020). Transmission dynamics of the COVID-19 outbreak and effectiveness of government interventions: A data-driven analysis. *Journal of medical virology*, *92*(6), 645-659.

Feehan, D. M., & Mahmud, A. S. (2021). Quantifying population contact patterns in the United States during the COVID-19 pandemic. *Nature communications*, *12*(1), 893.

Ferguson, N. (2007). Capturing human behaviour. *Nature*, *446*(7137), 733-733. https://doi.org/10.1038/446733a

Forrester, J. W. (1961). Industrial dynamics mit press cambridge. *MA.[Google Scholar]*.

Funk, S., Bansal, S., Bauch, C. T., Eames, K. T. D., Edmunds, W. J., Galvani, A. P., & Klepac, P. (2015). Nine challenges in incorporating the dynamics of behaviour in infectious diseases models. *Epidemics*, *10*, 21-25. https://doi.org/https://doi.org/10.1016/j.epidem.2014.09.005

Funk, S., Salathé, M., & Jansen, V. A. A. (2010). Modelling the influence of human behaviour on the spread of infectious diseases: a review. *Journal of The Royal Society Interface*, *7*(50), 1247-1256. https://doi.org/10.1098/rsif.2010.0142

Gonzalez, M. C., Hidalgo, C. A., & Barabasi, A.-L. (2008). Understanding individual human mobility patterns. *Nature*, *453*(7196), 779-782.

Guidotti, R., Monreale, A., Rinzivillo, S., Pedreschi, D., & Giannotti, F. (2016). Unveiling mobility complexity through complex network analysis. *Social Network Analysis and Mining*, *6*, 1-21.

Hsiang, S., Allen, D., Annan-Phan, S., Bell, K., Bolliger, I., Chong, T., Druckenmiller, H., Huang, L. Y., Hultgren, A., & Krasovich, E. (2020). The effect of large-scale anti-

contagion policies on the COVID-19 pandemic. *Nature*, *584*(7820), 262-267. https://www.nature.com/articles/s41586-020-2404-8.pdf

Huang, B., Wang, J., Cai, J., Yao, S., Chan, P. K. S., Tam, T. H.-w., Hong, Y.-Y., Ruktanonchai, C. W., Carioli, A., & Floyd, J. R. (2021). Integrated vaccination and physical distancing interventions to prevent future COVID-19 waves in Chinese cities. *Nature Human Behaviour*, *5*(6), 695-705. https://www.nature.com/articles/s41562-021-01063-2.pdf

LeJeune, L., Ghaffarzadegan, N., Childs, L. M., & Saucedo, O. (2025). Formulating human risk response in epidemic models: exogenous vs endogenous approaches. *European Journal of Operational Research*.

Liu, H., Wang, J., Liu, J., Ge, Y., Wang, X., Zhang, C., Cleary, E., Ruktanonchai, N. W., Ruktanonchai, C. W., & Yao, Y. (2023). Combined and delayed impacts of epidemics and extreme weather on urban mobility recovery. *Sustainable Cities and Society*, 104872.

Oraby, T., Tyshenko, M. G., Maldonado, J. C., Vatcheva, K., Elsaadany, S., Alali, W. Q., Longenecker, J. C., & Al-Zoughool, M. (2021). Modeling the effect of lockdown timing as a COVID-19 control measure in countries with differing social contacts. *Scientific reports*, *11*(1), 3354.

Osi, A., & Ghaffarzadegan, N. (2024). Parameter estimation in behavioral epidemic models with endogenous societal risk-response. *PLoS Computational Biology. In-press*.

Pardo-Araujo, M., García-García, D., Alonso, D., & Bartumeus, F. (2023). Epidemic thresholds and human mobility. *Scientific reports*, *13*(1), 11409.

Perra, N. (2021). Non-pharmaceutical interventions during the COVID-19 pandemic: A review. *Phys Rep*, *913*, 1-52. https://doi.org/10.1016/j.physrep.2021.02.001

Rahmandad, H., Xu, R., & Ghaffarzadegan, N. (2022a). Enhancing long-term forecasting: Learning from COVID-19 models. *PLoS Comput Biol*, *18*(5), e1010100. https://doi.org/10.1371/journal.pcbi.1010100

Rahmandad, H., Xu, R., & Ghaffarzadegan, N. (2022b). A missing behavioural feedback in COVID-19 models is the key to several puzzles. *BMJ Glob Health*, *7*(10). https://doi.org/10.1136/bmjgh-2022-010463

Ruktanonchai, C. W., Lai, S., Utazi, C. E., Cunningham, A. D., Koper, P., Rogers, G. E., Ruktanonchai, N. W., Sadilek, A., Woods, D., & Tatem, A. J. (2021). Practical geospatial and sociodemographic predictors of human mobility. *Scientific reports*, *11*(1), 15389. https://www.nature.com/articles/s41598-021-94683-7.pdf

Shakeel, S. M., Kumar, N. S., Madalli, P. P., Srinivasaiah, R., & Swamy, D. R. (2021). COVID-19 prediction models: A systematic literature review. *Osong public health and research perspectives*, *12*(4), 215.

Sterman, J. D. (2000). Business Dynamics: Systems thinking and modeling for a complex world. *MacGraw-Hill Company*.

Verelst, F., Willem, L., & Beutels, P. (2016). Behavioural change models for infectious disease transmission: a systematic review (2010–2015). *Journal of The Royal Society Interface*, *13*(125), 20160820. https://doi.org/10.1098/rsif.2016.0820

Warren, M. S., & Skillman, S. W. (2020). Mobility changes in response to COVID-19. *arXiv preprint arXiv:2003.14228*.

Xi, W., Pei, T., Liu, Q., Song, C., Liu, Y., Chen, X., Ma, J., & Zhang, Z. (2020). Quantifying the time-lag effects of human mobility on the COVID-19 transmission: a multi-city study in China. *Ieee Access*, *8*, 216752-216761.

Xu, R., Rahmandad, H., Gupta, M., DiGennaro, C., Ghaffarzadegan, N., Amini, H., & Jalali, M. S. (2021). Weather, air pollution, and SARS-CoV-2 transmission: a global analysis. *The Lancet Planetary Health*, *5*(10), e671-e680.

3. Essay 2: Debiasing Human Response Estimations in Dynamic Models: Exploring the Significance of Delay Structure and Asymmetries

3.1. Abstract

From how public opinion responds to economic outcomes to impact of risk perception on social interactions during a pandemic, many important social processes include the assimilation of information to shape opinions and perceptions, which then inform individual and societal actions. While such perception delays are well recognized, empirically identifying them is non-trivial. We study this problem in the context of human response to changes in the state of a disease mediated by public risk perception. Public risk perception changes through an information diffusion process with significant delays where perception adjustment delay may depend on whether risk is increasing or decreasing. Despite these complexities, most models either assume fixed-delay structures or exponential structures with symmetric delay periods. Leveraging synthetic data (where ground-truth is known) we show that incorrect delay structures and the assumption of symmetric delay periods can lead to biased and misleading estimates. We explore alternative ways of identifying appropriate delay structures that may overcome these challenges. We then apply the asymmetric delay structures to state-wide US COVID-19 Mobility data to showcase how the estimation of public's sensitivity to death is influenced by the method used for estimation. We also compare these alternative methods to flexible statistical approaches for capturing complex lag structures (ARDL) in projecting mobility out of sample.

3.2. Introduction

Social sciences deal with understanding human choices as affected by changes in incentives and environmental factors. Understanding the dynamics of social processes, ranging from how economic outcomes influence future voting patterns to the impact of risk perception on social interactions during a pandemic, underscores the importance of assimilating information to shape opinions and perceptions. These processes, integral to individual and societal actions, necessitate dynamic models that carefully quantify how humans perceive environmental changes, such as economic, political incentives, or health risks, and incorporate them into their considerations and actions. Achieving a precise representation of the causal mechanisms between the environment and human response demands an understanding of how humans receive information and respond, which often involves accounting for information delays not only in the physics of social processes but also in perception and response.

Consider the recent pandemic as an example. It prompted significant individual and societal responses to the infection risks. For example, during the COVID-19 pandemic, notable shifts in mobility patterns occurred, with many individuals choosing to limit their outside interactions by staying home or minimizing unnecessary travel. Notably, the change in pandemic risk perception

lagged the actual risk due to the time required for information dissemination and change in behavior: it takes time for individuals to grasp the risks through various channels such as the media and word of mouth and to adopt alternative patterns of behavior. The process by which information is communicated to the public and influences their behavior encompasses several system delays, corresponding to the time it takes for measurement of risk signals and for different groups to perceive risks and respond accordingly. While many studies correlate risks, represented by daily deaths or cases, with mobility patterns or consider a fixed delay period between risks and responses by shifting risk data forward, the dissemination of information does not necessarily follow a fixed delay. Moreover, there may be asymmetries in the time taken to perceive and act. For instance, as the number of cases increases, people may adapt their mobility more swiftly than letting down their guard when risks decline.

In modeling many problems, such as the example of COVID-19, modelers will need to quantify human responses to changes in their environment by systematically identifying delay structures. In this paper, we explore some basic methods for doing so and the value of correctly identifying delay structures in the causal representation of an external event on human response. We demonstrate that oversimplification of delay structures, such as assuming fixed-delay processes or exponential periods with symmetric periods for systems with asymmetric delay structures, can lead to biased and misleading estimates of human response. We achieve this in two steps: first, by demonstrating the importance of delay identification in a synthetic setting with known ground truth values for perception and impact mechanisms, and then by applying the method to state-level data tracking COVID-19 and mobility in the United States.

3.3. Background

Social and environmental changes such as epidemics, natural disasters, and significant policy changes, drive the public's response in complex manners (Abouk & Heydari, 2021; Feola, 2015). Especially as these responses unfold gradually and persist over time, it leads to delayed and diffused responses. There is often feedback from the public response to how the disruptive event takes shape, and people are made aware, through alternative sources, of the impact of their behavior as a whole (Rahmandad et al., 2022b). Through this information, people build a perception of the risks or rewards of their behavior, which later make further changes in thoughts, behaviors, and polices (Slovic, 1987). In certain processes, such as estimating wait times in queues, delays can be relatively straightforward to predict due to the availability of well-defined distributions. In contrast, quantifying delays in behavioral responses presents greater complexity, as the variability in social reactions to events renders both the average duration and the distribution of delays uncertain and not directly observable (Wibral et al., 2013). As a result, various studies adopt simplifying assumptions regarding the mechanisms by which external factors impact delayed behavioral responses. Some studies choose not to account for delayed responses, instead assuming immediate behavioral changes in response to acute natural disasters

(Li et al., 2022). Other studies adopt the assumption of a fixed delay between the external stimuli and observed behavioral changes without estimating the length and distribution of the delay (Jiao et al., 2021). These approaches overlook the complex dynamics of behavioral responses over time, potentially leading to biased estimations of the true effects. Individuals respond to external changes at varying rates, creating a distribution of responses across the period of change. Consequently, delays are not fixed but follow probabilistic distributions (Griliches, 1967). Disregarding or mis-characterizing these delays can result in unreliable and inconsistent estimates of key concepts, such as the responsiveness of individuals and communities to risk (De Boef & Keele, 2008).

Modeling the delayed impact of various factors is a common problem across different research communities. Several econometric methods are available for estimating delay distributions, with one of the more general being the autoregressive distributed lag (ARDL) models (De Boef & Keele, 2008). The ARDL model includes both past values of the dependent variable (autoregressive component) and past and current values of the independent variables (distributed lag component). ARDL incorporates different lags for both dependent and independent variables allowing a very flexible view of delays (Pesaran et al., 2001). While this method often provides very good (in-sample) fit to data, its flexibility comes with certain trade-offs. Firstly, the number of estimated parameters depends on the inclusion of lagged effects, which can grow substantially, thereby complicating theoretical interpretation (Hamilton, 1994). Secondly, without imposing constraints on the parameters, there is an increased risk of overfitting the model to historical data. Consequently, out-of-sample predictions based on these estimates may become unreliable (Kripfganz & Schneider, 2020; Narayan, 2005). Thirdly, projections become tricky when data on the dependent variables are unavailable until the previous period, a common issue for longer-term forecasts (Pesaran et al., 2001). Finally, this method by default does not allow for asymmetrical delay structures, complicating application to problems where asymmetry is suspected (Shin et al., 2014).

In epidemiological modeling, researchers have adopted a range of strategies to incorporate the delays inherent in human behavioral responses to infectious disease risk, and in a wider range of cases modelers ignore delays. Some models assume that behavior adjusts instantaneously to current conditions, effectively ignoring any delay; this “no-delay” approach is common in early behavioral–disease models and game-theoretic formulations (Funk et al., 2010; Reluga, 2010). In contrast, other models incorporate a fixed lag in the behavioral response to reflect the constant time interval between when information (such as rising case counts) becomes available and when individuals alter their behavior (Fenichel et al., 2011; Schecter, 2021; Xu et al., 2020; Zhang et al., 2023); for example, Schecter (2021) uses geometric singular perturbation theory to analyze an epidemic model in which “sticky” behavior introduces a fixed delay in the adjustment process. An alternative approach is modeling the delay structure. This can be done by employing exponential smoothing, whereby the behavioral response is modeled as depending on an exponentially weighted history of past incidence data, thereby capturing a gradual “memory-

effect" in risk perception(LeJeune et al., 2025). Another method of modeling delays uses an information index which is defined as an integral over past states (such as past infection levels) weighted by a memory kernel which acts to delay the effect of changes in the epidemic by representing how past information (or perceptions) is retained and gradually fades over time (Buonomo et al., 2025). Finally, few models allow for asymmetric delays, meaning that the time lag for adopting protective behaviors when infection levels rise is different from the delay in reverting to normal behavior as incidence falls, a structure that reflects the notion that people may react more quickly to increasing risk than they relax their caution once the risk has subsided (Rahmandad, 2022; Rahmandad & Sterman, 2022). This classification underscores how the specific formulation of behavioral delays can profoundly influence model predictions, including the timing and amplitude of epidemic peaks and the overall epidemic trajectory.

Nevertheless, modeling delays is not limited to infectious disease models but also present in many general behavioral modeling approaches. Similarly, some studies have not considered delays in their modeling of human behavior. For instance, several evacuation models used in building safety research omit the time it takes occupants to process cues and begin evacuating effectively "ignoring" behavioral delay (Kuligowski, 2008). Other studies incorporate delays in a very simple, fixed-lag manner. In many models of motor control or reaction time, such as in intermittent control tasks, the delay between stimulus and response is assumed to be constant. For example, Suzuki et al. (2018) modeled human response delay in a virtual stick-balancing task by using a fixed delay term in a delay-differential equation framework (Suzuki et al., 2018). This fixed-delay approach can capture some average response properties, though it may miss the inherent variability in human reaction times. A different modeling strategy uses methods from time-series forecasting, such as exponential smoothing to capture delay effects in human behavior (Okada et al., 2020). Finally, some researchers have proposed that delays in human decision processes are not symmetric meaning that the "cost" or subjective effect of a delay may depend on whether a reward is sped up versus delayed. For instance, recent work on temporal discounting has noted a delay–speedup asymmetry: people may prefer an immediate, smaller gain when a delay is framed as "added value" yet choose a larger, later reward when both options are postponed (Ruggeri et al., 2022). Together, these examples illustrate that researchers have taken quite different approaches when incorporating delays into models of human behavior: from ignoring delays entirely to representing them with fixed lags, smoothing functions, or even asymmetric structures. These distinctions are important when considering the trade-offs between model simplicity and behavioral realism

In dynamic modeling literature such perception delays are typically modeled as first or third order exponential delay functions (Forrester, 1961; Sterman, 2000). Other delay orders in traditional modeling (which yield Erlang distributions of different shapes in continuous-time models or Pascal distributions for discrete-time models) may be used and are occasionally applied in building of models (Li et al., 2022) Delay length and order are often assumed based on qualitative knowledge of the problem at hand, though empirical estimation for delay structure is

also occasionally pursued, often limited to the average length of the delay as an estimated parameter (e.g., see (Rahmandad et al., 2022)). These common practices thus assume a distribution and at best use empirical data to estimate delay lengths rather than identifying that distribution. Moreover, the assumed distribution is most commonly symmetrical, that is, the perceptions of increases and decreases in the phenomenon of interest happen with the same adjustment rate (i.e., delay length) (Espinoza et al., 2024; Zhang et al., 2023).

This assumption may be problematic. For example, extensive research in behavioral psychology shows that individuals have varying levels of sensitivity to desired versus undesired news. For example, in assessing the effect of wealth on happiness, individuals tend to experience a greater loss in happiness from a reduction in wealth compared to the happiness gained from an equivalent increase in wealth (Kahneman & Tversky, 1979). Such an asymmetry in response to positive and negative stimuli underscores the complex nature of human judgment processes.

To build intuition on the impact of delay structure, consider the illustrative example shown in Figure 3.1. Imagine a new disease that causes 1 death per day over a 4-day period and then ceases to cause mortality (Figure 3.1, graph 1, the dashed blue line). Now, consider asking people about their level of concern regarding this disease over those days and beyond. What would be the population's perceived levels of risk? The graph illustrates the imaginary trajectories of perceived risk for an average delay period of five days but under various assumptions about the order of the delay and the existence of asymmetry in the increase versus decrease in risks. With a fixed delay structure, the output is simply the input shifted by five days (graph 2, red line). This shows the assumption used in simple regressions. With a third order exponential delay structure, the impact on people’s risk perception starts earlier and finishes later than the fixed delay (graph 3, green line). Considering asymmetric delays requires a decision on the length of delay for up/down-ward adjustments. For example, with an asymmetric delay structure with the delay periods of 2.5 days when risk increases and 7.5 days when risk declines, we observe a more pronounced risk perception as if the impact of risk has been higher on individuals (graph 4, grey line).

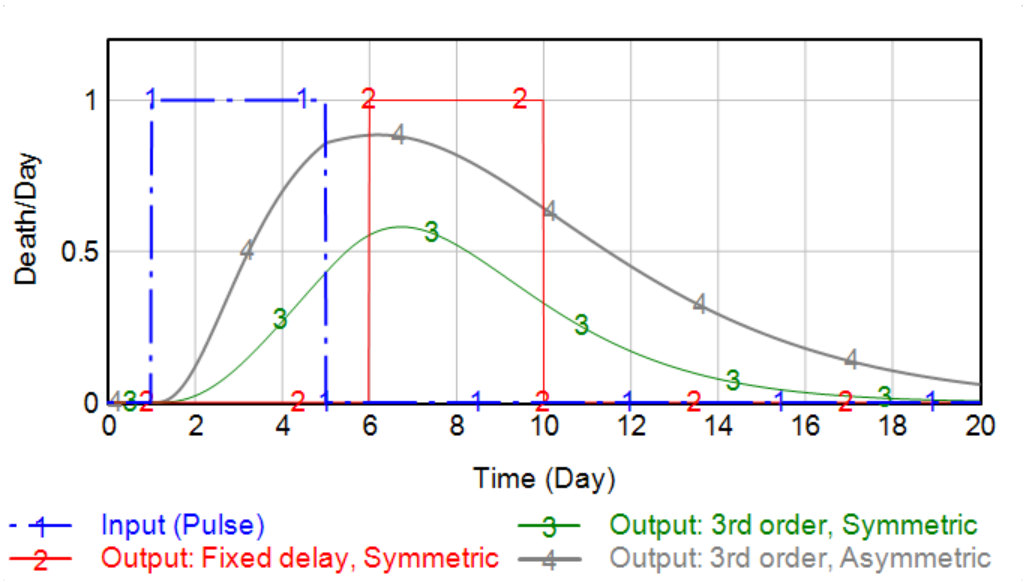

Figure 3.1: An illustration of the impact of delay asymmetries on formulating human risk perception. Note: Input is daily death formulated as a pulse function, starting from day one, for 4 days (blue line). The first output in red is a fixed delay structure, and the second and third outputs, in green and grey, are 3rd order delay structures with symmetric and asymmetric delay periods, respectively. The delay period for symmetric cases (including fixed delay) is 5 days, and for the asymmetric case the delay periods are 2.5 days and 7.5 days depending on the direction of change in input.

Despite the potential implications of improperly identifying delay structures, there has been limited research comparing various assumptions about these structures. This study addresses this gap by investigating the extent to which misidentification of delay structures can mislead examinations of causal relationships between environmental factors and human responses. Particularly resonating with classic modeling papers (Hamilton, 1980) advocating for operational thinking (Richmond, 1994), this study emphasizes representing causal relations through their mechanistic causal paths rather than mere correlational relationships.

We specifically focus on the problem of estimation of behavioral responses during pandemics as a case study. The primary reason for selecting this context is the existence of several critical feedback mechanisms indicated in various modeling papers (Rahmandad et al., 2021; Rahmandad & Sterman, 2022). For example, perception of risk impacts behaviors (e.g., masking, vaccination, mobility, social interactions) and policies (e.g., school closures, vaccine mandates) which then regulate disease transmission and future risk evolution. Estimating such human reactions lies at the core of improving long-term pandemic forecasting (Rahmandad et al., 2022a). Crucial to formulating these human reactions is an accurate representation of public risk perception, which influences compliance with non-pharmaceutical interventions (Osi & Ghaffarzadegan, 2024). We hypothesize that: 1) proper identification of the delay structure is crucial in investigating the effect of changes in pandemic risks on public response, and 2) in the

real world, changes in public risk perception have been observed to lag with asymmetric delays compared to changes in pandemic risks, challenging the validity of conclusions that do not account for this asymmetry.

3.4. Study 1: Significance of proper delay structure identification

3.4.1. Method

In the first study, we perform synthetic-data experiments using a parametrized delay structure model to generate (synthetic) data. The model's presumed parameter values, i.e., delay period, delay order, and effect size, serve as the ground truth to be recovered in the next step. Then we use this synthetic data to recover the effect size (and, where relevant, the delay period and order) and assess the impact of different assumptions on recovering the effect size accurately.

Specifically, we use the following approaches for generating synthetic data. To represent delay in a continuous format, we adopt an exponential delay kernel structure, as described below. The input represents "risk indicator" (e.g., daily case rate during a pandemic) and the output represents the "perception of risk" (e.g., perceived case rate corresponding to perceived risks). The perception variable is formulated using the exponential smoothing structure of an exponential delay kernel, incorporating a (potentially) asymmetric delay structure. This perception value is then scaled by a constant K that represents the "effect size" (e.g., change in public social distancing due to change in perceived risk) of the input on the output. To account for measurement error, we add normally-distributed i.i.d. noise to the output.

Equation 1.1 to 1.3 show the formulations, where X_i is the input (risk indicator) at time i, S_i is lagged input (the perceived case rate, i.e., perceived risk), and $\boldsymbol{E}$ is the final output (effect). Only $\boldsymbol{X}$ and $\boldsymbol{E}$ are observable. In our experiment the input is created by using a sinusoidal function with multiplicative auto-correlated noise added to resemble noisy oscillatory patterns in various real-world phenomena:

$$X_i = sin(\alpha \cdot i).N \qquad (1.1)$$

where N is input noise which is an auto-correlated Gaussian noise function with mean of 1 and standard deviation of 0.25 and correlation period of 5 days; α is a constant multiplier set to 0.1. As X is observable, the parameters generating X are not of primary concern here and only play a role in producing X values that qualitatively resemble real world data-generating processes.

The delay structure follows these equations where O is the delay order, and $S_{i,j}$ represents the delayed output for order j at time i. $S_{i,O}$ is also called the n-th order exponential smoothing function.

$$\frac{dS_{i,j}}{dt} = \begin{cases} \frac{(X_i - S_{i,j})}{(L/O)} & for\ j = 1 \\ \frac{S_{i,j-1} - S_{i,j}}{(L/O)} & for\ j \in (2, \dots, n) \end{cases}$$

$$\mathrm{L} = \begin{cases} L_1 & X_i \geq S_{i,O} \\ L_2 & X_i < S_{i,O} \end{cases} \qquad (1.2)$$

L_1 and L_2 are delay periods depending on the direction of change in the input (L_1 for updating perception when risk is increasing and L_2 for decreasing trends) we call L_1 upward delay and L_2 downward delay. O is the delay order, an integer. The final output is scaled by a factor of K representing the effect size which is the coefficient of interest to be recovered:

$$E_i = KS_{i,O} + \varepsilon \qquad (1.3)$$

where ε is a normally distributed noise in output with mean 0 and standard deviation of 0.25. The model is used to create 100 sets of synthetic data. Specifically, we randomly select 100 pairs of the four parameters in these intervals: L_1 (1,45), L_2 (1,90), O (1,5; integer values), and K (-5,5). For each set, we simulate the model to generate data series for 100 time periods of the output E.

Next, we implement a simple regression model of $E_t = \beta \hat{X}_t + \varepsilon$ to recover the effect size, where β is our estimation of the effect size, *K*, and $\hat{X}_t$ is a transformation of X_t to account for delay. We assess the performance of four different transformation methods with different assumptions about delay structure:

- Ignoring delay: Assuming immediate effect, that is $\hat{X}_t = X_t$;
- Fixed delay structure: A constant shift of L period in all input data, that is $\hat{X}_t = X_{t-L}$; with L estimated in the process.
- Symmetric exponential delay: consistent with equation 1.2, but assuming $L_1 = L_2 = L$; estimating O and L.
- Asymmetric exponential delay: consistent with equation 1.2, with possibly different values for L_1 and L_2; also estimating L_1, L_2, and O.

The general idea of this experiment is to test whether, in comparison to the correctly specified model of the delay structure (fourth approach), a simplified (first and second approaches) or a symmetrically specified delay structure (third approach) would still be able to a) fit the outcome to the data well and b) accurately recover effect size (K).

Note that besides K, in approaches 2-4 we also estimate the delay period(s), and in approaches 3-4 delay order is also estimated. While the regression in equation 1.3 is conducted using a simpler linear regression framework, for the other parameters we conduct a grid search looking for values that minimize the sum of squared errors for the final estimates of E. For example, in the fourth approach, we explore the solution space for ${L_1}^*, {L_2}^*, o^*$ such that

$$ {L_1}^*, {L_2}^*, o^* := \arg\min_{L_1, L_2, o>0} \frac{1}{n} \sum_{i=1}^{n} \left(E_i - \beta \hat{X}_{L1,L2,o}\right)^2 $$

In each of the four approaches, we report our best estimates of the effect size. The best estimation for approaches 2-4 is the coefficient of the regression model (β) with the optimal values of delay period(s) and order.

3.4.2. Results

First, for the purpose of demonstration, we report results from a single test based on one simulation run. In this test, the ground truth values in synthetic data generation are set to L_1=10, L_2=30, O=3, and K=1. Figure 4.2a depicts input (X, green) and output data (E, black). We follow the described process in the method section and estimate the effect size K using four different approaches, in addition to delay and order where relevant. Figure 4.2b shows the estimated E values for the four different transformation models in comparison to the synthetic data.

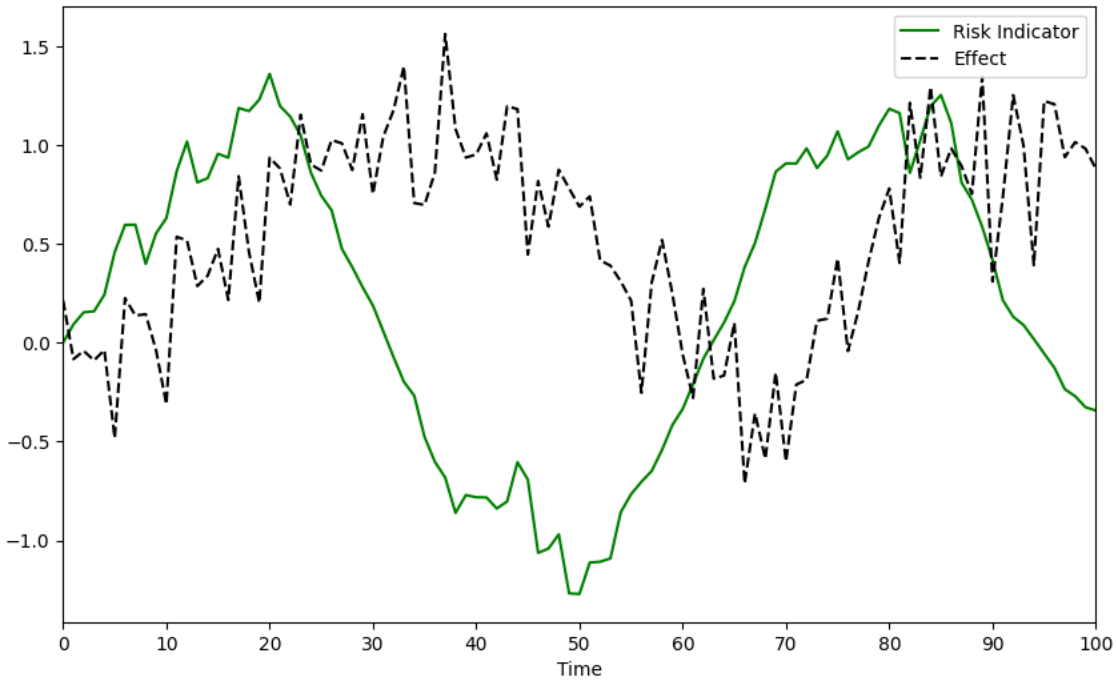

Figure 3.2a: Visualization of the two variables (Risk Indicator and Effect) used in the first simulation case

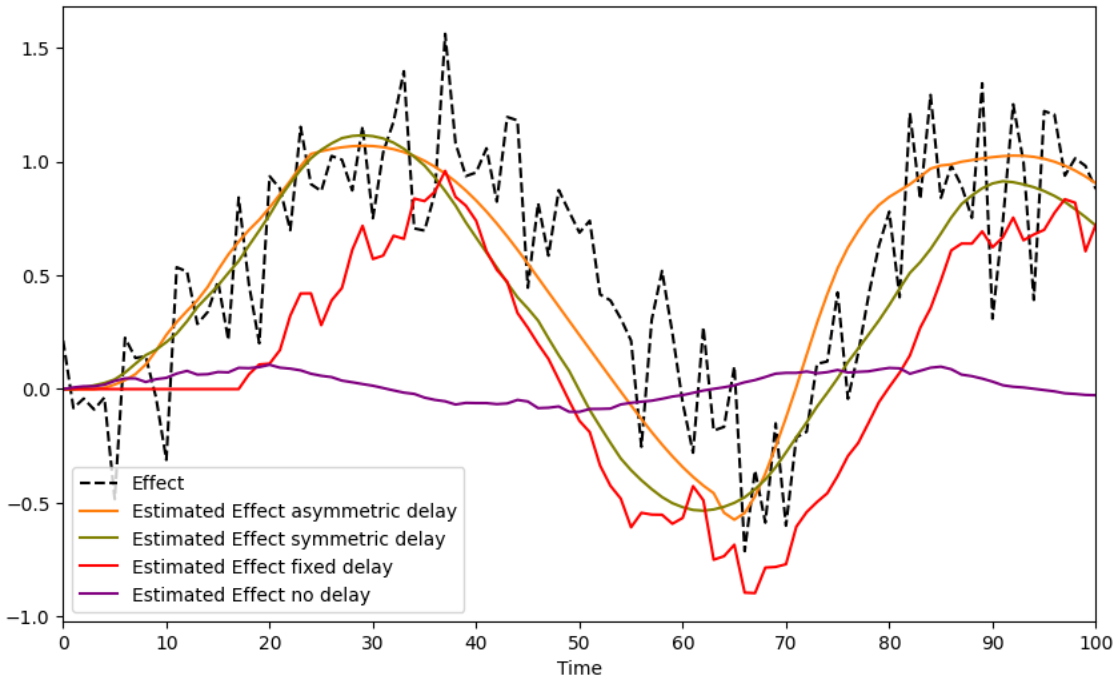

Figure 3.2b: Actual vs. fitted effect values across four delay structures included in the estimation framework

The estimated parameter values along with the measures of fitness are presented in Table 4.1.

Table 3.1: Comparison of different measures across four delay structures in the illustrative example

	L_1	L_2	L	O	K	MSE	MAE	R^2	BIC
Ground truth	**10**	**30**	**-**	**3**	**1**	-	-	-	-
Estimation with no delay	-	-	-	-	(-0.11, 0.27)	0.54	0.62	0.01	228.83
Estimation with fixed delay	-	-	17	∞	(0.56, 0.85)	0.28	0.46	0.49	162.42
Estimation with symmetric delay	-	-	49	1	(2.94, 3.74)	0.15	0.30	0.73	97.46
Estimation with asymmetric delay	10	31	-	4	(0.90, 1.03)	0.06	0.19	0.89	3.07

Note: L_1 and L_2 are delay lengths for increasing and decreasing trends respectively, and L is applicable to delay structures with a single delay period; O is the delay order; K is the effect size.

The results show that with the asymmetric delay structure the ground truth value is correctly identifiable ($0.90 \leq K \leq 1.03$). All other delay structures misidentify K, offering estimates that do not include true K(=1) in their confidence intervals. This is notable as misidentification of the delay structure not only results in an incorrect estimation of the delay period but also affects the estimation of the impact of the environment on people's behavior. Moreover, despite biased estimations for average delay period, delay order, and effect size, the symmetric delay condition still yields a reasonably high R^2, comparable to the asymmetric structure. This observation suggests that relying solely on R^2 in this scenario can be misleading.

The described case was a single experiment to demonstrate the approach. As described in the method section, to illustrate the differences more systematically when including different delay structures, 100 synthetic datasets are generated with different delay structures and effect sizes. The average absolute error in recovering the parameters in each method along with average fitting measurements are reported in Table 4.2. The results in Table 4.2 demonstrate that the error in K estimation substantially decreases with an asymmetric delay structure in the inverse problem. The estimated delay period and order are also much closer to the ground truth than in other cases. All fitness measures including BIC (that considers the number *of* parameters in assessing fit) improve with asymmetric delay structure.

Table 3.2: Average absolute error in delay and effect size and average fit measures over 100 simulation runs in four different delay structures included in the estimation framework.

	Average Absolute Error					**Average Model Fit**			
	L_1	L_2	**L**	**O**	**K**	**MSE**	**MAE**	**R^2**	**BIC**
Estimation with no delay	-	-	-	-	2.32	2.09	1.02	0.07	272.32
Estimation with fixed delay	-	-	20.32	-	1.23	1.15	0.71	0.43	208.5
Estimation with symmetric delay	-	-	40.92	1.26	10.16	0.43	0.42	0.7	122.99
Estimation with asymmetric delay	**4.81**	**5.4**	**-**	**0.96**	**0.32**	**0.1**	**0.23**	**0.79**	**37.1**

Note: L_1 and L_2 are delay lengths for increasing and decreasing trends respectively, and L is applicable to delay structures with a single delay period; The error size for the L estimation is reported based on the difference between the estimated symmetric delay period and the average of L_1 and L_2 in ground truth; O is delay order; K is the effect size.

Over the 100 simulations, the distribution of error in estimating delay structure (delay lengths and order) and effect size (K) are calculated. For the asymmetric method, two delays are considered, and the error represents the difference between the actual delay length values form the simulation runs and the best estimate values. In the methods using a single delay (fixed delay estimation and symmetric delay estimation) the error term is derived from the calculation of the difference between the average of the actual two delay lengths from the simulation runs and the best estimate for single delay. if we differentiate the simulation runs into two groups of K>0 and K<0, the biases in estimation methods become clear. This reveals that the earlier apparent unbiased estimation is due to the symmetric range selected for K and not because of the estimation method itself. Only the asymmetric delay structure inclusion consistently produces an unbiased estimation of K. In fact, the use of symmetric delay, despite otherwise a more flexible, and correct, delay structure, leads to more misleading K values (than the use of fixed delay or ignoring delays all together).

3.5. Study 2: Application to real-world data

3.5.1. Method

In the second study, we apply the methods discussed in study one to empirical data on COVID-19 in the US. State-level COVID-19 data yield weekly case rates per million population (Centers for Disease Control and Prevention, 2023; U.S. Department of Commerce, 2022). We merge COVID-19 case rate data with weekly state-level mobility data (Google, 2024). This data measures the daily deviation from a baseline mobility rate defined as the median pre-pandemic mobility index value for a location on the corresponding day of the week. We then calculate the weekly average mobility index change for each state. In sum, the data span all 50 states and Washington, D.C. for the period February 20, 2020-October 12, 2022.

We start by considering the asymmetric delay structure transformation from the synthetic analysis (i.e., different delay periods depending on the direction of change in case data) to account for the delayed impact of case rate on mobility in the simple regression:

$$\ln\left(mobility_{i,t}\right) \sim k_i \hat{C}_{i,t} \qquad (1.4)$$

The conceptual parameters used in the synthetic case can be mapped into the empirical case. The dependent variable in the synthetic case, y, is $\ln\left(mobility_{i,t}\right)$ in the empirical case (corresponding to "effect" in the synthetic case), and $\hat{C}_{i,t}$, the independent variable, is lagged cases which conceptually represents perceived case rate. We use equation 1.2 to calculate $\hat{C}_{i,t}$ given $C_{i,t}$. The subscript i refers to the individual state, t refers to the week number. k_i is the effect size representing the change in (logarithm of) state-level mobility for one additional case per million population.

While this initial model is informative of the general structure, it is too simplistic as it lacks other critical features of real-world mobility responses to changing risks. For example, an important behavioral component missed here is adherence fatigue. Adherence fatigue refers to the decline over time of public response to risk over the course of the pandemic. A possible proxy for this term can be calculated based on cumulative cases which we use in our updated model shown below:

$$\ln\left(mobility_{i,t}\right) \sim \frac{k_i \hat{C}_{i,t}}{\left(\sum C_t\right)^{\alpha}} \qquad (1.5)$$

where $\sum C_t$ represents cumulative cases since the beginning of the pandemic, and the parameter α represents the non-linearity in the effect of cumulative cases. In this formulation, as the pandemic continues, and thus cumulative cases grow, the effect of an additional case per million on change in mobility declines. To avoid division by zero, we hard code the pre-pandemic mobility to 1.

As in the synthetic data case, we estimate delay periods and order, as well as α in an iterative optimization minimizing mean squares errors of log mobility. We allow delay lengths to vary between 1 and 200 weeks, and delay order to be an integer between 1 and 10. We report the model fit statistics and estimated k_i (with 95% CI). We also plot the delay lengths (L_1 and L_2) against each other to showcase the importance of asymmetric delay estimation.

This illustrates the differences in sensitivity to cases we measure the implied impact on an extra case (per million per week) on mobility under values of cumulative cases spanning 100, 1000, and 10000 in each scenario. These plots provide an intuitive measure of the importance of the behavioral response effect, k_i.

Finally, we offer a comparison between two methods of estimation: Method A is the asymmetric delay model with the inclusion of adherence fatigue discussed above. Method B uses the ARDL model, a workhorse of econometric tools to estimate the lagged effects of both the dependent variable (mobility) and independent variable (cases). It is important to note that in Method B we are estimating mobility directly whereas in Method A the estimation is done through log of mobility.

First, we determine the number of lagged variables to include in the model. After doing so, we divide our data into two periods of test and train to not only do estimation on training data but also do projection on the test data. This division is done such that the first 85 weeks (Feb 19, 2020, until Sep 29, 2021) are in the training data and the rest of the 54 weeks are in the testing data (Oct 6, 2021, until Oct 12, 2022). This division includes at least one wave of the epidemic in the testing data. ARDL model projections rely on lagged values of dependent variable, which should be very informative but are not available/used in method A. To keep the comparisons on equal footing we use the estimated (rather than actual) mobility values during the test period (but not in the training period) to create projections of the ARDL model. We then compare the

performance of these two methods in the test period, noting that we should expect the ARDL model to produce a much better fit during the training period. In short, this test offers a fair head-to-head comparison between two methods, A benefiting from the explicit consideration of asymmetric delays, but with more restrictive assumptions on structure of delays (order and adherence fatigue effects), compared to the more flexible ARDL method that includes more degrees of freedom but does not explicitly allow for asymmetric delays.

3.5.2. Results

Using the same procedures as in the synthetic experiment, and based on the regression model 1.5, we apply the asymmetric delay distribution estimation framework to real-world state-level data capturing weekly COVID-19 case rates per million people and mobility rates (normalized to baseline mobility). For each state, we assess the prediction for the delay parameters and the relationship k_i between perceived case rates and mobility.

Detailed results for each state are shown in Figure 4.3. We also plot the national level estimates. These come from the state-level mobility estimates, with population-weighted estimates across all states (orange) aggregated and plotted against US data (blue) (Figure 4.4). The fit does a good job of capturing the overall trend, specifically the three waves of the disease.

Figure 4.5 plots the estimated delays (when case rate is increasing vs. decreasing) recovered from the asymmetric delay estimation framework in logarithmic scale. If there was no meaningful difference in risk perception when increasing and decreasing cases we would expect both delays to be equal, forming the line $L_1 = L_2$. However, most states show $L_2 > L_1$. The model implies a significantly quicker reaction to increasing risk than decreasing ones, consistent with our theoretically motivated hypothesis.

In Figure 4.6 we plot estimated K values. A negative K value indicates that an increase in perceived risk based on cases is associated with a reduction in mobility, while a positive K value indicates the opposite. As expected, most states indicate a negative value with only MT and WY deviating, both lightly populated states with significant tourism which may change their endogenous dynamics. Also, we find significant variation across states in responsiveness to risk, perhaps reflecting important cultural, demographic, and policy differences (Lim et al., 2023).

To better illustrate sensitivity to cases, we plot three different scenarios in one plot, where each scenario has a stable cumulative case value, and for that specific value, we compare how the addition of cases changes mobility. K and α are kept constant here. as shown in Figure 4.7 there is an inverse relationship between cases and mobility, and in all three cases an increase in cases would lead to a lower mobility. however, we see that the sensitivity to one additional case is greater in scenario one, where there are a total of 100 cases in comparison to scenario three where there is a total of 10000. With more cases mobility decreases but the sensitivity declines as we move to higher cumulative cases.

Finally, we test the projection performance of the two approaches. Method A is the asymmetric delay with adherence fatigue; and Method B is the ARDL model. First, we determine the optimal number of lagged variables for mobility and cases in the ARDL model. By comparing the BIC values produced in models with a max of 8 lagged variable for both mobility and cases we reach the best BIC value for each state. Based on this setting we produce the model fits and projections for each method. Results are reported in table 4.3 and Figure 4.8. While using lagged dependent variables the ARDL model can produce almost perfect fit in the training period, its projection performance deteriorates rapidly (the training and test periods are separated by the dotted black line). On the other hand, the asymmetric delay model suffers less from overfitting and offers more accurate predictions during the testing period. Various measures of out-of-sample projections in table 4.3 support this general conclusion.

Figure 4.3. Actual vs. fitted mobility values across all US states and DC

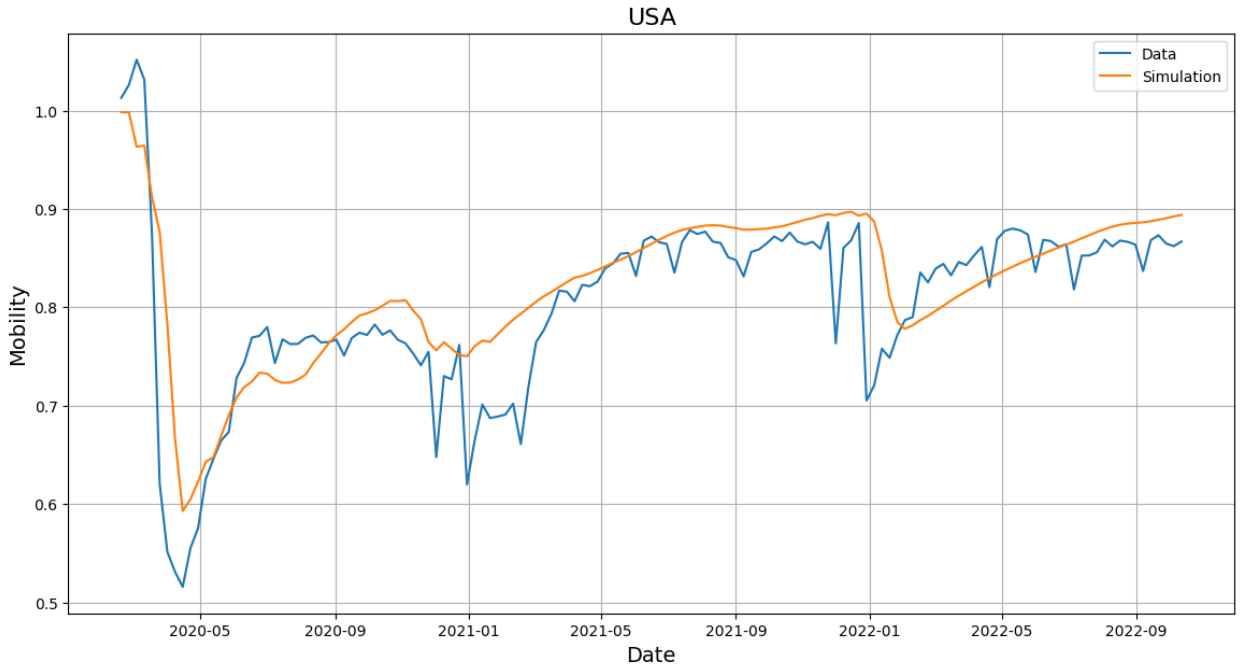

Figure 3.3: US mobility data compared to population-weighted estimations of aggregated state level data, R2=0.68

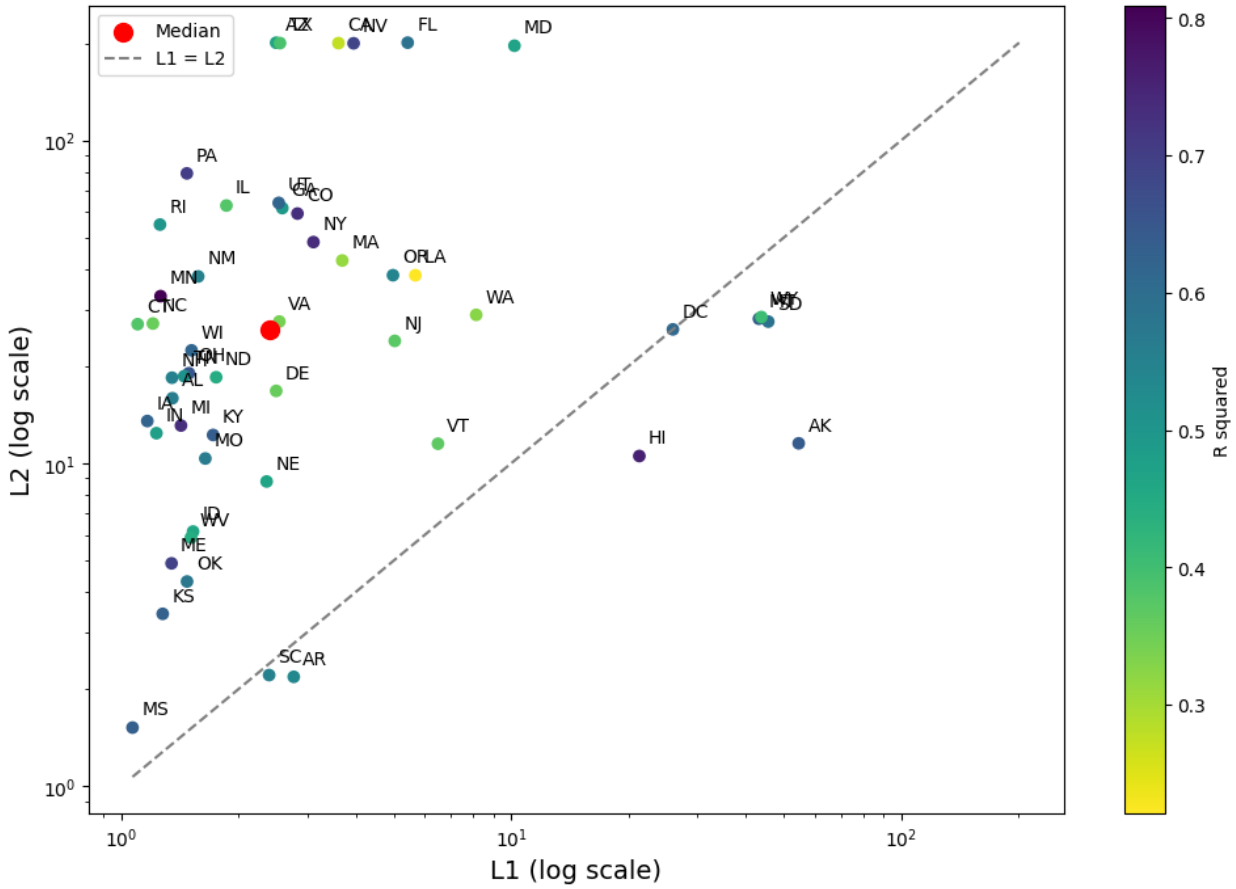

Figure 3.4: Estimated delay in weeks for perceiving increased case rate (Delay 1) vs. decreased case rate (Delay 2) for each state, color-coded by R2 value (increasing in value from light yellow to deep purple), and the median across all states (in red).

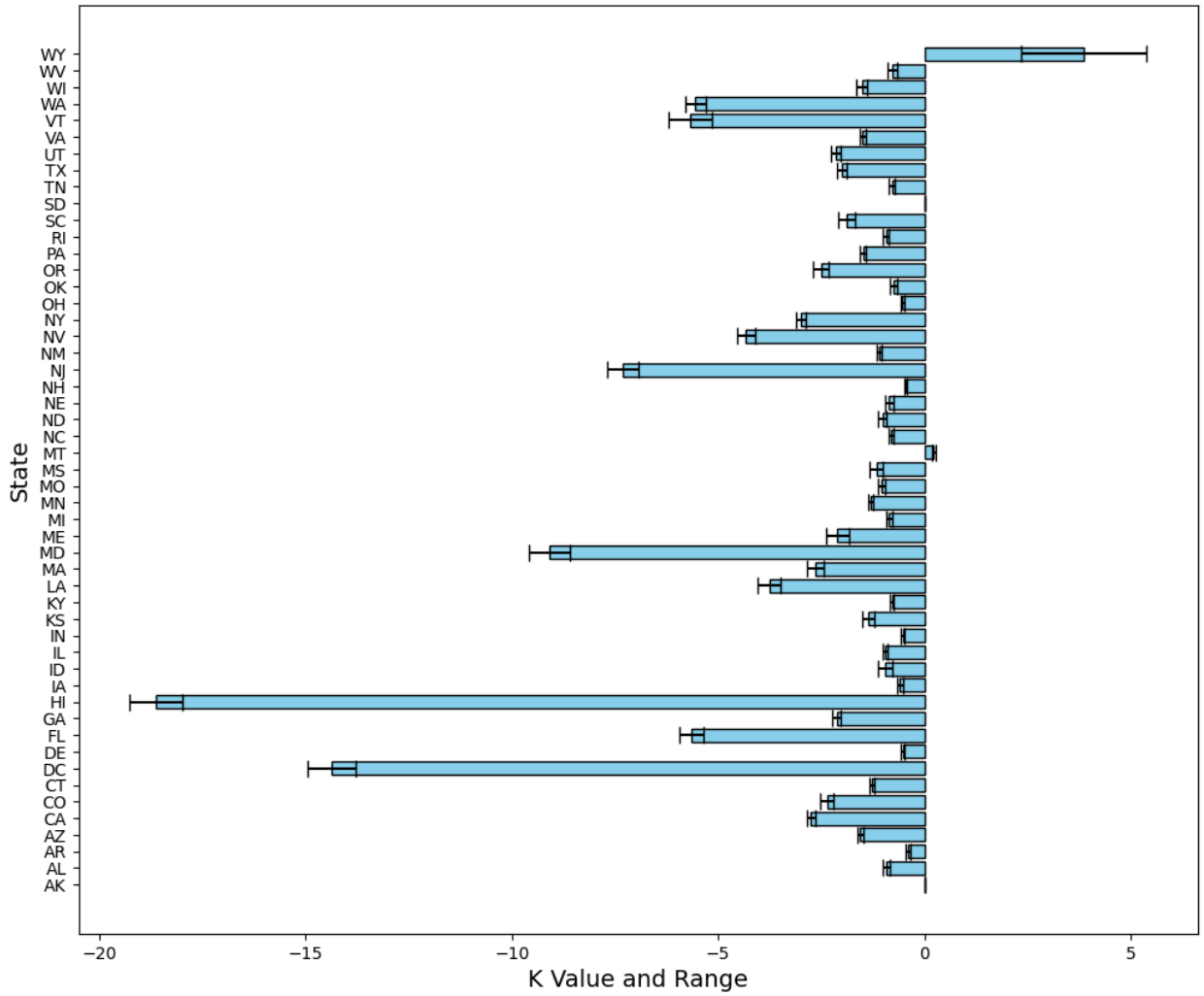

Figure 3.5: K values in an asymmetric delay estimation framework for each state, with 95% confidence intervals.

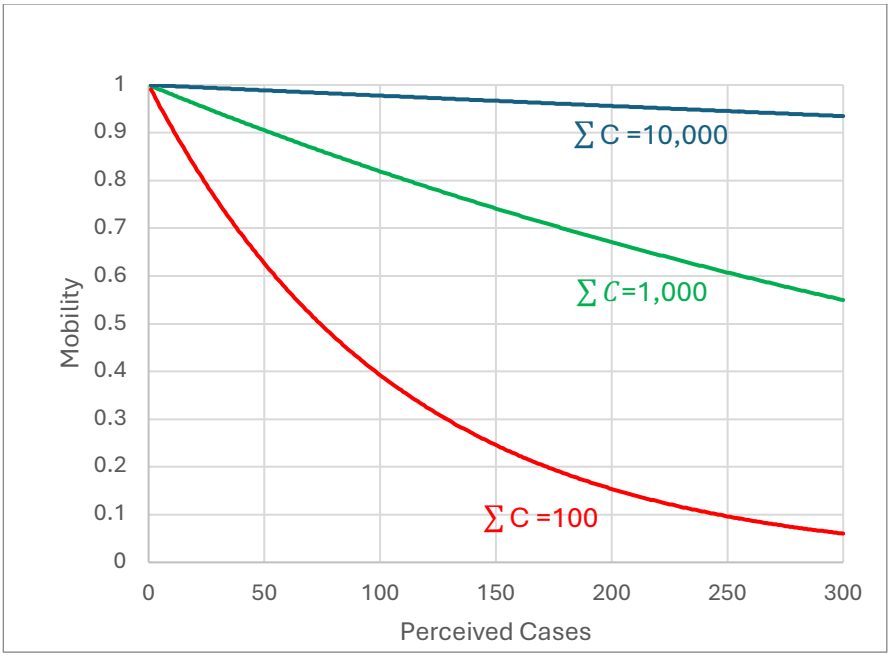

Figure 3.6: illustration of change in mobility for addition of cases in three levels of prior cumulative cases ()

	R^2	BIC	RMSE	MAE	MAPE
Method A median	0.14	**-269.5**	**0.08**	**0.07**	**7.33**
Method B median	**0.21**	-229.8	0.09	**0.07**	8.28
Method A mean	0.19	**-262.9**	**0.10**	**0.08**	**9.86**
Method B mean	**0.21**	-222	0.12	0.10	12.08

Table 3.3: Median and mean values of out of sample (test period) fit statistics across all states and DC comparing Method A (Asymmetric delay) and Method B (ARDL)

Figure 4.8. Method A: (Asymmetric delay) vs. Method B: (ARDL) fitted and projected values

3.6. Discussion

In this paper we assessed the impact of different assumptions for estimating perception delay structures from empirical data. Common to many social phenomena, those delays moderate how causes lead to effects, e.g., when people should assimilate information and change behaviors and policies in response to those perceptions. Using synthetic data experiments and empirical state-

level data from changes in mobility in response to COVID-19 in the US, we show the assumptions on delay structures matter and may lead to qualitatively different findings. Specifically, mis-specifying the length, shape (i.e., order), and symmetry of delay can lead to significantly biased parameter estimates that incorrectly identify the theoretical and practical parameters of interest, such as how responsive people are to risks of disease.

At one level, this realization is trivial. Every statistician will tell you that mis-specifying a model will lead to unreliable parameter estimates. Yet, it is also broadly recognized that "all models are wrong"(Box, 1976; Sterman, 2000). The resolution is not to give up on building and estimating models, but to identify the assumptions that matter versus the simplifications that are harmless. Our exploration shows that assuming a fixed-delay (common in statistical models of social processes) or even the practice of using a first or third order symmetric delay (common in dynamic modeling literature) is not innocuous and could lead to significant errors. Thus, a more nuanced empirical treatment of delay structures is called for when perception and action adjustments induce delays between causes and effects.

Our analysis provides one way forward that combines the strengths of standard statistical estimation with a formal acknowledgement of the possibility of more complex delay structures. Specifically, we separate two steps of creating the independent variables (perception as a delayed function of reality), and estimation of the theoretical relationship of interest (impact of perception on the estimated effect). Our method calls for a procedure (typically simulations of a simple delay model) that calculates the perception as a function of some inputs (i.e., delay length and order), before feeding that into a standard regression procedure needed to estimate the impact of perception on the estimated effect. The two steps are linked in a loop, where perception is created using different delay structures, and the quality of fit from the regression allows us to select the best fitting delay structure using an optimization process. By separating these two steps we can explore complex delay structures while benefiting from standard regression packages that may not accommodate those delays natively but otherwise offer standard and scalable estimation. Here we only explored standard Erlang lag distributions (corresponding to Smooth/Delay functions of different orders in dynamic modeling literature) but the method can easily be applied to any lag structure one can hypothesize and model explicitly.

Of course, this method is not the only viable option, and others are available and potentially promising. On the one hand, there are statistical methods developed by econometricians for estimating more complex delay structures as part of regression workflows. From (vector) autoregressive models (Sims, 1980) to distributed lags (Almon, 1965) and various panel data models with lagged variables, these methods provide opportunities for estimating very flexible lag structures, and many are assisted in predictive power by inclusion of lagged dependent variables. Two limitations may be noted for this category of methods. First, flexibility may come at the cost of interpretability. Resulting lagged models do not offer the clarity of delay length and shape parameters, and indeed including lagged dependent variables further complicates a clear

cause-effect interpretation. Second, despite their flexibility, incorporation of asymmetric delays in these frameworks is sometimes infeasible or, when feasible, becomes complicated very quickly. Absent accounting for those asymmetries, we find sophisticated ARDL method may perform worse than the significantly simpler asymmetric delay structure we proposed. Though we note that this finding depends on limiting both methods from direct access to lagged dependent variable during the projection period.

A different path may follow nonlinear estimation of the combined model that includes both the estimation of the delay structure and that of the perception to estimated effect relationship. Bringing the two steps together allows for assessing the joint (posterior) distribution of delay structure and the core cause-effect relationship in question, offering confidence bounds on delay order and length for example. It may also prove computationally more efficient when the resulting optimization for estimation is not too complex. However, it would require additional coding and figuring out the appropriate estimation method for the more complex joint model. Future research can compare these broader alternatives for specific categories of problems, though conceptual similarity with our approach suggests the gains would be more computational than qualitative.

In the conceptual space, our paper shows that on average, allowing for delay length and order to vary and allowing for asymmetric delays improves model fit, in some cases, drastically. However, there are some settings in which the fit is not improved by adding this more realistic structure in an albeit simple regression framework. Whether that is a characteristic of the data or of the regression framework, though, is unclear and warrants further exploration. The results of this analysis suggest that states whose models yielded delay asymmetry in the form of longer times to act on case rates decreasing and shorter times to react to case rates increasing are better fit to the data. This provides important evidence that people were faster to change in the face of heightened danger than they were to let their guards down and increased their mobility when that danger lessened.

Overall, we hope this paper provides a bridge between the appreciation for importance of perception delays in the dynamic modeling community, and the empirical issues related to estimating those delays reliably. Better integration of empirical data with SD models can promise more effective and convincing research and policy.

3.7. Acknowledgement

We thank Ran Xu and Gaofei Zhang for their constructive feedback. This research is funded by the US National Science Foundation, Division of Mathematical Sciences and Division of Social and Economic Sciences (Award No. 2229819).

3.8. References

Abouk, R., & Heydari, B. (2021). The immediate effect of COVID-19 policies on social-distancing behavior in the United States. *Public health reports*, *136*(2), 245-252.

Almon, S. (1965). The distributed lag between capital appropriations and expenditures. *Econometrica: journal of the Econometric Society*, 178-196.

Box, G. E. (1976). Science and statistics. *Journal of the American Statistical Association*, *71*(356), 791-799.

Buonomo, B., Messina, E., Panico, C., & Vecchio, A. (2025). An integral renewal equation approach to behavioural epidemic models with information index. *Journal of Mathematical Biology*, *90*(1), 8.

Centers for Disease Control and Prevention, C.-R. (2023). Weekly United States COVID-19 Cases and Deaths by State.

De Boef, S., & Keele, L. (2008). Taking time seriously. *American journal of political science*, *52*(1), 184-200.

Espinoza, B., Saad-Roy, C. M., Grenfell, B. T., Levin, S. A., & Marathe, M. (2024). Adaptive human behaviour modulates the impact of immune life history and vaccination on long-term epidemic dynamics. *Proceedings B*, *291*(2033), 20241772.

Fenichel, E. P., Castillo-Chavez, C., Ceddia, M. G., Chowell, G., Parra, P. A. G., Hickling, G. J., Holloway, G., Horan, R., Morin, B., Perrings, C., Springborn, M., Velazquez, L., & Villalobos, C. (2011). Adaptive human behavior in epidemiological models. *Proceedings of the National Academy of Sciences*, *108*(15), 6306-6311. https://doi.org/10.1073/pnas.1011250108

Feola, G. (2015). Societal transformation in response to global environmental change: A review of emerging concepts. *Ambio*, *44*(5), 376-390.

Forrester, J. W. (1961). Industrial dynamics mit press cambridge. *MA.[Google Scholar]*.

Funk, S., Salathé, M., & Jansen, V. A. A. (2010). Modelling the influence of human behaviour on the spread of infectious diseases: a review. *Journal of The Royal Society Interface*, *7*(50), 1247-1256. https://doi.org/10.1098/rsif.2010.0142

Google. (2024). Google COVID-19 Community Mobility Reports. https://www.google.com/covid19/mobility/

Griliches, Z. (1967). Distributed lags: A survey. *Econometrica: journal of the Econometric Society*, 16-49.

Hamilton, J. D. (1994). Time Series Analysis. In: Princeton University Press.

Hamilton, M. S. (1980). Estimating lengths and orders of delays in system dynamics models. *Elements of the system dynamics method*, 162-182.

Jiao, J., Bhat, M., & Azimian, A. (2021). Measuring travel behavior in Houston, Texas with mobility data during the 2020 COVID-19 outbreak. *Transportation Letters*, *13*(5-6), 461-472.

Kahneman, D., & Tversky, A. (1979). Prospect Theory: An Analysis of Decision under Risk. *Econometrica*, *47*(2), 263. https://doi.org/10.2307/1914185

Kripfganz, S., & Schneider, D. C. (2020). Response surface regressions for critical value bounds and approximate p-values in equilibrium correction models 1. *Oxford Bulletin of Economics and Statistics*, *82*(6), 1456-1481.

Kuligowski, E. D. (2008). Modeling human behavior during building fires.
LeJeune, L., Ghaffarzadegan, N., Childs, L. M., & Saucedo, O. (2025). Formulating human risk response in epidemic models: exogenous vs endogenous approaches. *European Journal of Operational Research*.
Li, W., Wang, Q., Liu, Y., Small, M. L., & Gao, J. (2022). A spatiotemporal decay model of human mobility when facing large-scale crises. *Proceedings of the National Academy of Sciences*, *119*(33), e2203042119.
Lim, T. Y., Xu, R., Ruktanonchai, N., Saucedo, O., Childs, L. M., Jalali, M. S., Rahmandad, H., & Ghaffarzadegan, N. (2023). Why Similar Policies Resulted In Different COVID-19 Outcomes: How Responsiveness And Culture Influenced Mortality Rates: Study examines why similar policies resulted in different COVID-19 outcomes in using data from more than 100 countries. *Health Affairs*, *42*(12), 1637-1646.
Narayan, P. K. (2005). The saving and investment nexus for China: evidence from cointegration tests. *Applied economics*, *37*(17), 1979-1990.
Okada, M., Yamanishi, K., & Masuda, N. (2020). Long-tailed distributions of inter-event times as mixtures of exponential distributions. *Royal Society open science*, *7*(2), 191643.
Osi, A., & Ghaffarzadegan, N. (2024). Parameter estimation in behavioral epidemic models with endogenous societal risk-response. *PLoS Computational Biology. In-press*.
Pesaran, M. H., Shin, Y., & Smith, R. J. (2001). Bounds testing approaches to the analysis of level relationships. *Journal of applied econometrics*, *16*(3), 289-326.
Rahmandad, H. (2022). Behavioral responses to risk promote vaccinating high-contact individuals first. *System Dynamics Review*, *38*(3), 246-263.
Rahmandad, H., Lim, T. Y., & Sterman, J. (2021). Behavioral dynamics of COVID-19: estimating underreporting, multiple waves, and adherence fatigue across 92 nations. *System Dynamics Review*, *37*(1), 5-31.
Rahmandad, H., & Sterman, J. (2022). Quantifying the COVID-19 endgame: Is a new normal within reach? *System Dynamics Review*, *38*(4), 329-353.
Rahmandad, H., Xu, R., & Ghaffarzadegan, N. (2022a). Enhancing long-term forecasting: Learning from COVID-19 models. *PLoS Comput Biol*, *18*(5), e1010100. https://doi.org/10.1371/journal.pcbi.1010100
Rahmandad, H., Xu, R., & Ghaffarzadegan, N. (2022b). A missing behavioural feedback in COVID-19 models is the key to several puzzles. *BMJ Glob Health*, *7*(10). https://doi.org/10.1136/bmjgh-2022-010463
Reluga, T. C. (2010). Game theory of social distancing in response to an epidemic. *PLOS Computational Biology*, *6*(5), e1000793.
Richmond, B. (1994). System dynamics/systems thinking: Let's just get on with it. *System Dynamics Review*, *10*(2-3), 135-157.
Ruggeri, K., Panin, A., Vdovic, M., Većkalov, B., Abdul-Salaam, N., Achterberg, J., Akil, C., Amatya, J., Amatya, K., & Andersen, T. L. (2022). The globalizability of temporal discounting. *Nature Human Behaviour*, *6*(10), 1386-1397.
Schecter, S. (2021). Geometric singular perturbation theory analysis of an epidemic model with spontaneous human behavioral change. *Journal of Mathematical Biology*, *82*(6), 54.

Shin, Y., Yu, B., & Greenwood-Nimmo, M. (2014). Modelling asymmetric cointegration and dynamic multipliers in a nonlinear ARDL framework. *Festschrift in honor of Peter Schmidt: Econometric methods and applications*, 281-314.

Sims, C. A. (1980). Macroeconomics and reality. *Econometrica: journal of the Econometric Society*, 1-48.

Slovic, P. (1987). Perception of risk. *Science*, *236*(4799), 280-285.

Sterman, J. D. (2000). Business Dynamics: Systems thinking and modeling for a complex world. *MacGraw-Hill Company*.

Suzuki, T., Lubashevsky, I., & Zgonnikov, A. (2018). Complexity of human response delay in intermittent control: The case of virtual stick balancing. *arXiv preprint arXiv:1808.05002*.

U.S. Department of Commerce, B. o. t. C. (2022). Population Estimates Program 2022 and 2020 Decennial Census. https://www.ers.usda.gov/data-products/county-level-data-sets/county-level-data-sets-download-data/

Wibral, M., Pampu, N., Priesemann, V., Siebenhühner, F., Seiwert, H., Lindner, M., Lizier, J. T., & Vicente, R. (2013). Measuring information-transfer delays. *Plos One*, *8*(2), e55809.

Xu, W.-J., Zhong, C.-Y., Ye, H.-F., Chen, R.-D., Qiu, T., Ren, F., & Zhong, L.-X. (2020). Coupled effects of epidemic information and risk awareness on contagion. *arXiv preprint arXiv:2009.05327*.

Zhang, X., Scarabel, F., Murty, K., & Wu, J. (2023). Renewal equations for delayed population behaviour adaptation coupled with disease transmission dynamics: A mechanism for multiple waves of emerging infections. *Mathematical biosciences*, *365*, 109068.

4. Essay 3: Optimal Vaccination Policies in the Presence of Behavioral Response

4.1. Abstract

Among the most critical health policy decisions are those pertaining to vaccine distribution during epidemics, specifically, decisions concerning prioritization and the pace of distribution. A common question is which group of receivers should be prioritized when vaccines are limited. The question has been widely explored using compartmental models. In their conventional form, such models assume human behavior is constant in the course of a pandemic. Yet we know that human contact rate is affected by their risk perception which can be influenced by the state of the disease.

In this study, we employ a behavioral epidemic model to determine optimal vaccination strategies under conditions that account for behavioral responses. Our focus is on a feedback loop that represents how a rise in number of infectious cases and mortalities affected societal risk perception, decreasing their contact rate, slowing down infection. The central hypothesis of this study is that including such behavioral feedback will change policy suggestions in contrast to models that ignore this feedback loop. To that end, we will compare and contrast two models that include or ignore this mechanism in terms of their suggested optimal vaccination policy.

This research includes two major steps. First in a simple aggerate model we examine how varying levels of a) vaccination coverage and b) vaccination speed affect the spread of the disease in two models that exclude or include the behavioral mechanism. Second, in age-stratified model, we explore whether incorporating behavioral responses alters the optimal vaccination policy and quantify the marginal benefits of optimal policies compared to less effective alternatives.

Our results show that accounting for behavioral feedback meaningfully changes both the estimated thresholds and the ranking of vaccination policies. In the homogeneous model, the behavioral SEIRbV structure requires higher coverage and capacity to suppress the epidemic than a conventional SEIRV model and reveals a stronger premium on starting vaccination earlier. In the age-stratified model, behavioral responses make vaccination speed more important than age-based prioritization: across a wide range of conditions, increasing rollout capacity saves more lives than switching between young-first and old-first allocation rules.

Keywords: Policy analysis, Epidemic modeling, Human behavior, Vaccination

4.2. Introduction

Policy decisions in public health and other domains have far-reaching consequences, from shaping individual behavior to influencing societal outcomes. When policymakers determine guidelines, whether about resource allocation (WHO, 2000), vaccine prioritization (National Academies of Sciences & Medicine, 2020), or risk mitigation (Ferguson et al., 2020), they can also shift perceived risk and, in turn, protective behavior, creating feedback loops between policy, behavior, and disease dynamics (Rahmandad et al., 2022b).

However, many policy-oriented frameworks and the models that inform them rely on simplified, population-average representations of behavior. For instance, many compartmental models assume static population responses or ignore the ways in which individuals adapt to policy changes over time (Funk et al., 2010). Other modelling perspectives such as agent-based approaches emphasize how heterogeneous individuals and their interactions (Bruch & Atwell, 2015) yet often assume agent-level preferences are fixed. These simplifying assumptions can potentially have implications on model-based policy recommendations. For example, interventions that appear optimal when behavior is treated as fixed or externally imposed may perform differently once behavioral responses are modeled as endogenous to perceived risk (LeJeune et al., 2025).

In the absence of a nuanced understanding of human behavior, policymakers risk underestimating or overestimating the impact of interventions (Rahmandad, 2022). By focusing solely on epidemiological parameters, such as reproduction numbers, mortality rates, or hospital capacity, policy guidelines may miss the fact that human beings quickly adapt their behavior in response to perceived risks, mandates, and social norms (Osi & Ghaffarzadegan, 2024). When these behavioral adaptations are not incorporated, policies may struggle to sustain adherence to recommended preventive measures, given the strong link between risk-related beliefs and preventive behavior (Kamran et al., 2021).

Behavioral modeling captures the feedback loops between individual decision-making and the broader system (Z. Zhang et al., 2025). Individuals are not passive recipients of policy directives; they respond based on perceptions of risk, personal values, social pressures, and available incentives (Verelst et al., 2016). By explicitly representing risk-responsive behavior in epidemic models, either as time-varying (exogenous) changes or as an endogenous feedback tied to the evolving state of the outbreak, analysts can better reproduce observed epidemic patterns and improve the longer-horizon projections that inform policy design. (LeJeune et al., 2024). The importance of behavioral modeling lies in its ability to capture dynamic changes, like how people reduce contacts when they sense rising infection risks or how they might become more complacent once a vaccine is announced. These shifting behaviors feed back into disease transmission rates, creating feedback loops that can amplify or dampen an epidemic (Rahmandad et al., 2021).

Incorporating behavioral modeling into policy setting helps bridge the gap between theoretical models and real-world outcomes. When policymakers consult epidemiological models that accurately reflect human responses, they gain insights that are otherwise hidden in simpler models. Moreover, behavioral modeling can inform adaptive policy approaches (Fenichel et al., 2011). Instead of instituting rigid, one-size-fits-all guidelines, decision-makers can adjust policies in real time based on observed shifts in behavior. For instance, if contact-tracing data reveal that certain groups are increasingly mobile or if vaccine hesitancy remains high in particular communities, targeted measures can be enacted swiftly (Bavel et al., 2020). By aligning policy with real behavioral patterns, governments and organizations can increase the likelihood of achieving desired outcomes, such as higher vaccination uptake or sustained adherence to social distancing (van Heusden et al., 2023).

A clear illustration of the importance of behavioral feedback loops is found in vaccination strategies. Conventional policy approaches might prioritize vaccinating the elderly first, as they are more vulnerable to severe illness and have higher mortality rates (Levin et al., 2020). This approach makes intuitive sense and aligns with a purely epidemiological perspective centered on reducing deaths. However, when behavioral responses and infection dynamics are incorporated, a more nuanced picture can emerge: vaccinating high-contact individuals first may actually shorten the pandemic and reduce the overall burden of disease (Rahmandad, 2022).

High-contact individuals, such as essential workers or those with extensive social networks, are more likely to encounter and spread the virus. By immunizing them early, the number of interactions between susceptible and infected individuals decreases (Buckner et al., 2021). This indirect reduction in spread can also protect people at highest risk of severe outcomes, even if they are vaccinated later. As a result, under some conditions, prioritizing high-transmission groups can avert more deaths and bring infections down faster than an age-only strategy (Matrajt et al., 2021).

This paper asks how much optimal vaccine policy recommendations change once we stop treating human contact behavior as fixed and instead model it as a feedback response to perceived epidemic risk. Specifically, we compare a conventional SEIRV framework with constant contact rates to a behavioral SEIRbV framework in which perceived risk (proxied by recent mortality) endogenously reduces contacts with a perception delay, thereby altering transmission dynamics. We run two model-based experiments: Study 1 uses a homogeneous population to examine how optimal vaccination coverage and rollout speed shift when behavioral feedback is included, and Study 2 extends the analysis to an age-stratified population in which daily doses can be allocated between younger, high-contact individuals and older, high-risk individuals. Across both settings, we treat vaccination policy as a simulation-based optimization problem over coverage, speed, and (in Study 2) age allocation, and evaluate policies by their implications for epidemic burden (e.g., cumulative cases, peak prevalence, and deaths). Our central objective is to determine whether incorporating behavioral feedback materially changes (i) the coverage/capacity thresholds needed for epidemic control and (ii) the relative importance of who is vaccinated first versus how fast vaccination proceeds.

In this paper, we develop and compare a standard SEIRV model and a behavioral SEIRbV model with endogenous risk-driven contact reduction to examine how behavioral feedback reshapes optimal vaccination policy. We ask how optimal coverage, rollout speed, and age-based prioritization change when contact rates respond to perceived mortality risk in both homogeneous and age-structured populations, and whether improving vaccination speed or fine-tuning prioritization rules has the larger impact on total infections and deaths.

The key contribution of this study lies in its comprehensive analysis of vaccination policies and the ways in which behavioral feedback loops shape optimal policy choices. In particular, we investigate whether incorporating behavioral responses into the model alters which policy emerges as optimal, and we quantify the marginal gains when comparing these optimal strategies with less effective alternatives. As such, we propose the following hypothesis:

H: Optimal vaccination policies are different in a model that neglects behavioral feedback (the control model) vs. a model that includes behavioral feedback (the treatment model).

This study is aimed at testing whether optimal solutions for vaccine distribution and coverage are sensitive to incorporating behavioral feedback.

4.3. Background

4.3.1. Literature Review

The rapid development of effective vaccines was one of the few clear successes in the response to COVID-19, one of the most disruptive global crises in recent history. However, once vaccines existed, scaling up production and delivering them efficiently proved to be a persistent challenge. More broadly, deciding how to prioritize vaccination for new and emerging diseases is an ongoing problem that extends well beyond COVID-19 (Rahmandad, 2022).

When vaccine supply or delivery capacity is constrained, "who should be vaccinated first?" becomes a quantitative question with multiple defensible answers because different studies optimize different outcomes and assume different vaccine mechanisms. Lipsitch and Dean frame this as a trade-off between direct protection (vaccinating those at highest risk of severe disease/death) and indirect protection (vaccinating those most responsible for transmission to reduce spread), noting that which pathway dominates depends on the vaccine's effects and the epidemic context (Lipsitch & Dean, 2020). Fitzpatrick and Galvani make a similar point in the context of age-specific strategies: optimal targeting depends on whether the goal is minimizing deaths or minimizing infections (Fitzpatrick & Galvani, 2021). Because vaccines can generate both direct and indirect protection, evaluations that ignore intergroup mixing can miss-evaluate the impact of vaccination (Gallagher et al., 2021).

A first family of studies answers the prioritization question using static, risk-based calculations that aggregate direct benefits within groups, without explicitly simulating between-group transmission. Goldstein et al., for example, use a simplified demographic framework to compare age-prioritized versus age-neutral rollouts and argue that age-prioritization can avert substantially more deaths largely because mortality risk rises steeply with age; they also explicitly note that their approach focuses on direct lives saved and does not incorporate reduced transmission effects (Goldstein et al., 2021). Wrigley-Field et al. similarly evaluate alternative eligibility schemes, age alone versus age combined with race/ethnicity or geography, by asking how well eligibility rules target groups with the highest observed COVID-19 mortality risk (using 2020 mortality as a proxy) and argue that adding geographic prioritization can better align eligibility with mortality risk and improve equity compared with age thresholds alone (Wrigley-Field et al., 2021). These designs are useful for clarifying "who is at highest observed mortality risk," but by construction they do not capture dynamic indirect effects that arise when vaccinating one group changes the infection risk faced by others.

A second family uses dynamic transmission models (typically age-structured or stratified by occupation) to represent those interdependencies and evaluate how vaccinating one subgroup changes infections and deaths in the rest of the population. Bubar et al. use an age-structured model to compare prioritization strategies under different vaccine assumptions and show that prioritizing adults 20–49 can minimize cumulative incidence when the vaccine strongly blocks transmission, whereas prioritizing older adults (>60) minimizes deaths and years of life lost in most scenarios (Bubar et al., 2021). Buckner et al. extend this logic by explicitly representing "essential workers" as a group with limited ability to socially distance and find that optimal/dynamic prioritization often vaccinates essential workers early (when the objective includes reducing transmission), then shifts toward older adults as marginal returns change (Buckner et al., 2021). Moore et al. use an age-structured UK model and conclude that targeting older age groups first is optimal for minimizing deaths or QALY losses across a range of assumptions about vaccine action and efficacy (Moore et al., 2021). In the Canadian context, Jentsch et al. compare multiple strategies and report that an oldest-first strategy yields the largest projected mortality reduction (with alternative strategies close behind but generally inferior on deaths under their assumptions) (Jentsch et al., 2021).

Importantly, transmission conclusions can reverse when contact structure and the feasibility of distancing differ by occupation. Buckner et al. show that prioritizing essential workers can be strongly favored under many scenarios because it targets a high-contact group that sustains transmission while remaining exposed (Buckner et al., 2021). This mechanism is consistent with evidence that infection risk and mixing are not uniform across groups, and with findings that younger groups can have higher observed prevalence during surge periods (Rumain et al., 2021), even while older adults face much higher fatality risk conditional on infection (Levin et al., 2020).

Across these papers, different conclusions often trace back to differences in (i) the objective function (deaths vs cases vs YLL), (ii) assumptions about vaccine effects on transmission, (iii) how finely heterogeneity is represented (age only vs age + worker status vs geography), and (iv) whether behavior is treated as fixed. Empirical evidence suggests behavior is not fixed; for example, age groups differ in risk perception and distancing behavior, which motivates extending prioritization analyses to settings where contact rates adapt endogenously rather than remaining constant by assumption (Masters et al., 2020)

Overall, prior studies consistently recommend prioritizing older adults for vaccination, often after the critical-care workforce. Given that the infection fatality rate (IFR) for the elderly is orders of magnitude higher than that of younger age groups (Levin et al., 2020), these findings are also intuitively appealing and also have been applied in many countries. However, these studies largely overlook how people and governments change their behavior as the perceived risk of the disease evolves (Rahmandad, 2022). This behavioral response affects the transmission rates endogenously and creates a feedback mechanism (Bagnoli et al., 2007; Funk et al., 2010).

Only a few models include an endogenous behavioral response function. Among which, one study using such structure finds that vaccinating high contact adults first (young adults) would be more beneficial (Rahmandad, 2022). Reducing deaths through vaccination can lower perceived risk, leading people and policymakers to relax precautions, which in turn causes a rebound in cases and deaths. Vaccinating high-contact groups, or those less responsive to risk, first allows more cautious groups to remain careful and keep deaths low until they are vaccinated. By contrast, if high-contact groups are deprioritized, the rebound will be strongest among them: seeing early declines in deaths as older adults are protected, they may increase their interactions, keeping the reproduction number high and the disease circulating for longer, and ultimately raising total deaths.

While some prior work has started to incorporate behavioral feedback in epidemic models, its implications for vaccination priority remain less well understood, yet potentially important. How different is the "optimal" vaccination policy when behavioral responses are explicitly modeled versus ignored? And in a behavioral setting, is it still worth investing substantial effort in fine-tuning prioritization rules, or is it more effective to focus on increasing vaccination speed and coverage? In this paper, we address these questions directly.

4.3.2. Experimental Design

Our experimental design is summarized in Table 5.1 and includes two families of tests which will be conducted in a base run Scenario. For each test we compare optimal solutions from two models (with and without behavioral feedback). In study 1, we cover the first test where there is no age-stratified model and there exists no vaccination distribution based on age. This study uses a homogeneous-population SEIR framework and compares a standard SEIRV model (control) with a behavioral SEIRbV model (treatment) that endogenizes risk-driven contact reduction. In study 2, we make the model more realistic by adding two age groups (young and old) and redo the analysis while considering the effect of age-based vaccine distribution. This study extends both structures to an age-stratified setting, contrasting an age-structured SEIRV model with its behavioral counterpart in a population partitioned into younger, high-contact individuals and older, high-risk individuals.

Table 4.1: Experimental design

Test 1 (Study 1)	Test 2 (Study 2)
Model 1: SEIR (control)	Age-stratified SEIR (control)
Model 2: SEIRb (treatment)	Age-stratified SEIRb (treatment)

Optimal vaccine coverage and speed. Objective function: Minimize cumulative cases, deaths, and peak of pandemic	Optimal vaccine coverage, speed, and distribution. Objective function: Minimize cumulative cases, deaths, and peak of pandemic

Across both studies, vaccination policy is treated as an optimization problem over three decision variables: (i) overall vaccination coverage, (ii) vaccination speed, and (iii) in Study 2, the allocation of doses between younger and older age groups. Coverage represents the total fraction of the population that can be vaccinated over the simulation horizon; speed is the daily vaccination capacity as a share of the population; and the age-allocation parameter specifies the proportion of available doses directed to older adults.

For each model and study, we systematically vary these policy levers and simulate epidemic trajectories under a common base-run scenario, in which disease and vaccine parameters are fixed and neither vaccine-induced nor disease-induced immunity wanes over time. We compute cumulative cases, peak prevalence, and vaccination costs, and use these outcomes in a payoff function to identify combinations of coverage, speed, and (for Study 2) age allocation that minimize the overall burden of the epidemic.

4.4. Study 1

4.4.1. Method

In Study 1, we analyze a homogeneous SEIR-type model with vaccination, comparing a standard structure without behavioral feedback (SEIRV, hereafter SEIR) to a behavioral variant with endogenous risk response (SEIRbV, hereafter SEIRb). The population is partitioned into six compartments: susceptible (S), exposed (E), infectious (I), recovered (R), dead (D), and vaccinated (V) with homogeneous mixing. Infection occurs at rate $\lambda(t)S$, where the force of infection is given by $\lambda(t) = \beta_0\, c(t)\, I/N$. In the SEIR model, the contact modifier $c(t)$ is fixed at 1. In the SEIRb model, $c(t)$ adjusts endogenously to perceived risk $P(t)$ through an exponential response $c(t) = \exp(-k\, P(t))$, where $P(t)$ tracks the current death rate with a perception delay τ_P. Vaccination is represented as a flow $v(t)S$ from S to V, constrained by daily vaccination capacity κN and total coverage θN, and activated after a start time t_{start}. Disease progression from exposure to infection, recovery, and death follows standard latent and infectious periods (T_E and T_I) and an infection fatality rate f. The complete stock–flow structure is shown in Figure 5.1, and the corresponding differential equations, auxiliary functions, and parameter values for the base-run scenario are summarized in Table 5.2.

Using this model, we run multiple simulations and sensitivity analysis runs to understand the progression of the disease under the two model assumptions of SEIR and SEIRb. First, we do simple simulations showing the progression of the disease over a short-term period and long-term period comparing the SEIR and SEIRb model behavior. Next, we do multiple sensitivity analysis runs comparing total deaths and maximum number of infected versus different vaccination coverage and vaccination speed values. And finally, we analyze the effect of vaccination starting time by doing sensitivity analysis runs where we change the vaccination starting time to see how it affects total deaths.

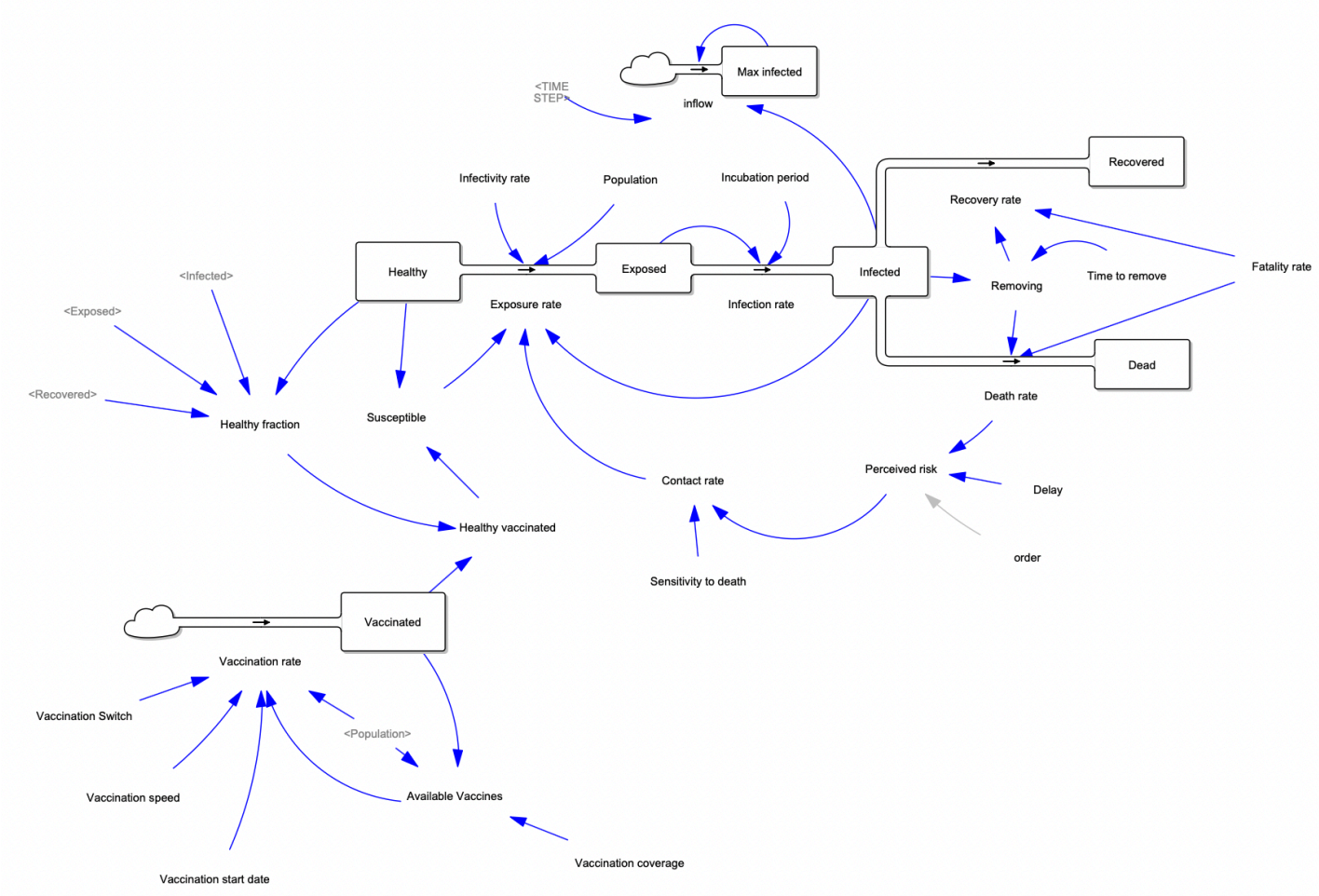

Figure 4.1. Stock flow diagram used in Study 1

Table 4.2: Formulations

Differential Equations

$dS/dt = -\lambda(t)S - v(t)S$

$dE/dt = \lambda(t)S - E/T_E$

$dI/dt = E/T_E - I/T_I$

$dR/dt = (1-f)I/T_I$

$dD/dt = fI/T_I$

$dV/dt = v(t)S$

Key Functions

Force of infection:

$\lambda(t) = \beta_0 c(t) I/N$

Vaccination rate:

$v(t) = \min(AV, \kappa N) \times STEP(1, t_{start})$

Available vaccines:

$AV = \theta N - V$

Contact modifier:

$c(t) = \exp(-kP(t))$

Perceived risk:

$dP/dt = (\delta(t) - P)/\tau_P$

where $\delta(t) = fI/T_I$

Population:

$N = S + E + I + R + D + V$

Parameters

Symbol	Description	Value
N	Total population	**1,000,000**
β_0	Baseline transmission rate	**0.30**
T_E	Latent period	**5 days**
T_I	Infectious period	**10 days**
f	Infection fatality rate	**0.005**
k	Sensitivity to death	**0 for SEIR** **1 for SEIRb**
τ_P	Perception delay	**30 days**
κ	Vaccination speed	**0.003**
θ	Vaccination coverage	**0.10**
t_{start}	Vaccination start	**30 days**

4.4.2. Results

We begin by plotting the total deaths over time with and without the presence of vaccine and over different time periods. Panels A and B in figure 5.2 show the total number of deaths over a 1-year period for SEIR versus SEIRb models. The blue line indicates the no vaccine scenario, and the red line indicates the with vaccine. Panels C and D provide a similar comparison for the longer period of period of 10,000 days.

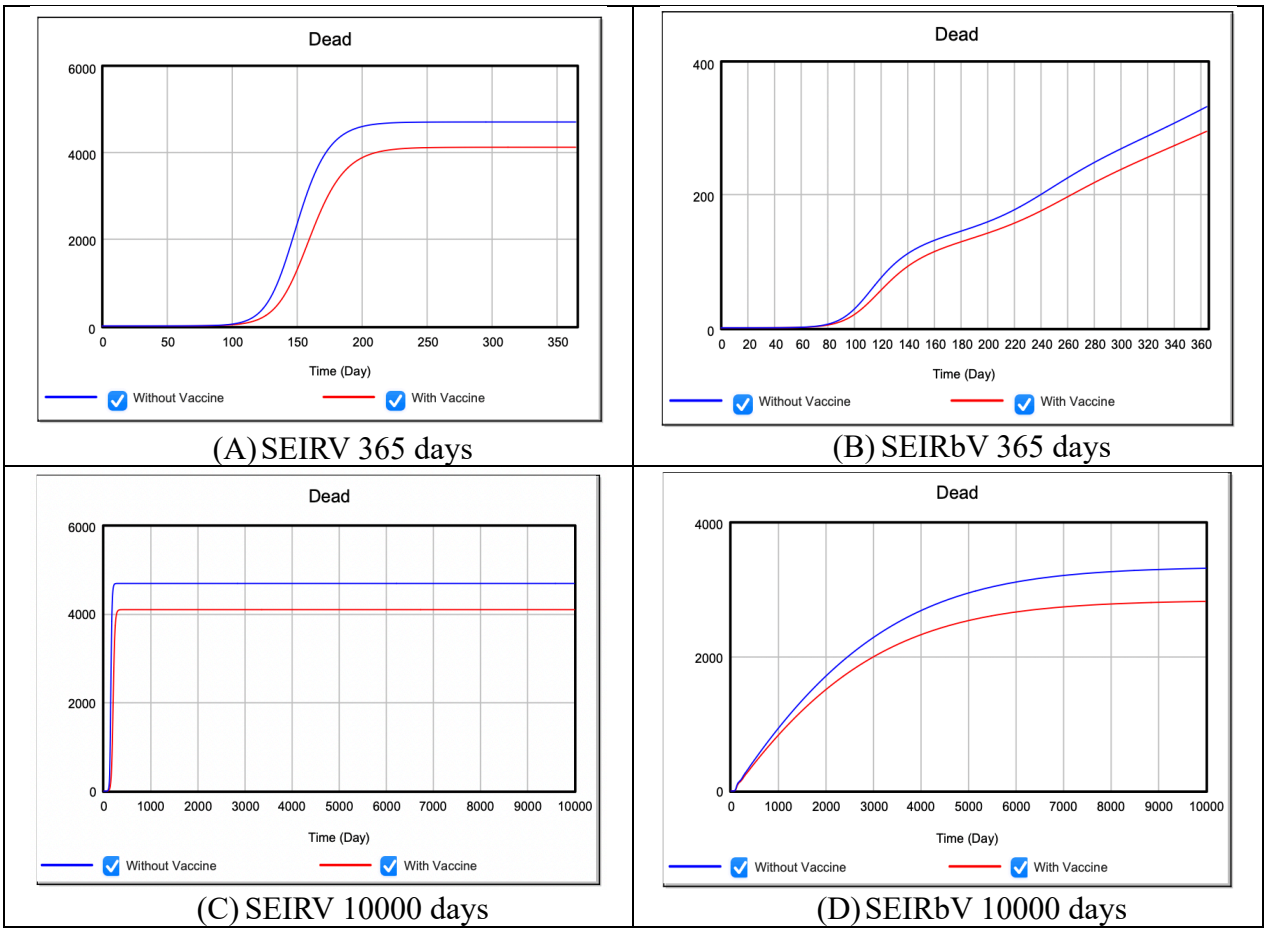

Figure 4.2. Base run SEIR vs SEIRb with and without Vaccination

Figure 5.2 illustrates the basic dynamics: without vaccination, the SEIR model generates a sharp, high first wave, whereas the SEIRb model flattens and stretches the epidemic by reducing contacts as deaths rise. When vaccination is introduced, both models display lower peaks and fewer cumulative deaths, but the SEIRb trajectories remain more spread out over time, reflecting the interaction between risk-driven distancing and vaccine-induced immunity.

Figure 5.3 depicts the change of contact rate over time in the SEIRb model in the presence and absence of vaccination. As the SEIR model does not include a behavioral loop the contact rate for that model is constant at 1.

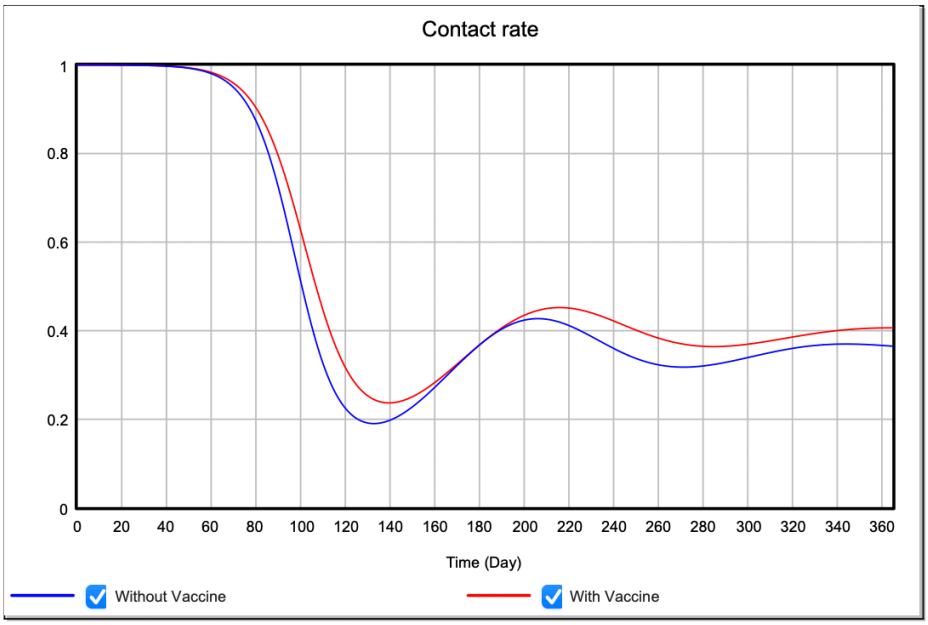

Figure 4.3. Contact rate over time in SEIRb models

Figure 5.3 makes this mechanism explicit: in the behavioral model the contact rate falls sharply as deaths increase, then gradually relaxes as the epidemic subsides, while the non-behavioral SEIR model maintains a constant contact rate.

Next, we compare cumulative death over a period of 365 days and under varying values of vaccination coverage and vaccination speed. Y-axis shows cumulative deaths from time t = 1 until the end of simulation period time t = 365. In panels A and B, X axis represents the vaccination coverage and there are eleven colored lines each representing a value for vaccination speed. Panel A in Figure 5.4 is for a model with no behavioral feedback (k=0), and panel B is results from the model with behavioral feedback (k=1). In Figure 5.5, For panels A and B, the X axis represents the vaccination speed and the eleven colored lines each represent a certain value for vaccination coverage.

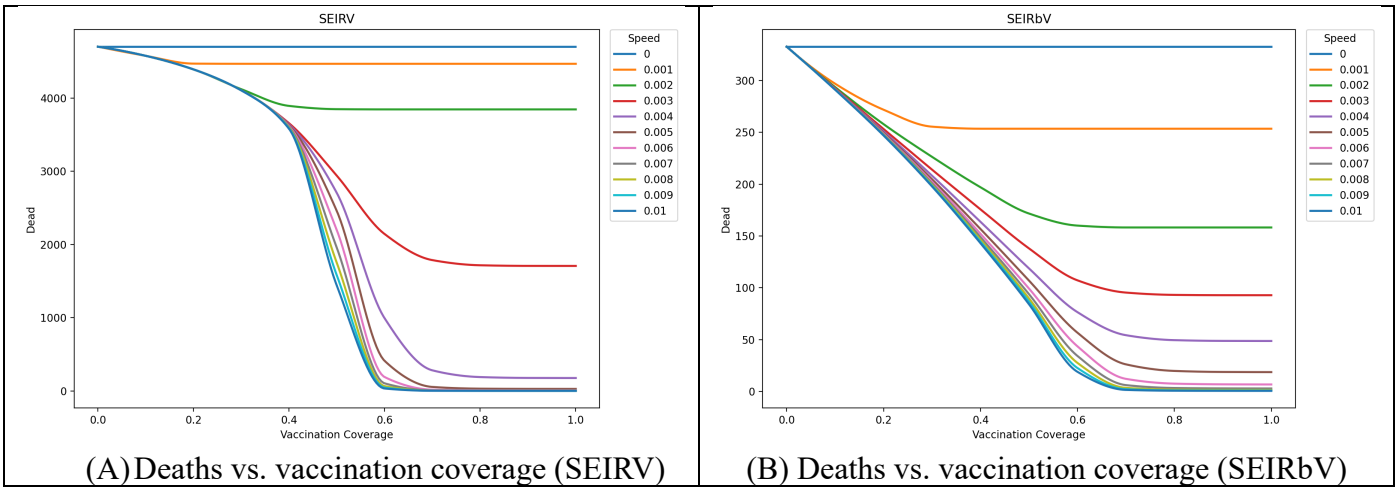

(A) Deaths vs. vaccination coverage (SEIRV) (B) Deaths vs. vaccination coverage (SEIRbV)

Figure 4.4. Simulation results of SEIRV vs SEIRbV comparing deaths to vaccination coverage for different values of vaccination speed

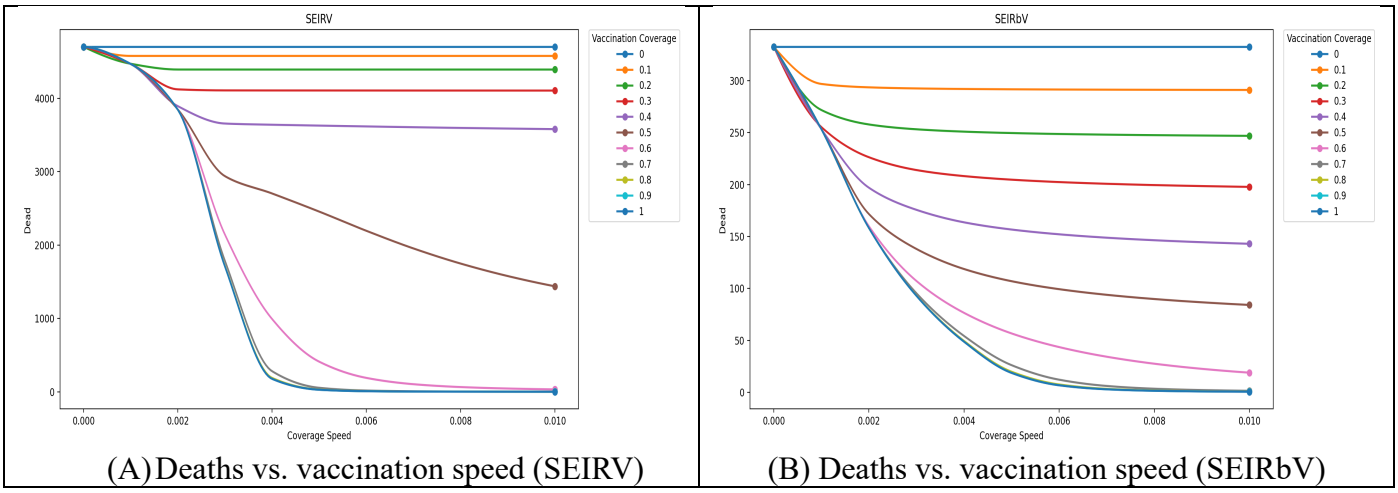

(A) Deaths vs. vaccination speed (SEIRV) (B) Deaths vs. vaccination speed (SEIRbV)

Figure 4.5. Simulation results of SEIRV vs SEIRbV comparing deaths to vaccination speed for different values of vaccination coverage

Figures 5.4 and 5.5 then show how vaccination coverage and speed jointly shape total deaths. In both SEIR and SEIRb, moving along either axis, raising coverage at a fixed speed (Figure 5.4) or increasing speed at a fixed coverage (Figure 5.5), reduces mortality, but with diminishing returns at very high levels. The panels also reveal that in the behavioral model, outcomes are more sensitive to vaccination speed: when contacts adjust endogenously, faster rollout produces a much steeper reduction in deaths, especially at intermediate coverage levels, whereas simply adding more doses at a slow pace delivers smaller gains.

To get a better sense of the difference in SEIR and SEIRb death estimates, we plot figure 5.6 where in it three values of vaccination speed are shown for both models, totaling 6 different scenarios.

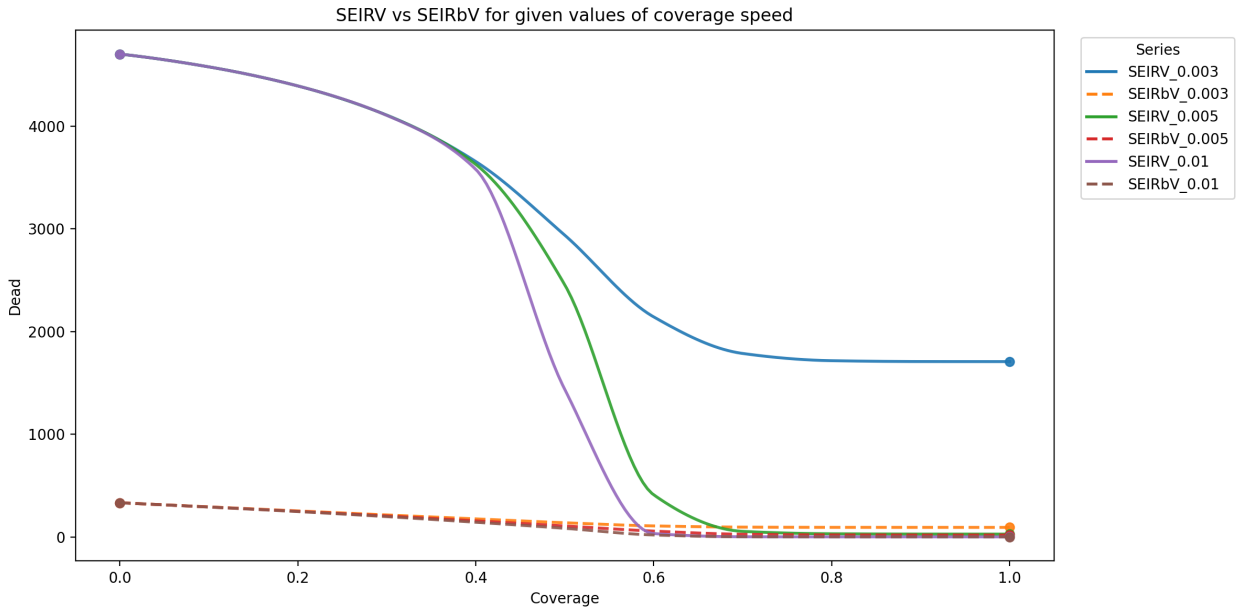

Figure 4.6. Comparing results from SEIRV (continuous lines) vs SEIRbV (dotted lines) in terms of deaths for different values of vaccination coverage and speed.

Figures 5.6 and 5.7 summarize these patterns in a more compact form. Figure 5.6 visualizes total deaths as a function of coverage and speed for both SEIR and SEIRb, highlighting a ridge of high mortality at low coverage and low speed, and a low-mortality region at high coverage and high speed. The contours tilt, indicating that coverage and speed are partially substitutable but not equivalent: in the behavioral model, moving "up" in speed often compensates more for low coverage than in the non-behavioral case.

Figure 5.7 compares the peak of pandemics (defined as all-time maximum number of cases in day) across different scenarios for the two models.

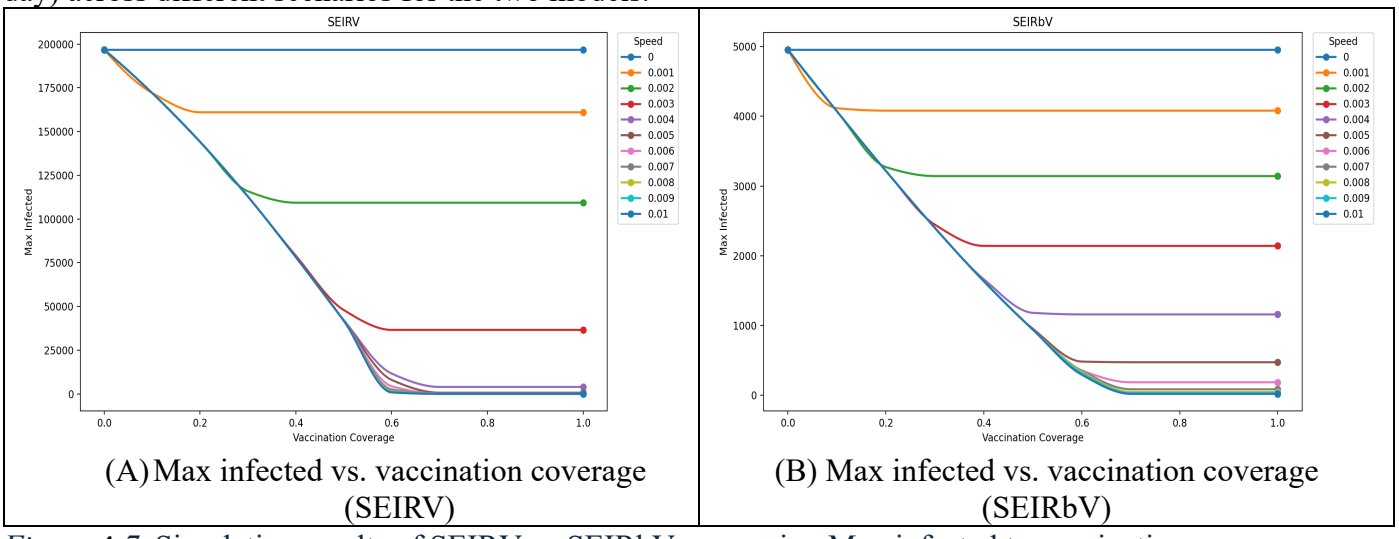

(A) Max infected vs. vaccination coverage (SEIRV)

(B) Max infected vs. vaccination coverage (SEIRbV)

Figure 4.*7.* Simulation results of SEIRV vs SEIRbV comparing Max infected to vaccination coverage for different values of vaccination speed

Figure 5.7 focuses directly on the difference between the two models across the coverage–speed plane, showing that the gap is largest at intermediate values where behavioral responses are strongly activated but vaccination has not yet fully suppressed transmission. In this region, behavioral feedback makes vaccination speed particularly valuable, shifting the policy emphasis from maximizing total doses to delivering available doses as early and as quickly as possible.

Sensitivity analysis for vaccination starting time

It is important to consider the vaccination starting time and the effect it has on the progression of the disease. In the real world, vaccination is not available from the very first day that the disease begins. To explore this, Figures 5.8 and 5.9 vary the vaccination start date from 0 to 100 days. In Figure 5.8, we group vaccination coverage values into three levels (0.3, 0.6, and 0.9) and vaccination speed into three levels (0.001, 0.002, and 0.003), creating nine scenarios that allow us to compare total deaths over a one-year simulation horizon for different vaccination start dates. In Figure 5.9, we visualize the same relationships using three-dimensional plots, where each panel represents a different vaccination start date. Panel A shows total deaths as a function of vaccination speed and coverage when vaccination begins at day 0, panel B for a start date of 30 days, and panel C for a start date of 100 days.

These sensitivity analyses show that the value of starting vaccination earlier depends strongly on vaccination speed. When vaccination capacity is low, shifting the start date forward has only a modest effect on total deaths because rollout is too slow to substantially change the first epidemic wave. At higher speeds, however, earlier start dates yield large reductions in mortality: in our base parameterization, bringing the start of vaccination forward from 100 days to 0–30 days can reduce deaths over the first year by more than half. Together, Figures 5.8 and 5.9 highlight that early rollout and high capacity are complementary: starting vaccination earlier is most beneficial when the system can also deliver doses quickly

In Figure 5.9, we visualize this concept in three-dimensional plots where each panel represents a different starting date for vaccination. Plot A shows the comparison of total deaths versus vaccination speed versus vaccination coverage in a one-year period given a vaccination start date of 0, plot B shows the same comparison for the start date of 30 days, and finally, plot C shows it for the start date of 100 days.

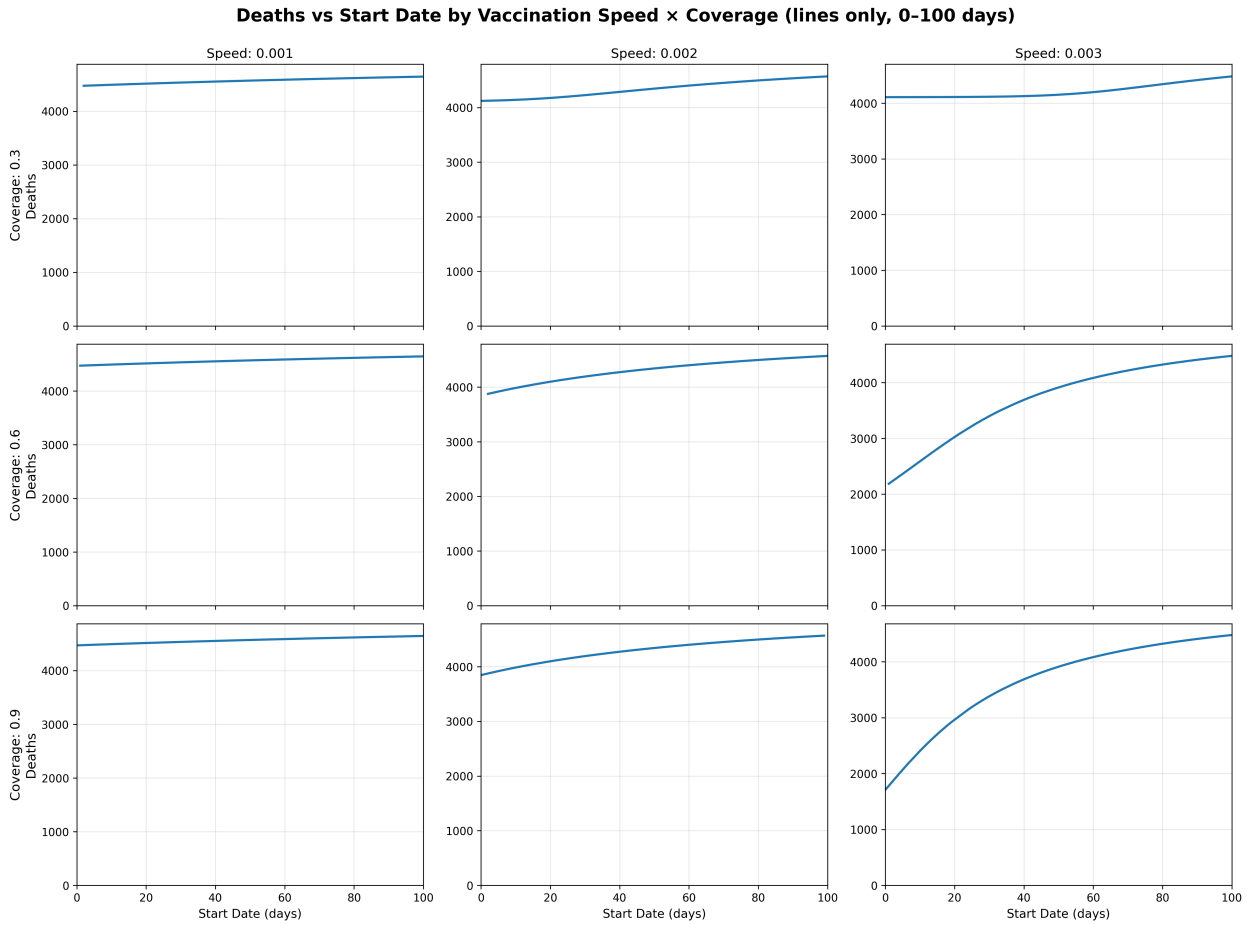

Figure 4.8. Sensitivity analysis of vaccination start date: comparing deaths with different values of vaccination speed and coverage over different vaccination start dates.

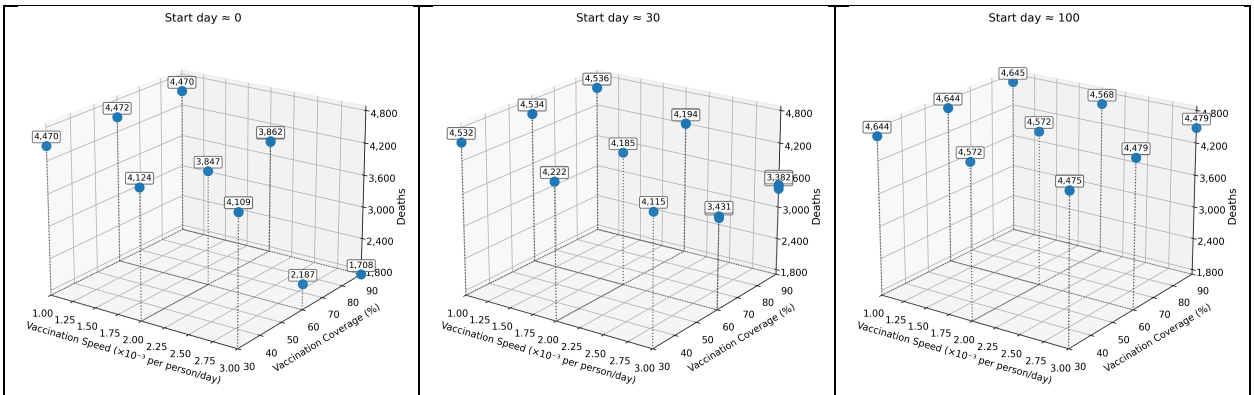

(A) Deaths vs coverage vs speed at start day of 0

(B) Deaths vs coverage vs speed at start day of 30

(C) Deaths vs coverage vs speed at start day of 100

Figure 4.9. Total deaths vs vaccination speed vs vaccination coverage at start dates of 0, 30, and 90 days

4.5. Study 2

4.5.1. Method

Upon completion of study 1 and the first test, we move to the second test in study 2 where we add age stratification to our model. The model structure mostly stays the same with the difference of having two stock and flow structures, one for young adults and the other for elderly adults. Below, you can see these two stock and flow diagrams.

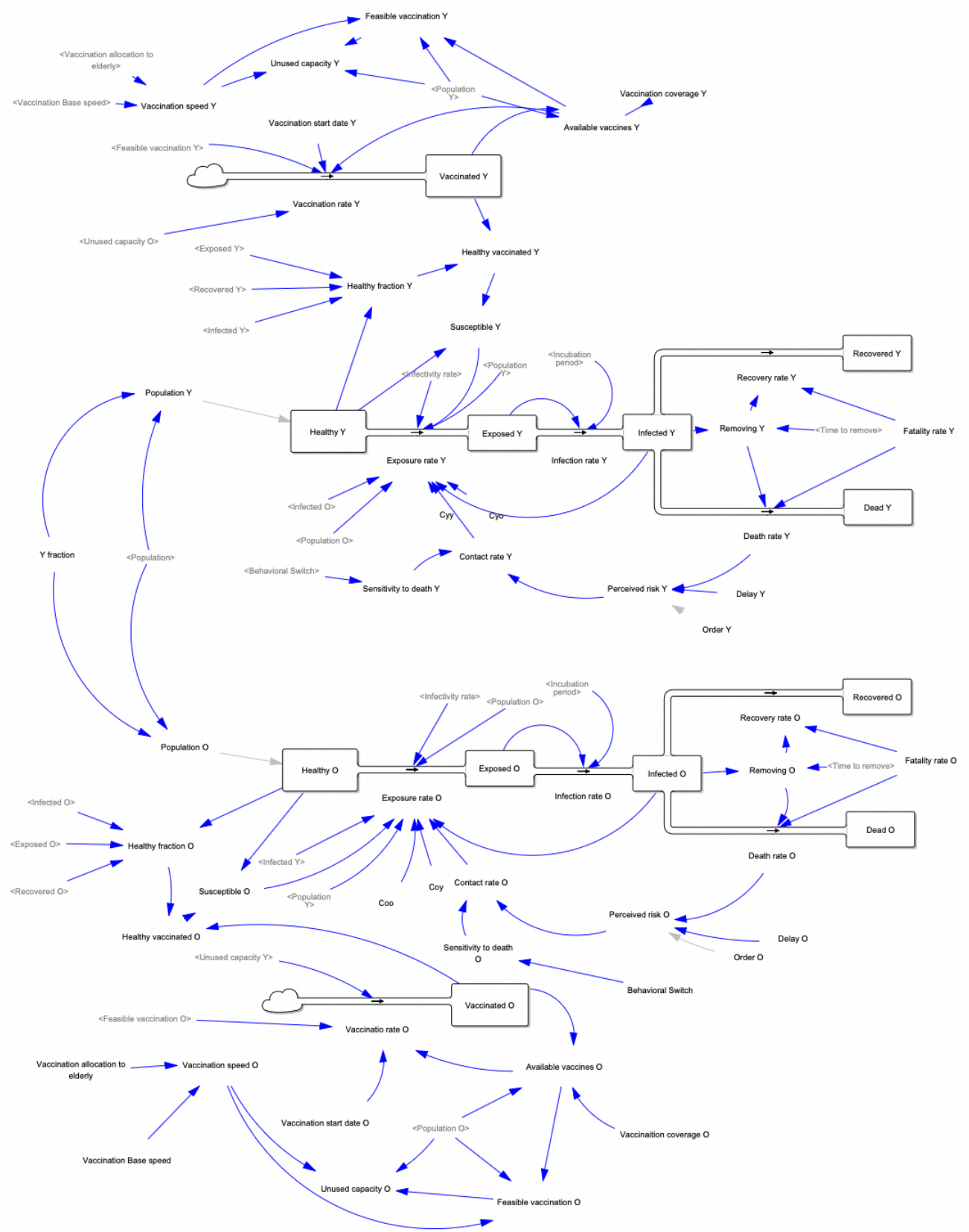

Figure 4.10. Stock-flow diagram used in study 2

The additional assumptions and formulations compared to the first study are presented below.

In Study 2 we extend the homogeneous-population model of Study 1 to a simple age-structured setting with two groups. The total population is partitioned into "young" individuals Y (0–59 years) and "old" individuals O (60+ years). The age-60 threshold is chosen to capture the sharp increase in COVID-19 severity that is consistently observed in epidemiological data and keeps the model parsimonious while allowing for strong age gradients in risk.

To reflect age-specific severity, we assign group-specific infection fatality rates f_Y and f_O. Young individuals face an IFR of $f_Y = 0.001$ (0.1%), while older individuals face an IFR of $f_O = 0.01$ (1.0%), capturing the order-of-magnitude higher mortality risk observed for older age groups in empirical COVID-19 data e.g., (Levin et al., 2020; O'Driscoll et al., 2021). These values are intended as stylized but realistic magnitudes rather than pathogen- or setting-specific estimates.

Transmission is governed by a 2×2 age-specific contact matrix C_{ij}, where $i, j \in Y, O$ index the age group of the "from" and "to" individuals. We specify

$$C = \begin{pmatrix} c_{YY} & c_{YO} \\ c_{OY} & c_{OO} \end{pmatrix} = \begin{pmatrix} 15 & 3 \\ 3 & 6 \end{pmatrix},$$

measured in average contacts per person per day. This stylized parameterization is consistent with empirical age-structured contact studies e.g., (Mossong et al., 2008; Prem et al., 2017) which show that working-age adults have substantially higher within-group contact rates than older adults and that intergenerational mixing is limited relative to within-group mixing. In our setting, young individuals have roughly 2.5 times as many within-group contacts as older adults ($c_{YY} = 15$ vs. $c_{OO} = 6$), while between-group contacts occur at a lower and approximately symmetric rate ($c_{YO} = c_{OY} = 3$).

Apart from replicating the SEIRV/SEIRbV compartments for young and old groups and modifying the forces of infection to incorporate the 2×2 contact matrix, all epidemiological and behavioral parameters use the same values as in Study 1; the only new parameters are the age-specific fatality risks and the contact matrix entries.

Proceeding with the analysis, we begin by comparing the simulation results of deaths over time, death rate over time, and infection rate over time given three scenarios of no vaccination, young vaccination, and old vaccination.

Finally, in Study 2 we treat age-prioritization as a continuous decision variable. We define an allocation parameter $a_O \in [0,1]$ that specifies the share of daily vaccination capacity directed to older adults. On each day, $a_O \kappa N$ doses are allocated to the older group (up to the remaining susceptible population), and the remaining $(1 - a_O)\kappa N$ doses go to younger adults. Varying a_O from 0 to 1 thus spans policies from "young-first" ($a_O = 0$) to "old-first" ($a_O = 1$),

with intermediate values representing mixed allocation strategies. We evaluate how outcomes change along this allocation continuum while holding total coverage and vaccination speed fixed.

We do multiple sensitivity analysis runs to assess how total number of deaths and cases change over a 1 year and 10-year period with varying values of vaccination allocation to elderly. Lastly, we compare the best versus worst policy (based on vaccination allocation to elderly) with vaccination speed to analyze which factor plays a more important role.

4.5.2. Results

In this section, we begin by comparing deaths, death rate, and infection rate over the simulation period of 365 days for three scenarios of no vaccination, young vaccination, and old vaccination. In plot A, C, and E the young first vaccination policy is tested and compared with a case of no vaccination. The dotted lines represent the no vaccine cases. On the other hand, in plot B, D, and F the Old first vaccination policy is being compared with the no vaccination policy.

To be more precise, in plot A, we visualize 6 lines, where the solid green line represents total deaths in the young first vaccination policy and the dotted line shows the same value for the no vaccination policy. The blue and red solid lines respectively show old and young deaths over time under young-first vaccination policy, and the blue and red dotted lines respectively show the same values under no vaccination policy. The same logic follows for plots B to F. these nine plots are illustrated in figure 5.11 below.

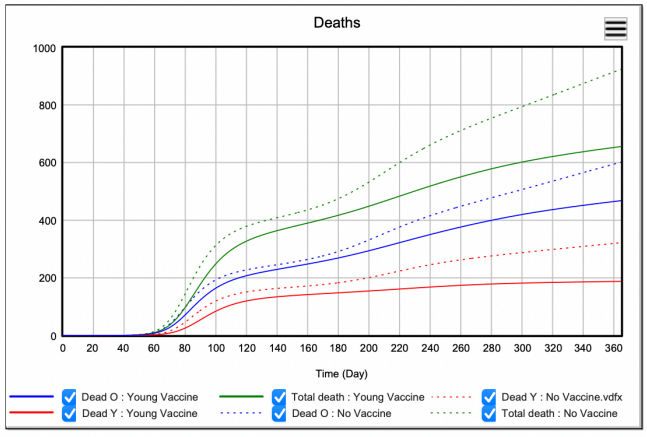

(A) Cumulative Deaths over time: Young vaccination

(B) Cumulative Deaths over time: Old Vaccination

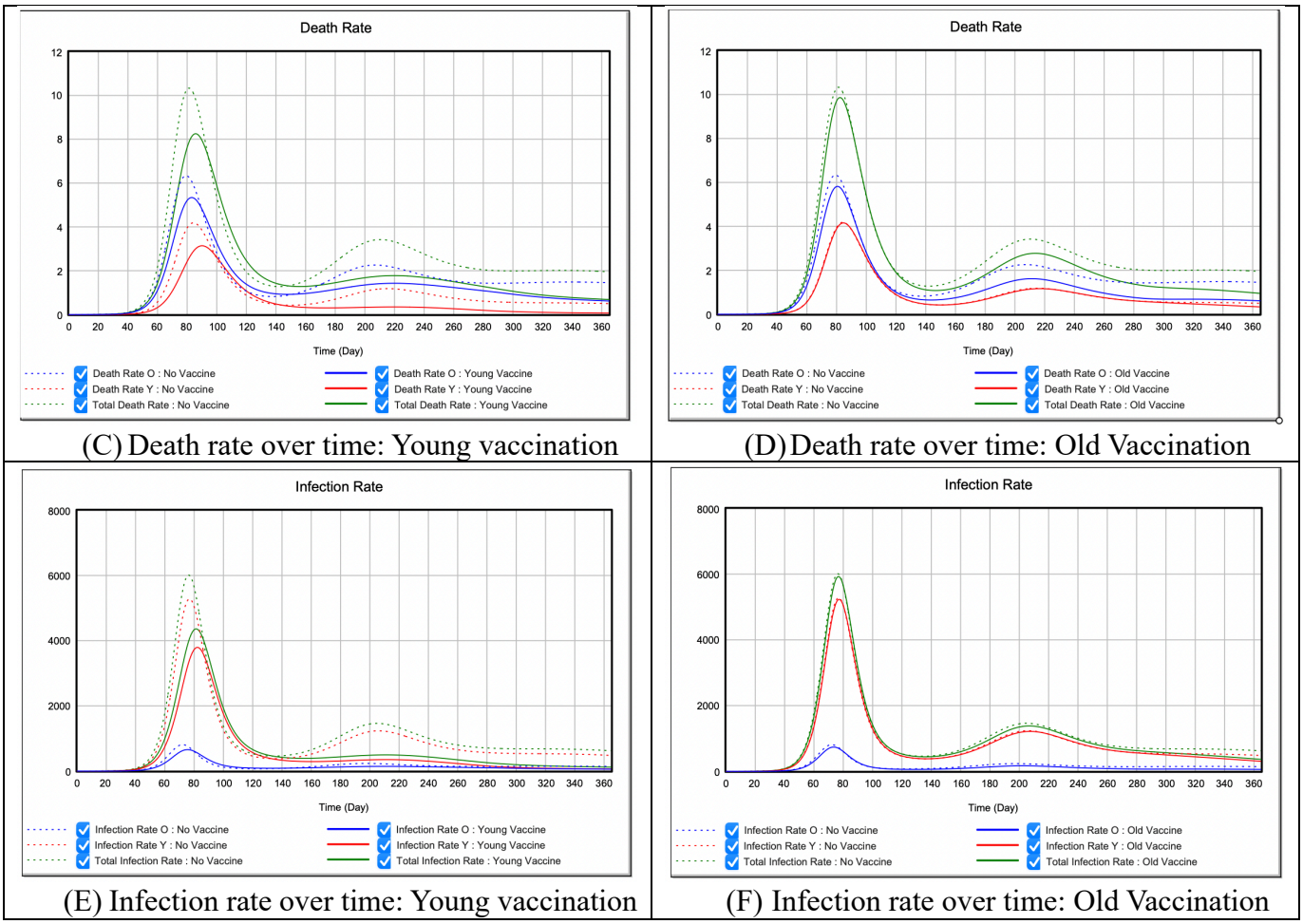

(C) Death rate over time: Young vaccination

(D) Death rate over time: Old Vaccination

(E) Infection rate over time: Young vaccination

(F) Infection rate over time: Old Vaccination

Figure 4.11.Baseline simulation of deaths, death rate, and infection rate over time for two cases of young vaccination priority and old vaccination priority

Figure 5.11 illustrates these trade-offs in more detail. In panels A and B, both young-first and old-first vaccination policies substantially reduce total deaths compared to the no-vaccination baseline (dotted lines), but they do so in different ways. Under the young-first strategy (panel A), vaccinating high-contact younger adults slows transmission in both age groups, so deaths in both the young and old populations accumulate more gradually, and the epidemic peak is lower. Under the old-first strategy (panel B), deaths among older adults drop sharply relative to the baseline, reflecting direct protection of the high-risk group, while deaths among younger adults are closer to the no-vaccination trajectory. Panels C–F make this pattern clearer by focusing on instantaneous rates: young-first vaccination produces the largest reduction in infection and death rates, especially around the epidemic peak, whereas old-first vaccination yields a stronger and more immediate reduction in mortality among older adults but a smaller effect on infection rates overall. Together, these panels highlight the central tension in age-based prioritization: vaccinating younger, high-contact individuals is more effective at suppressing transmission, while vaccinating older, high-risk individuals delivers larger direct mortality benefits in the short run.

Next, we plot total cases and deaths over the simulation period of 1 and 10 years given different values of vaccination allocation to elderly and different values of vaccination speed. In figure 5.12, 4 plots are visualized that represent cases over time and the 4 Panels in figure 5.13 represent deaths over time. to elaborate, in each of the two figures, there are four Panels: Panel A showcases how the total number of cases change with vaccination allocation to elderly changing from 0 to 1 given 10 different scenarios of vaccination speed. These 10 vaccination speeds are shown with colored lines in each Panel. Furthermore, Panel A visualizes this setting in a one-year period with and SEIR model assumption. Panel C on the other hand, shows the same case but in a ten-year period. Panels B and D are using the SEIRb model assumption, and they also visualize the one year and ten-year period simulations. Figure 5.13 shows the same setting with the only difference of showcasing deaths over time.

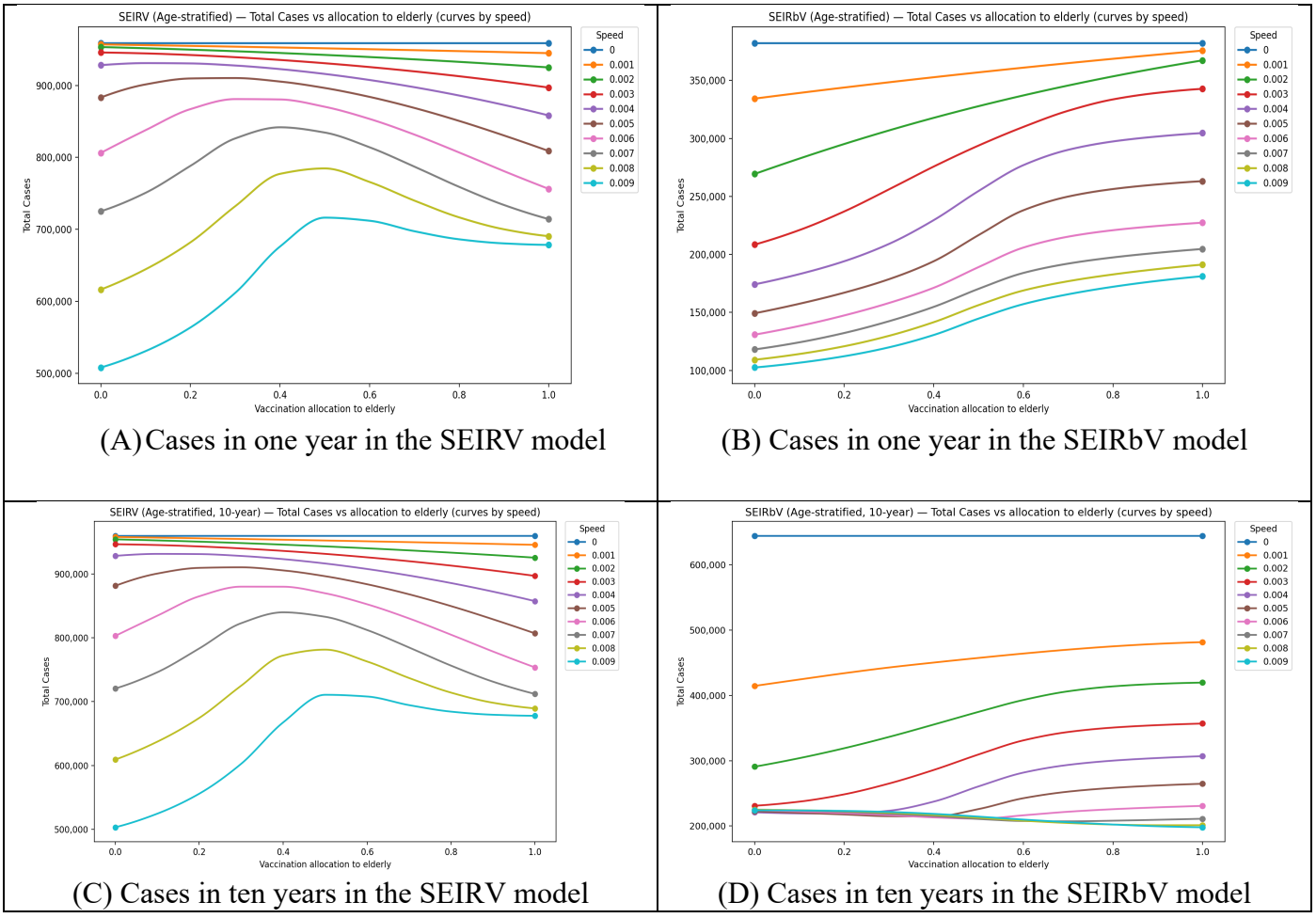

(A) Cases in one year in the SEIRV model

(B) Cases in one year in the SEIRbV model

(C) Cases in ten years in the SEIRV model

(D) Cases in ten years in the SEIRbV model

Figure 4.12.Sensitivity analysis of total cases vs allocation to elderly for different values of vaccination speed in one and ten years

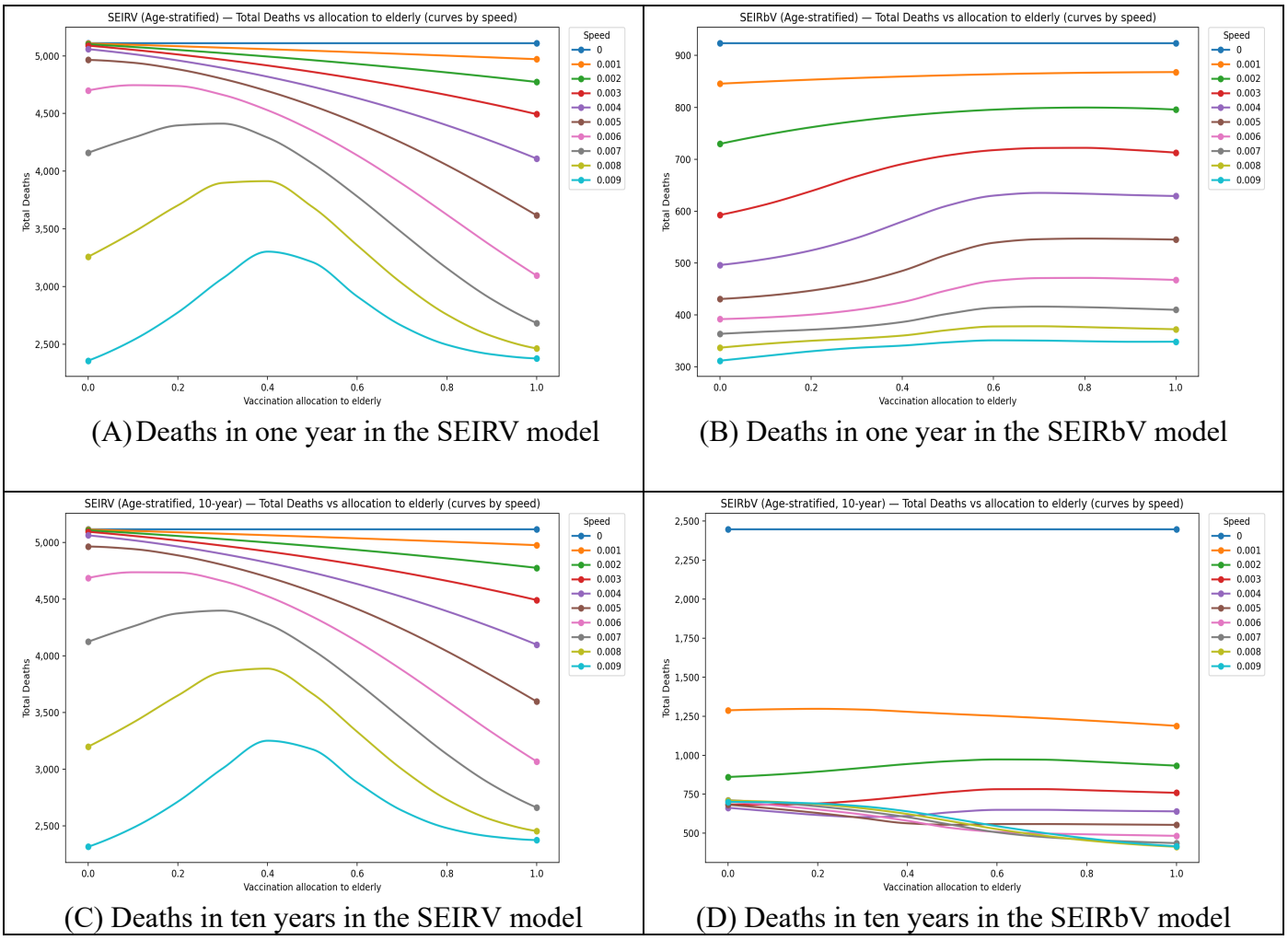

(A) Deaths in one year in the SEIRV model

(B) Deaths in one year in the SEIRbV model

(C) Deaths in ten years in the SEIRV model

(D) Deaths in ten years in the SEIRbV model

Figure 4.*13.* Sensitivity analysis of total deaths vs allocation to elderly for different values of vaccination speed in one and ten years

Figures 5.12 and 13 summarize how vaccination speed and age allocation interact over short and long horizons. Figure 5.12 focuses on total cases. In each panel, moving along the horizontal axis from left to right corresponds to shifting the allocation from young-first (low allocation to elderly) to old-first (high allocation to elderly), while the colored lines represent different vaccination speeds. In both SEIRV (panels A and C) and SEIRbV (panels B and D), allocating more doses to younger, high-contact individuals tends to reduce cumulative infections, especially when vaccination speed is moderate to high. At low speeds, the curves are relatively flat: limited capacity means that changing who is prioritized has only a modest effect on total cases. As speed increases, however, the separation between lines becomes more pronounced and the benefits of vaccinating high-contact younger adults first become clearer, particularly over the 10-year horizon where repeated waves can occur.

Figure 5.13 shows the same set of scenarios but for total deaths rather than total cases. Here, the trade-offs between age allocation and speed are much sharper. In the SEIRV panels (A and C), when vaccination speed is low, allocating more doses to older adults substantially reduces deaths, because those doses go directly to the group with the highest infection fatality risk. As speed increases, the advantage of strongly old-first policies shrinks: once rollout is fast, vaccinating younger high-contact individuals can nearly match the mortality performance of elderly-first strategies by suppressing transmission more quickly. In the SEIRbV panels (B and D), vaccination speed clearly dominates age allocation. Differences between young-first and old-first policies are relatively small compared to the large vertical gaps between slow and fast rollout lines, particularly over 10 years, where behavioral feedback generates multiple waves. Together, Figures 5.12 and 13 show that in a purely epidemiological model the choice of age priority can matter a great deal when speed is limited, whereas in the behavioral model increasing vaccination speed reliably saves more lives than fine-tuning the allocation between young and old.

Finally, in figure 5.14 we look at the how total deaths in the simulation period change with different values of vaccination speed (varying from 0 to 0.009). Two lines separate the best and worst policy which is derived from the previous analysis: best policy comes from the vaccination allocation value that produced the least number of deaths, and the worst vaccination policy comes from the vaccination allocation that produced the greatest number of deaths. Best policy is shown by the blue line whereas the orange line represents the worst policy. Plots A, C, and E use the SEIR model assumption whereas plots B, D, and F assume the SEIRb model structure. To elaborate further on each of the plots, we begin by plot A and B where the simulation is done over 1 year. Plots C and D normalize the values calculated in plot A and B such that all the value are between 0 and 1. Lastly, plot E and F continue with the normalized approach; however, they analyze the number of deaths over a 10-year period.

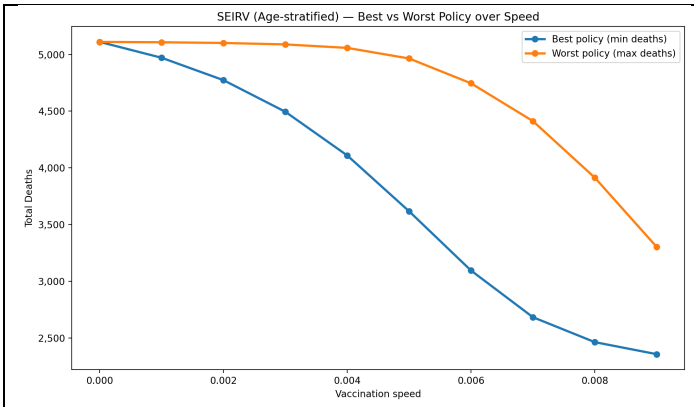

(A) Deaths vs vaccination speed in SEIRV for one year: best vs worst policy

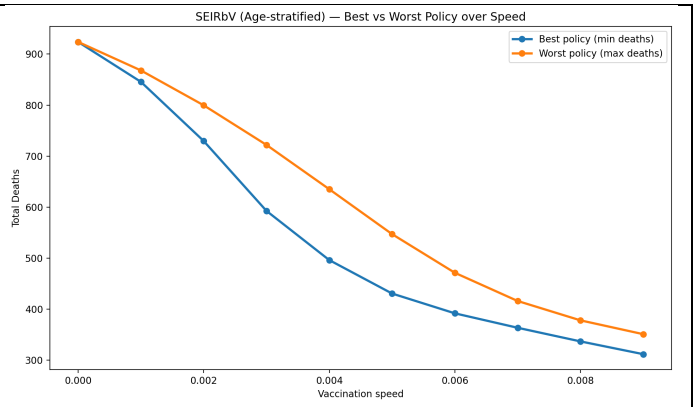

(B) Deaths vs vaccination speed in SEIRbV for one year: best vs worst policy

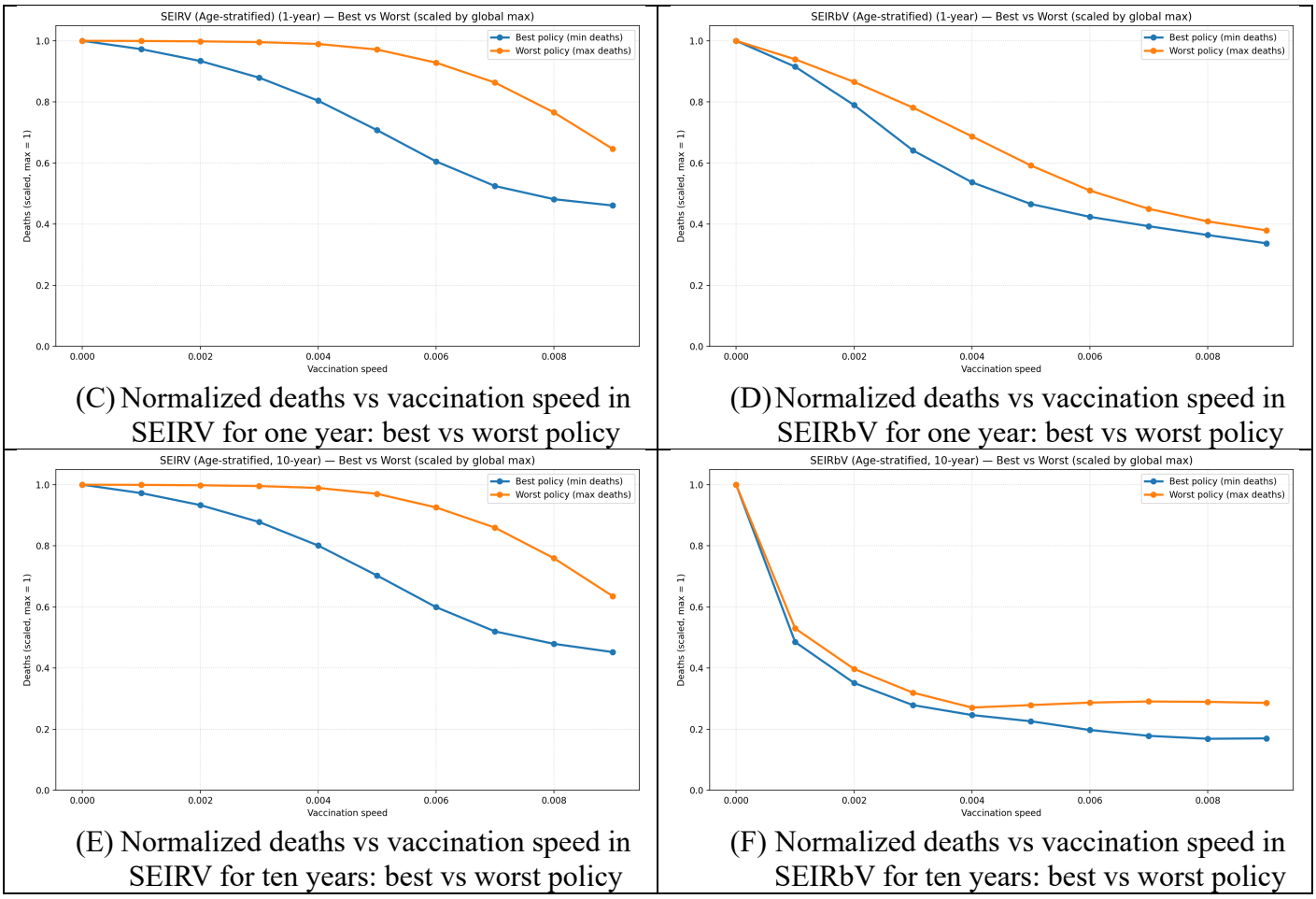

(C) Normalized deaths vs vaccination speed in SEIRV for one year: best vs worst policy

(D) Normalized deaths vs vaccination speed in SEIRbV for one year: best vs worst policy

(E) Normalized deaths vs vaccination speed in SEIRV for ten years: best vs worst policy

(F) Normalized deaths vs vaccination speed in SEIRbV for ten years: best vs worst policy

Figure 4.14. Analyzing vaccination speed vs Young-Old priority policies. Raw and normalized values over 1 and 10 years.

Figure 5.14 summarizes how vaccination speed interacts with age-prioritization, focusing on the best and worst allocation rules identified in Figures 5.12–5.13. For each vaccination speed between 0 and 0.009, we select the best policy as the allocation to older adults that minimizes total deaths and the worst policy as the allocation that maximizes total deaths. Panels A and B show raw death counts over a 1-year horizon in SEIRV and SEIRbV, respectively, with the best policy (blue line) and worst policy (orange line) plotted as functions of vaccination speed. Panels C and D display the same relationships but on a normalized scale, and panels E and F extend the normalized analysis to a 10-year horizon.

In the normalized panels (C–F), we rescale deaths within each model–horizon combination so that values lie between 0 and 1. Specifically, for each panel we subtract the minimum number of deaths observed across all speeds and policies and divide by the resulting range, so that 0 represents the lowest deaths in that panel and 1 represents the highest. This normalization removes differences in absolute scale between SEIRV and SEIRbV and between 1- and 10-year horizons, allowing a cleaner visual comparison of how fast deaths fall with increasing vaccination speed and how large the gap remains between the best and worst allocation rules.

Read from left to right, Panels A and B show that in both models total deaths decline as vaccination speed increases, but the relative role of age prioritization differs sharply. In SEIRV (panel A), the vertical distance between the best and worst policies is substantial at low speeds and remains visible even at higher speeds, indicating that who is prioritized continues to matter alongside how fast vaccination proceeds. In SEIRbV (panel B), by contrast, both lines drop steeply with speed and lie much closer together, suggesting that once behavioral feedback is included, increasing vaccination speed produces much larger gains than switching between young-first and old-first allocation. The normalized panels over 1 and 10 years (C–F) reinforce this pattern: in SEIRV, the normalized gap between best and worst policies is wide at low speeds and narrows only gradually, whereas in SEIRbV the gap is small across most of the speed range and both lines follow a similar downward trajectory. Taken together, Figure 5.14 highlights the central result of Study 2: in a behaviorally responsive epidemic, vaccination speed dominates age-based prioritization, and the difference between "good" and "bad" allocation rules is much smaller than the difference between slow and fast rollout.

4.6. Discussion

In many epidemic settings, the effectiveness of vaccination policy depends not only on biological and logistical constraints, but also on how people adjust their behavior in response to perceived risk. Vaccines are introduced into populations that are simultaneously changing contact patterns, reacting to reported cases and deaths, and responding to policy signals. In this paper, we compared a standard vaccination model without behavioral feedback (SEIRV) to a behavioral variant (SEIRbV) to examine how endogenous risk response alters conclusions about optimal vaccination coverage, speed, and age-based allocation. Study 1 focused on a single, homogeneous population; Study 2 extended the analysis to an age-stratified population where vaccines can be directed toward younger, high-contact individuals or older, high-risk individuals.

At one level, the importance of model structure is obvious. Any statistician will recognize that mis-specifying feedback between risk, perception, and behavior can bias parameter estimates and policy recommendations. Yet all models simplify, and the practical question is which simplifications matter. Building on our previous work on delay estimation in behavioral epidemic models, we embedded a simple perception-and-response loop into an otherwise conventional SEIRV framework. Perceived risk adjusts toward the observed death rate with a delay and then feeds back into a contact multiplier that scales transmission. Rather than proposing a fully realistic behavioral theory, we used this stylized mechanism to ask a narrower question: to what extent does including behavioral feedback change what the model recommends about vaccination policies?

Study 1 shows that incorporating behavioral feedback substantially reshapes the vaccination policy landscape. In both SEIRV and SEIRbV, there is a clear tipping frontier in the coverage capacity space beyond which peak infections and deaths in the simulation window essentially drop to zero; below that frontier, increases in coverage and capacity yield large but rapidly diminishing gains. However, SEIRV underestimates how much coverage is needed to reach this frontier: it suggests control around 60% coverage, whereas SEIRbV requires closer to 70%. SEIRbV also reveals more structure in vaccination capacity: small changes in capacity (for example, from 0.005 to 0.006) generate visible improvements even at full coverage, whereas

SEIRV tends to smooth over these differences. At the same time, SEIRV overestimates the severity of the epidemic relative to SEIRbV, producing much higher peaks in infections and deaths because it ignores risk-driven contact reductions. Once the system is above the tipping frontier, additional vaccination in SEIRbV mainly accelerates the return of contact rates toward normal levels, suggesting that in this regime the marginal benefit of extra doses is primarily economic and social rather than purely epidemiological. Finally, the value of starting vaccination earlier depends strongly on vaccination speed: when capacity is low, shifting the start date forward has limited impact, but at higher speeds an earlier start can more than halve total deaths.

Study 2 adds an age structure and highlights how behavioral feedback interacts with prioritization rules. In the baseline age-stratified simulations, young-first strategies (vaccinating younger, high-contact individuals) are more effective at reducing infections and lowering peak incidence, because they dampen transmission in the most connected part of the network. Old-first strategies (vaccinating older, high-risk individuals) produce larger immediate reductions in deaths, especially when vaccination speed is limited. Thus, each allocation rule has clear strengths and weaknesses: young-first policies excel at controlling spread, while old-first policies excel at directly reducing mortality.

The sensitivity analyses over 1 and 10-year horizons reveal that SEIRV and SEIRbV differ not only in levels but also in how policy rankings evolve over time. In SEIRV, the qualitative patterns at 1 year largely persist at 10 years: the relative ordering of young-first and old-first allocations is stable, and longer horizons mainly scale up the same underlying relationships. In SEIRbV, by contrast, extending the horizon from 1 to 10 years leads to substantial increases in total cases and deaths and to pronounced changes in the shapes of the policy curves, reflecting repeated waves and the cumulative effects of behavioral adaptation.

Within SEIRV, allocation to older adults matters most when vaccination speed is low: elderly-first strategies reduce deaths more than young-first strategies, because they directly protect those most likely to die. As speed increases, that advantage shrinks, and purely young-first policies can perform nearly as well, since rapid vaccination of high-contact individuals quickly suppresses transmission. In SEIRbV, however, vaccination speed clearly dominates age allocation. The differences between young-first and old-first strategies are modest compared to the differences induced by changing vaccination speed. As speed increases, deaths fall sharply and consistently, and the number of lives saved by vaccinating faster is larger than the gap between any two allocation rules. This pattern becomes especially clear when we compare the worst and best policies as a function of speed: in SEIRbV, these lines lie close together and both follow a steep downward trajectory, indicating that “how fast” is more consequential than “who first” in a behaviorally responsive epidemic. This is the central finding of Study 2.

Our findings speak to, and extend, three strands of existing work. First, in the vaccination prioritization literature, most compartmental and statistical models that treat behavior as fixed conclude that older adults or other high-risk groups should be vaccinated first to minimize deaths e.g., (Bubar et al., 2021; Buckner et al., 2021; Fitzpatrick & Galvani, 2021; Goldstein et al., 2021; Jentsch et al., 2021; Lipsitch & Dean, 2020; Moore et al., 2021). Our SEIRV results broadly reproduce this pattern: when vaccination speed is limited and contact rates are exogenous, prioritizing older adults yields the largest mortality reductions. However, by

embedding the same prioritization problem in a behavioral SEIRbV model, we show that this ranking is not robust once risk-driven contact changes are considered. In the behavioral setting, age-prioritization rules still matter, but their impact is dominated by vaccination speed, and young-first strategies can perform nearly as well as old-first strategies at realistic levels of capacity.

Second, our study connects this prioritization literature to the growing work on behavioral epidemic models that endogenize risk perception and contact reduction (Bagnoli et al., 2007; Fenichel et al., 2011; Funk et al., 2010; LeJeune et al., 2024; Osi & Ghaffarzadegan, 2024; Rahmandad et al., 2021; Rahmandad et al., 2022b; Verelst et al., 2016; G. Zhang et al., 2025). Those studies demonstrate that ignoring behavioral feedback can misestimate basic epidemiological quantities and produce puzzles around under-reporting, multiple waves, and adherence fatigue. Our contribution is to show that the same omission can also distort normative conclusions about vaccination policy. By systematically comparing a conventional SEIRV model to a behavioral SEIRbV counterpart under the same disease, vaccine, and capacity assumptions, we quantify how behavioral feedback shifts the coverage threshold for epidemic control, reshapes the payoff to faster rollout, and changes the relative importance of age-based prioritization versus speed.

Third, our results complement prior work that uses behavioral models to argue for vaccinating high-contact groups earlier (Gallagher et al., 2021; Rahmandad, 2022) and policy reports emphasizing both equity and speed in vaccine allocation (Bavel et al., 2020; National Academies of Sciences & Medicine, 2020; WHO, 2000). Relative to those studies, we contribute (i) a unified framework that analyzes coverage, speed, and age allocation in both homogeneous and age-structured populations; (ii) a systematic exploration of how behavioral feedback alters the "tipping frontier" in coverage–capacity space; and (iii) a direct comparison of the marginal benefits of speeding up vaccination versus fine-tuning prioritization rules over both one-year and ten-year horizons. In that sense, our work helps bridge the gap between theoretical behavioral epidemic models and the practical optimization questions that dominate the vaccination policy literature.

Framed in terms of the competing logics emphasized in the vaccine prioritization literature, our results help reconcile why different modeling traditions reach different recommendations. Under fixed-contact assumptions, the "direct protection" school, prioritizing those at highest clinical risk, naturally dominates mortality objectives, consistent with age–severity gradients and with many age-structured allocation studies that favor older-first strategies for minimizing deaths and years of life lost (Bubar et al., 2021; Goldstein et al., 2021; Jentsch et al., 2021; Lipsitch & Dean, 2020; Moore et al., 2021). At the same time, the "indirect protection" school, prioritizing groups that sustain transmission (often high-contact or essential-worker groups), can outperform age-only rules when vaccines meaningfully reduce infection or when contact opportunities differ by occupation (Buckner et al., 2021; Fitzpatrick & Galvani, 2021; Gallagher et al., 2021). Our contribution is to show that once risk-responsive behavior is endogenized, the relative gains from choosing one prioritization rule over another can compress, while investments that increase rollout speed become a more robust driver of outcomes across both logics, suggesting that policy debates centered narrowly on "young-first vs old-first" may be less consequential than expanding

delivery capacity, even as ethical and equity-oriented frameworks continue to shape which groups should not be left behind in practice.

Taken together, these comparisons suggest that our main qualitative conclusions, higher coverage thresholds than SEIRV would imply, strong complementarities between early start and high speed, and the dominance of rollout speed over age-based prioritization in behaviorally responsive epidemics, are not simply restatements of existing results, but extensions that arise specifically from integrating behavioral feedback into vaccination policy analysis

These results have several implications for vaccination policy design. First, behavioral dynamics can shift both the estimated coverage threshold for epidemic control and the marginal value of increasing capacity, making it risky to base coverage targets or capacity planning on models with fixed contact rates. Second, in populations that respond to risk, vaccination can deliver large indirect economic and social benefits by enabling a faster and safer return to normal contact patterns, even when the marginal gains in avoided deaths are small. Third, our age-structured results suggest that policy debates that focus narrowly on young- versus old-first prioritization may be incomplete: when behavioral feedback is taken seriously, building capacity to vaccinate quickly can dominate the gains from fine-tuning age priorities, particularly over longer horizons.

Our analysis is deliberately stylized. We work with a homogeneous population in Study 1 and a simple two-group age structure in Study 2, hold disease and vaccine parameters fixed, and represent behavior through a single perception delay and contact-response function. Real epidemics involve heterogeneous networks, spatial clustering, waning immunity, evolving variants, and richer behavioral patterns, including asymmetric responses to rising versus falling risk and the influence of information, norms, and trust. Future work should combine empirical estimation of delay and response structures with more detailed population heterogeneity and extend the objective function to include equity, fairness, and political feasibility alongside epidemiological and economic outcomes. Even within these simplifications, our results reinforce a central message from both this paper and our earlier work on delay estimation: behavior is not a nuisance add-on, but a core mechanism shaping optimal vaccination strategies. Accounting for how people respond to risk can change both parameter estimates and which policies appear best and should therefore be a standard ingredient in the design and evaluation of vaccination programs.

4.7. Acknowledgment

This research is funded by the US National Science Foundation, Division of Mathematical Sciences and Division of Social and Economic Sciences (Award No. 2229819).

4.8. Appendix

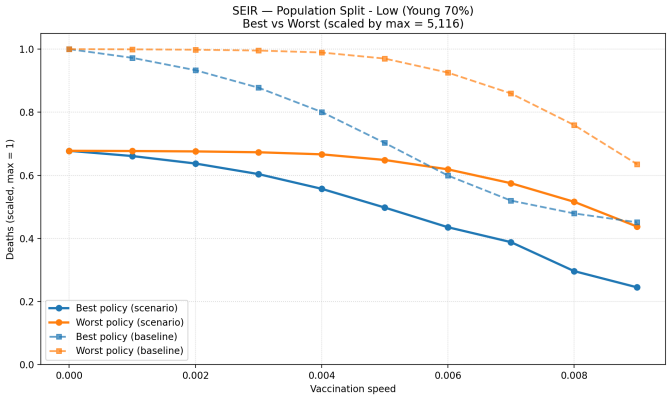

(A) Normalized deaths vs vaccination speed in SEIRV for one year: best vs worst policy Population split low

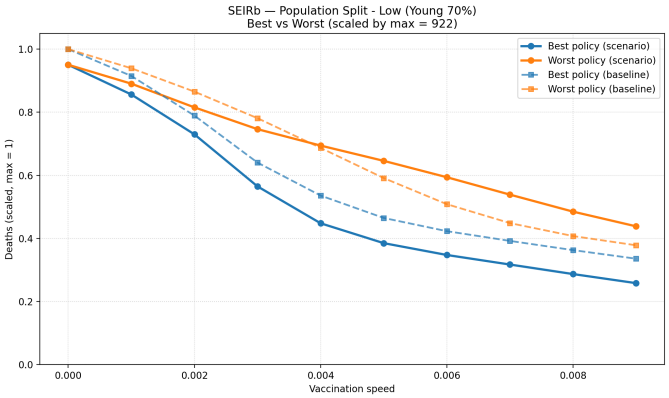

(B) Normalized deaths vs vaccination speed in SEIRbV for one year: best vs worst policy Population split low

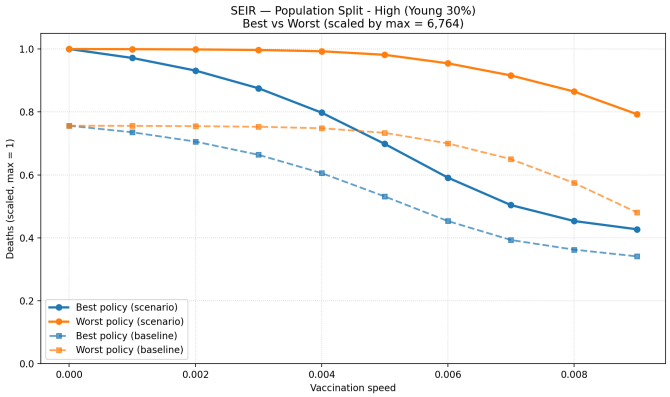

(C) Normalized deaths vs vaccination speed in SEIRV for one year: best vs worst policy Population split high

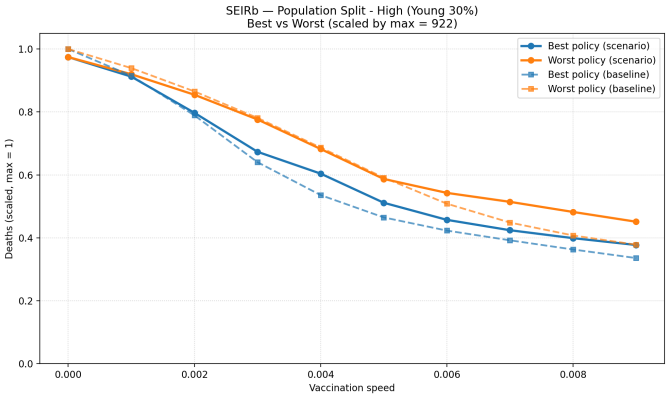

(D) Normalized deaths vs vaccination speed in SEIRbV for one year: best vs worst policy Population split high

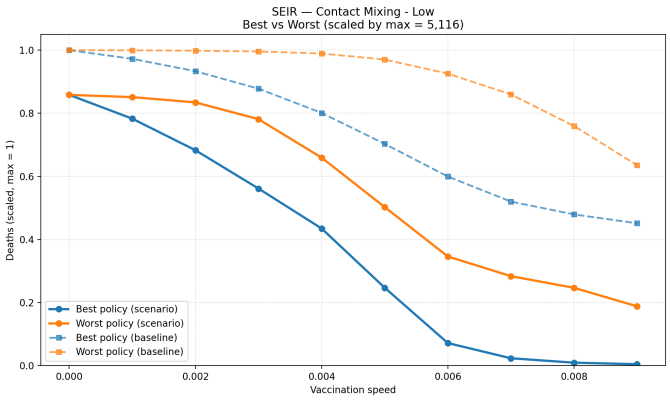

(E) Normalized deaths vs vaccination speed in SEIRV for ten years: best vs worst policy Contact mixing low

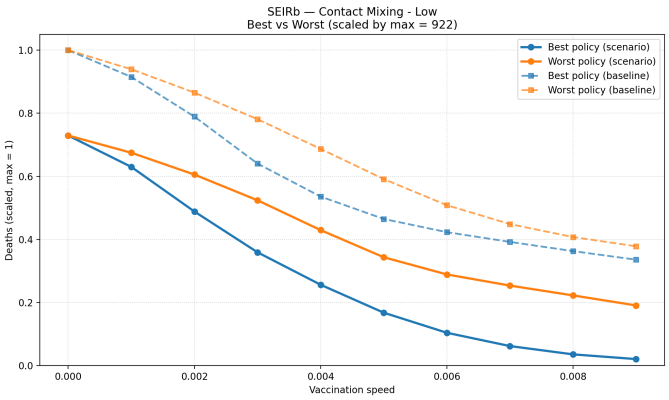

(F) Normalized deaths vs vaccination speed in SEIRbV for ten years: best vs worst policy Contact mixing low

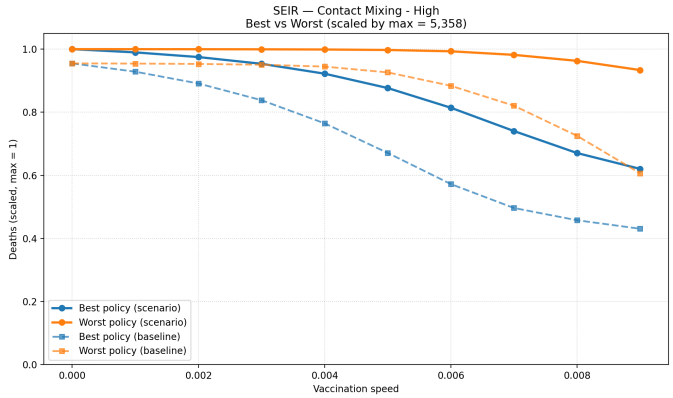

(G) Normalized deaths vs vaccination speed in SEIRV for one year: best vs worst policy Contact mixing high

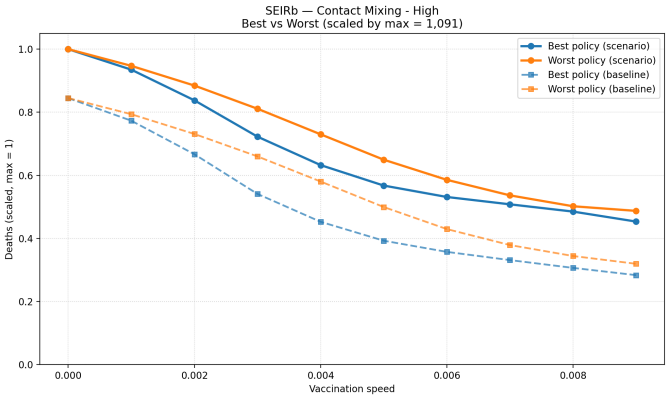

(H) Normalized deaths vs vaccination speed in SEIRbV for one year: best vs worst policy Contact mixing high

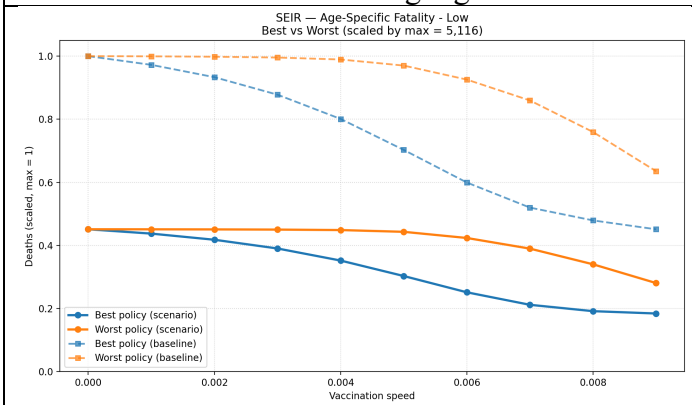

(I) Normalized deaths vs vaccination speed in SEIRV for one year: best vs worst policy Age specific fatality low

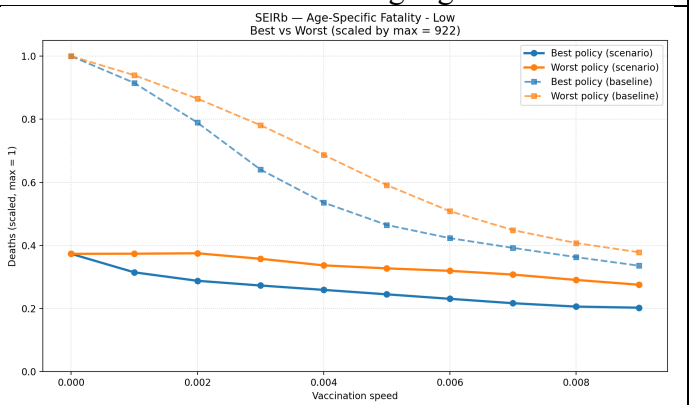

(J) Normalized deaths vs vaccination speed in SEIRV for one year: best vs worst policy Age specific fatality low

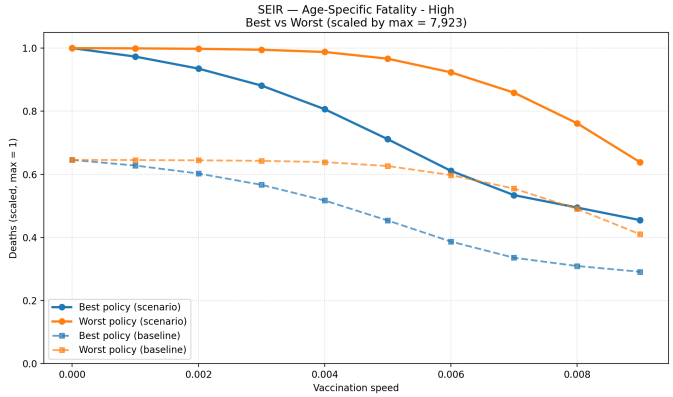

(K) Normalized deaths vs vaccination speed in SEIRV for one year: best vs worst policy Age specific fatality high

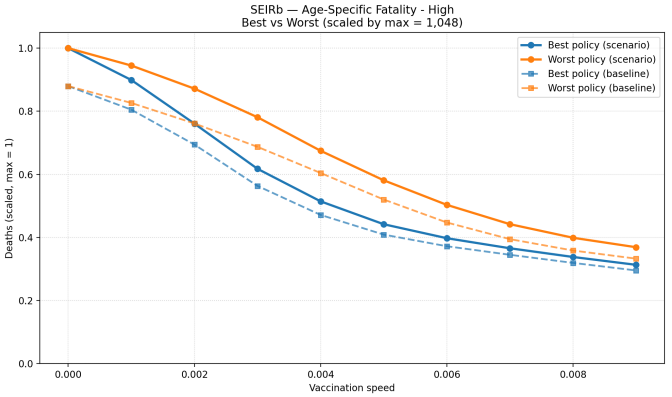

(L) Normalized deaths vs vaccination speed in SEIRV for one year: best vs worst policy Age specific fatality high

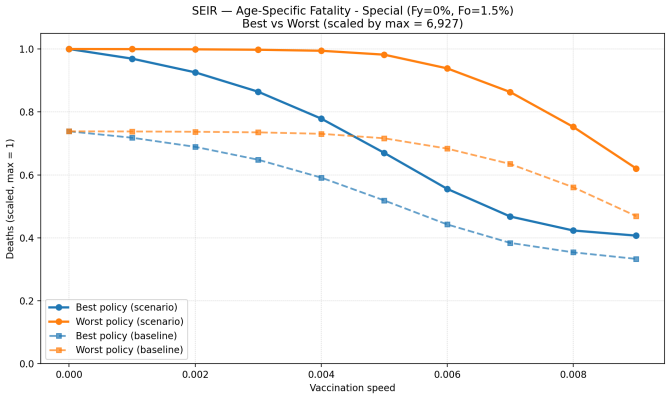

(M) Normalized deaths vs vaccination speed in SEIRV for one year: best vs worst policy fatality low for young high for old

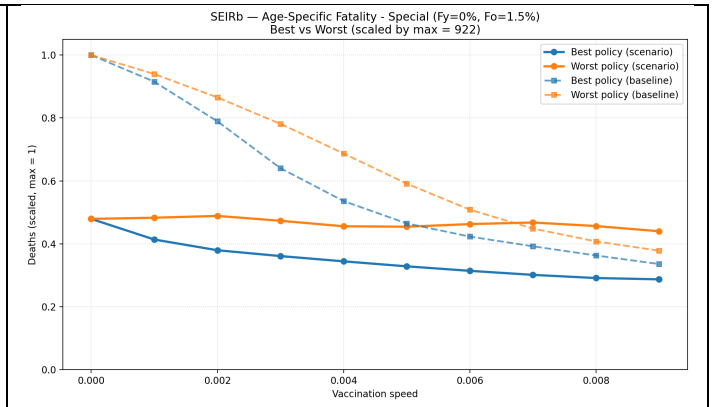

(N) Normalized deaths vs vaccination speed in SEIRV for one year: best vs worst policy fatality low for young high for old

Figure 5.15. Analyzing vaccination speed vs Young-Old priority policies. Sensitivity analyses for variating population split, contact mixing, and age specific fatality

4.9. References

Bagnoli, F., Lio, P., & Sguanci, L. (2007). Risk perception in epidemic modeling. *Physical Review E—Statistical, Nonlinear, and Soft Matter Physics*, *76*(6), 061904.

Bavel, J. J. V., Baicker, K., Boggio, P. S., Capraro, V., Cichocka, A., Cikara, M., Crockett, M. J., Crum, A. J., Douglas, K. M., & Druckman, J. N. (2020). Using social and behavioural science to support COVID-19 pandemic response. *Nature Human Behaviour*, *4*(5), 460-471.

Bruch, E., & Atwell, J. (2015). Agent-based models in empirical social research. *Sociological methods & research*, *44*(2), 186-221.

Bubar, K. M., Reinholt, K., Kissler, S. M., Lipsitch, M., Cobey, S., Grad, Y. H., & Larremore, D. B. (2021). Model-informed COVID-19 vaccine prioritization strategies by age and serostatus. *Science*, *371*(6352), 916-921.

Buckner, J. H., Chowell, G., & Springborn, M. R. (2021). Dynamic prioritization of COVID-19 vaccines when social distancing is limited for essential workers. *Proceedings of the National Academy of Sciences*, *118*(16), e2025786118.

Fenichel, E. P., Castillo-Chavez, C., Ceddia, M. G., Chowell, G., Parra, P. A. G., Hickling, G. J., Holloway, G., Horan, R., Morin, B., Perrings, C., Springborn, M., Velazquez, L., & Villalobos, C. (2011). Adaptive human behavior in epidemiological models. *Proceedings of the National Academy of Sciences*, *108*(15), 6306-6311. https://doi.org/10.1073/pnas.1011250108

Ferguson, N. M., Laydon, D., Nedjati-Gilani, G., Imai, N., Ainslie, K., Baguelin, M., Bhatia, S., Boonyasiri, A., Cucunubá, Z., & Cuomo-Dannenburg, G. (2020). *Report 9: Impact of non-pharmaceutical interventions (NPIs) to reduce COVID19 mortality and healthcare demand* (Vol. 16). Imperial College London London.

Fitzpatrick, M. C., & Galvani, A. P. (2021). Optimizing age-specific vaccination. *Science*, *371*(6532), 890-891.

Funk, S., Salathé, M., & Jansen, V. A. A. (2010). Modelling the influence of human behaviour on the spread of infectious diseases: a review. *Journal of The Royal Society Interface*, *7*(50), 1247-1256. https://doi.org/10.1098/rsif.2010.0142

Gallagher, M. E., Sieben, A. J., Nelson, K. N., Kraay, A. N., Orenstein, W. A., Lopman, B., Handel, A., & Koelle, K. (2021). Indirect benefits are a crucial consideration when evaluating SARS-CoV-2 vaccine candidates. *Nature medicine*, *27*(1), 4-5.

Goldstein, J. R., Cassidy, T., & Wachter, K. W. (2021). Vaccinating the oldest against COVID-19 saves both the most lives and most years of life. *Proceedings of the National Academy of Sciences*, *118*(11), e2026322118.

Jentsch, P. C., Anand, M., & Bauch, C. T. (2021). Prioritising COVID-19 vaccination in changing social and epidemiological landscapes: a mathematical modelling study. *The Lancet Infectious Diseases*, *21*(8), 1097-1106.

Kamran, A., Isazadehfar, K., Heydari, H., Azgomi, R. N. D., & Naeim, M. (2021). Risk perception and adherence to preventive behaviours related to the COVID-19 pandemic: a community-based study applying the health belief model. *BJPsych Open*, *7*(4), e133.

LeJeune, L., Ghaffarzadegan, N., Childs, L. M., & Saucedo, O. (2024). Mathematical analysis of simple behavioral epidemic models. *Mathematical biosciences*, *375*, 109250.

LeJeune, L., Ghaffarzadegan, N., Childs, L. M., & Saucedo, O. (2025). Formulating human risk response in epidemic models: exogenous vs endogenous approaches. *European Journal of Operational Research*.

Levin, A. T., Hanage, W. P., Owusu-Boaitey, N., Cochran, K. B., Walsh, S. P., & Meyerowitz-Katz, G. (2020). Assessing the age specificity of infection fatality rates for COVID-19: systematic review, meta-analysis, and public policy implications. *European journal of epidemiology*, *35*(12), 1123-1138.

Lipsitch, M., & Dean, N. E. (2020). Understanding COVID-19 vaccine efficacy. *Science*, *370*(6518), 763-765.

Masters, N. B., Shih, S.-F., Bukoff, A., Akel, K. B., Kobayashi, L. C., Miller, A. L., Harapan, H., Lu, Y., & Wagner, A. L. (2020). Social distancing in response to the novel coronavirus (COVID-19) in the United States. *Plos One*, *15*(9), e0239025.

Matrajt, L., Eaton, J., Leung, T., & Brown, E. R. (2021). Vaccine optimization for COVID-19: Who to vaccinate first? *Science Advances*, *7*(6), eabf1374.

Moore, S., Hill, E. M., Dyson, L., Tildesley, M. J., & Keeling, M. J. (2021). Modelling optimal vaccination strategy for SARS-CoV-2 in the UK. *PLOS Computational Biology*, *17*(5), e1008849.

Mossong, J., Hens, N., Jit, M., Beutels, P., Auranen, K., Mikolajczyk, R., Massari, M., Salmaso, S., Tomba, G. S., & Wallinga, J. (2008). Social contacts and mixing patterns relevant to the spread of infectious diseases. *PLoS medicine*, *5*(3), e74.

National Academies of Sciences, E., & Medicine. (2020). Framework for equitable allocation of COVID-19 vaccine.

O'Driscoll, M., Ribeiro Dos Santos, G., Wang, L., Cummings, D. A., Azman, A. S., Paireau, J., Fontanet, A., Cauchemez, S., & Salje, H. (2021). Age-specific mortality and immunity patterns of SARS-CoV-2. *Nature*, *590*(7844), 140-145.

Osi, A., & Ghaffarzadegan, N. (2024). Parameter estimation in behavioral epidemic models with endogenous societal risk-response. *PLoS Computational Biology. In-press.*

Prem, K., Cook, A. R., & Jit, M. (2017). Projecting social contact matrices in 152 countries using contact surveys and demographic data. *PLOS Computational Biology*, *13*(9), e1005697.

Rahmandad, H. (2022). Behavioral responses to risk promote vaccinating high-contact individuals first. *System Dynamics Review*, *38*(3), 246-263.
Rahmandad, H., Lim, T. Y., & Sterman, J. (2021). Behavioral dynamics of COVID-19: estimating underreporting, multiple waves, and adherence fatigue across 92 nations. *System Dynamics Review*, *37*(1), 5-31.
Rahmandad, H., Xu, R., & Ghaffarzadegan, N. (2022). A missing behavioural feedback in COVID-19 models is the key to several puzzles. *BMJ Glob Health*, *7*(10). https://doi.org/10.1136/bmjgh-2022-010463
Rumain, B., Schneiderman, M., & Geliebter, A. (2021). Prevalence of COVID-19 in adolescents and youth compared with older adults in states experiencing surges. *Plos One*, *16*(3), e0242587.
van Heusden, K., Stewart, G. E., Otto, S. P., & Dumont, G. A. (2023). Effective pandemic policy design through feedback does not need accurate predictions. *PLOS Global Public Health*, *3*(2), e0000955.
Verelst, F., Willem, L., & Beutels, P. (2016). Behavioural change models for infectious disease transmission: a systematic review (2010–2015). *Journal of The Royal Society Interface*, *13*(125), 20160820. https://doi.org/10.1098/rsif.2016.0820
WHO. (2000). *The world health report 2000: health systems: improving performance*. World Health Organization.
Wrigley-Field, E., Kiang, M. V., Riley, A. R., Barbieri, M., Chen, Y.-H., Duchowny, K. A., Matthay, E. C., Van Riper, D., Jegathesan, K., & Bibbins-Domingo, K. (2021). Geographically targeted COVID-19 vaccination is more equitable and averts more deaths than age-based thresholds alone. *Science Advances*, *7*(40), eabj2099.
Zhang, G., Osi, A., Ghaffarzadegan, N., Rahmandad, H., & Xu, R. (2025). Identifying delayed human response to external risks: an econometric analysis of mobility change during a pandemic. *BMC Medical Research Methodology*, *25*(1), 244.
Zhang, Z., Jalali, M. S., & Ghaffarzadegan, N. (2025). Behavioral Dynamics of Epidemic Trajectories and Vaccination Strategies: A Simulation-Based Analysis. *Journal of Artificial Societies and Social Simulation*, *28*(1).

5. Conclusion

This dissertation set out to enhance our understanding of behavioral responses in epidemic settings by focusing on a central, but often under-specified mechanism: the delays through which people perceive risk and translate that perception into changes in behavior and policy. Across the three essays, I argue that behavioral feedback is not merely a contextual complication; it is a structural feature of epidemic dynamics. When delays and feedbacks are ignored or simplified too aggressively, both empirical inference and policy evaluation can become unreliable. By combining synthetic experiments, empirical mobility analysis, and behavioral epidemic modeling for vaccination policy, the dissertation develops a coherent toolkit for incorporating delay structures into estimation and for evaluating how those structures shape optimal interventions.

The three essays are intentionally sequenced to move from identification to application. Essay 1 begins with the basic question of whether overlooking delays biases the estimation of human response, using mobility as a key behavioral indicator. Essay 2 then demonstrates that it is not enough to "add a lag": the assumed length, shape, and symmetry of perception delays can meaningfully alter conclusions about responsiveness, including whether people react differently when risk is rising versus falling. Essay 3 extends these insights to policy design, showing that when behavioral responses are endogenous and delayed, optimal vaccination strategies can shift in systematic ways. Together, the dissertation connects empirical measurement of behavioral response to decision-making: the way we estimate behavior influences the way we rank and design policies.

Essay 1 demonstrates that immediate-association approaches to mobility estimation can be misleading when risk signals diffuse through a system with time delays. Using a controlled synthetic setting, the essay shows that accounting for delay is essential for recovering both the magnitude of response (e.g., sensitivity to mortality risk) and the timing of that response. Importantly, the results highlight that a fixed-lag approach may improve fit yet still fail to recover the correct underlying behavioral mechanism if the true delay is distributed over time. To address this, Essay 1 introduces a regression-based delay representation grounded in the Erlang family of distributions and provides a practical algorithm for incorporating and estimating delay structures within common empirical workflows. The broader contribution is methodological: the framework offers a systematic way to reduce bias in time-series estimation when delayed responses are present, with applications that extend beyond epidemics to many domains where perception and action adjust gradually.

Essay 2 builds on this foundation by showing that the structure of delay, its length, order/shape, and potential asymmetry is not a technical detail but a substantive modeling choice that can change inference. Through synthetic experiments with known ground truth, the essay demonstrates how mis-specifying delay structure can generate biased estimates of the parameters researchers often care about most, such as how responsive behavior is to risk. It then applies these ideas to U.S. state-level COVID-19 mobility data, illustrating that alternative assumptions about delay structure lead to different conclusions about public sensitivity and about how quickly mobility adjusts when risk increases versus declines. To make delay identification tractable, the essay advances a two-step approach: constructing perceived risk from candidate delay structures and then estimating response parameters using standard regression tools, iterating to select the delay structure that best fits the data. By also benchmarking against flexible econometric alternatives such as ARDL-type approaches, the essay clarifies an important trade-off between flexibility and interpretability: highly flexible lag models may fit well, but they do not necessarily preserve the mechanistic meaning of delay parameters, and they can become difficult to extend to asymmetric responses.

Essay 3 shifts from measurement to intervention, asking whether incorporating endogenous behavioral response changes optimal vaccination policies and, crucially, how much it changes

them. Using a behavioral SEIRbV framework in which perceived risk reduces contact rates with a perception delay, the essay compares outcomes to a conventional SEIRV model with constant contacts. The analysis shows that behavioral feedback can alter both the thresholds required for suppression and the relative value of competing policy levers. In particular, when behavior responds to perceived risk, vaccination speed and early rollout can become especially valuable, sometimes outweighing the gains from switching among prioritization rules. This logic extends to an age-stratified setting: allocating doses between younger high-contact and older high-risk groups changes outcomes, but the presence of behavioral feedback can make the timing and pace of vaccination even more consequential for mortality reduction than the choice of "young-first" versus "old-first" strategies across a wide range of conditions. The broader implication is that vaccination policy evaluation should treat behavior as endogenous: policies shape disease trajectories, trajectories shape perceptions, and perceptions shape behavior in ways that feed back into policy effectiveness.

Across the three essays, the dissertation makes several integrated contributions. First, it provides a rigorous empirical framework for representing and estimating perception delays, emphasizing that distributed and asymmetric delay structures are often plausible and empirically consequential. Second, it demonstrates, using both synthetic ground-truth experiments and real mobility data that delay misspecification can bias behavioral parameter estimates and therefore distort our understanding of how quickly and how strongly people respond to risk. Third, it connects these estimation insights to policy design by showing that delayed behavioral feedback can change which vaccination strategies appear optimal and can shift attention toward levers such as earlier starts and higher rollout capacity. In combination, these contributions support a single overarching message: accurate modeling of behavioral feedback and delay is a prerequisite for both credible inference and credible policy evaluation in epidemic settings.

This dissertation also points to several directions for future work. Empirically, richer data sources and multiple risk signals could be incorporated to better distinguish perception, information diffusion, and action mechanisms, and to quantify heterogeneity across populations and contexts. Methodologically, delay identification could be embedded within broader joint-estimation frameworks that treat epidemiological and behavioral parameters simultaneously and provide uncertainty bounds on delay structure. Substantively, policy evaluation could extend beyond stylized settings to account for realistic population heterogeneity, spatial clustering, changing variants, waning immunity, and richer behavioral dynamics, including more complex asymmetries and the role of information environments, norms, and trust. Finally, the optimization framework could be expanded to incorporate equity, fairness, and political feasibility in addition to epidemiological and economic outcomes, recognizing that real vaccination programs are judged on multiple criteria.

In sum, the dissertation advances the study of behavioral-disease interactions by bringing delay structures to the forefront of both empirical modeling and policy analysis. By demonstrating how delay assumptions shape parameter estimates and how endogenous behavior reshapes optimal

vaccination choices, the three essays collectively move the field toward more realistic and policy-relevant epidemic modeling. A more faithful representation of behavioral feedbacks and delays can improve forecasting, sharpen causal inference, and better inform interventions, ultimately contributing to more effective public health responses and lives saved.

6. References

Abouk, R., & Heydari, B. (2021). The immediate effect of COVID-19 policies on social-distancing behavior in the United States. *Public health reports*, *136*(2), 245-252.

Almon, S. (1965). The distributed lag between capital appropriations and expenditures. *Econometrica: journal of the Econometric Society*, 178-196.

Arthur, R. F., Gurley, E. S., Salje, H., Bloomfield, L. S. P., & Jones, J. H. (2017). Contact structure, mobility, environmental impact and behaviour: the importance of social forces to infectious disease dynamics and disease ecology [Review]. *Philosophical Transactions of the Royal Society B-Biological Sciences*, *372*(1719), 9, Article 20160454. https://doi.org/10.1098/rstb.2016.0454

Bagnoli, F., Lio, P., & Sguanci, L. (2007). Risk perception in epidemic modeling. *Physical Review E—Statistical, Nonlinear, and Soft Matter Physics*, *76*(6), 061904.

Bao, H., Zhou, X., Zhang, Y., Li, Y., & Xie, Y. (2020). Covid-gan: Estimating human mobility responses to covid-19 pandemic through spatio-temporal conditional generative adversarial networks. Proceedings of the 28th international conference on advances in geographic information systems,

Bauch, C. T., & Galvani, A. P. (2013). Social Factors in Epidemiology. *Science*, *342*(6154), 47-49. https://doi.org/10.1126/science.1244492

Bavel, J. J. V., Baicker, K., Boggio, P. S., Capraro, V., Cichocka, A., Cikara, M., Crockett, M. J., Crum, A. J., Douglas, K. M., & Druckman, J. N. (2020). Using social and behavioural science to support COVID-19 pandemic response. *Nature Human Behaviour*, *4*(5), 460-471.

Bergman, N. K., & Fishman, R. (2023). Correlations of mobility and Covid-19 transmission in global data. *Plos One*, *18*(7), e0279484.

Bian, Z., Zuo, F., Gao, J., Chen, Y., Venkata, S. S. C. P., Bernardes, S. D., Ozbay, K., Ban, X. J., & Wang, J. (2021). Time lag effects of COVID-19 policies on transportation systems: A comparative study of New York City and Seattle. *Transportation Research Part A: Policy and Practice*, *145*, 269-283.

Box, G. E. (1976). Science and statistics. *Journal of the American Statistical Association*, *71*(356), 791-799.

Bruch, E., & Atwell, J. (2015). Agent-based models in empirical social research. *Sociological methods & research*, *44*(2), 186-221.

Bubar, K. M., Reinholt, K., Kissler, S. M., Lipsitch, M., Cobey, S., Grad, Y. H., & Larremore, D. B. (2021). Model-informed COVID-19 vaccine prioritization strategies by age and serostatus. *Science*, *371*(6352), 916-921.

Buckner, J. H., Chowell, G., & Springborn, M. R. (2021). Dynamic prioritization of COVID-19 vaccines when social distancing is limited for essential workers. *Proceedings of the National Academy of Sciences*, *118*(16), e2025786118.

Buonomo, B., Messina, E., Panico, C., & Vecchio, A. (2025). An integral renewal equation approach to behavioural epidemic models with information index. *Journal of Mathematical Biology*, *90*(1), 8.

Centers for Disease Control and Prevention, C.-R. (2023). Weekly United States COVID-19 Cases and Deaths by State.

Chang, S., Pierson, E., Koh, P. W., Gerardin, J., Redbird, B., Grusky, D., & Leskovec, J. (2021). Mobility network models of COVID-19 explain inequities and inform reopening. *Nature*, *589*(7840), 82-87.

Chernozhukov, V., Kasahara, H., & Schrimpf, P. (2021). Causal impact of masks, policies, behavior on early covid-19 pandemic in the US. *Journal of econometrics*, *220*(1), 23-62.

Childs, L., Dick, D. W., Feng, Z., Heffernan, J. M., Li, J., & Röst, G. (2022). Modeling waning and boosting of COVID-19 in Canada with vaccination. *Epidemics*, *39*, 100583.

De Boef, S., & Keele, L. (2008). Taking time seriously. *American journal of political science*, *52*(1), 184-200.

Dubey, P., Chen, Y., Gajardo, Á., Bhattacharjee, S., Carroll, C., Zhou, Y., Chen, H., & Müller, H.-G. (2022). Learning delay dynamics for multivariate stochastic processes, with application to the prediction of the growth rate of COVID-19 cases in the United States. *Journal of Mathematical Analysis and Applications*, *514*(2), 125677.

Espinoza, B., Saad-Roy, C. M., Grenfell, B. T., Levin, S. A., & Marathe, M. (2024). Adaptive human behaviour modulates the impact of immune life history and vaccination on long-term epidemic dynamics. *Proceedings B*, *291*(2033), 20241772.

Fang, Y., Nie, Y., & Penny, M. (2020). Transmission dynamics of the COVID-19 outbreak and effectiveness of government interventions: A data-driven analysis. *Journal of medical virology*, *92*(6), 645-659.

Feehan, D. M., & Mahmud, A. S. (2021). Quantifying population contact patterns in the United States during the COVID-19 pandemic. *Nature communications*, *12*(1), 893.

Fenichel, E. P., Castillo-Chavez, C., Ceddia, M. G., Chowell, G., Parra, P. A. G., Hickling, G. J., Holloway, G., Horan, R., Morin, B., Perrings, C., Springborn, M., Velazquez, L., & Villalobos, C. (2011). Adaptive human behavior in epidemiological models. *Proceedings of the National Academy of Sciences*, *108*(15), 6306-6311. https://doi.org/10.1073/pnas.1011250108

Feola, G. (2015). Societal transformation in response to global environmental change: A review of emerging concepts. *Ambio*, *44*(5), 376-390.

Ferguson, N. (2007). Capturing human behaviour. *Nature*, *446*(7137), 733-733. https://doi.org/10.1038/446733a

Ferguson, N. M., Laydon, D., Nedjati-Gilani, G., Imai, N., Ainslie, K., Baguelin, M., Bhatia, S., Boonyasiri, A., Cucunubá, Z., & Cuomo-Dannenburg, G. (2020). *Report 9: Impact of non-pharmaceutical interventions (NPIs) to reduce COVID19 mortality and healthcare demand* (Vol. 16). Imperial College London London.

Fitzpatrick, M. C., & Galvani, A. P. (2021). Optimizing age-specific vaccination. *Science*, *371*(6532), 890-891.
Forrester, J. W. (1961). Industrial dynamics mit press cambridge. *MA.[Google Scholar]*.
Funk, S., Bansal, S., Bauch, C. T., Eames, K. T. D., Edmunds, W. J., Galvani, A. P., & Klepac, P. (2015). Nine challenges in incorporating the dynamics of behaviour in infectious diseases models. *Epidemics*, *10*, 21-25. https://doi.org/https://doi.org/10.1016/j.epidem.2014.09.005
Funk, S., Salathé, M., & Jansen, V. A. A. (2010). Modelling the influence of human behaviour on the spread of infectious diseases: a review. *Journal of The Royal Society Interface*, *7*(50), 1247-1256. https://doi.org/10.1098/rsif.2010.0142
Gallagher, M. E., Sieben, A. J., Nelson, K. N., Kraay, A. N., Orenstein, W. A., Lopman, B., Handel, A., & Koelle, K. (2021). Indirect benefits are a crucial consideration when evaluating SARS-CoV-2 vaccine candidates. *Nature medicine*, *27*(1), 4-5.
Goldstein, J. R., Cassidy, T., & Wachter, K. W. (2021). Vaccinating the oldest against COVID-19 saves both the most lives and most years of life. *Proceedings of the National Academy of Sciences*, *118*(11), e2026322118.
Gonzalez, M. C., Hidalgo, C. A., & Barabasi, A.-L. (2008). Understanding individual human mobility patterns. *Nature*, *453*(7196), 779-782.
Google. (2024). Google COVID-19 Community Mobility Reports. https://www.google.com/covid19/mobility/
Griliches, Z. (1967). Distributed lags: A survey. *Econometrica: journal of the Econometric Society*, 16-49.
Guidotti, R., Monreale, A., Rinzivillo, S., Pedreschi, D., & Giannotti, F. (2016). Unveiling mobility complexity through complex network analysis. *Social Network Analysis and Mining*, *6*, 1-21.
Hamilton, J. D. (1994). Time Series Analysis. In: Princeton University Press.
Hamilton, M. S. (1980). Estimating lengths and orders of delays in system dynamics models. *Elements of the system dynamics method*, 162-182.
Hsiang, S., Allen, D., Annan-Phan, S., Bell, K., Bolliger, I., Chong, T., Druckenmiller, H., Huang, L. Y., Hultgren, A., & Krasovich, E. (2020). The effect of large-scale anti-contagion policies on the COVID-19 pandemic. *Nature*, *584*(7820), 262-267. https://www.nature.com/articles/s41586-020-2404-8.pdf
Huang, B., Wang, J., Cai, J., Yao, S., Chan, P. K. S., Tam, T. H.-w., Hong, Y.-Y., Ruktanonchai, C. W., Carioli, A., & Floyd, J. R. (2021). Integrated vaccination and physical distancing interventions to prevent future COVID-19 waves in Chinese cities. *Nature Human Behaviour*, *5*(6), 695-705. https://www.nature.com/articles/s41562-021-01063-2.pdf
Jentsch, P. C., Anand, M., & Bauch, C. T. (2021). Prioritising COVID-19 vaccination in changing social and epidemiological landscapes: a mathematical modelling study. *The Lancet Infectious Diseases*, *21*(8), 1097-1106.
Jiao, J., Bhat, M., & Azimian, A. (2021). Measuring travel behavior in Houston, Texas with mobility data during the 2020 COVID-19 outbreak. *Transportation Letters*, *13*(5-6), 461-472.

Kahneman, D., & Tversky, A. (1979). Prospect Theory: An Analysis of Decision under Risk. *Econometrica*, *47*(2), 263. https://doi.org/10.2307/1914185

Kamran, A., Isazadehfar, K., Heydari, H., Azgomi, R. N. D., & Naeim, M. (2021). Risk perception and adherence to preventive behaviours related to the COVID-19 pandemic: a community-based study applying the health belief model. *BJPsych Open*, *7*(4), e133.

Kripfganz, S., & Schneider, D. C. (2020). Response surface regressions for critical value bounds and approximate p-values in equilibrium correction models 1. *Oxford Bulletin of Economics and Statistics*, *82*(6), 1456-1481.

Kuligowski, E. D. (2008). Modeling human behavior during building fires.

LeJeune, L., Ghaffarzadegan, N., Childs, L. M., & Saucedo, O. (2024). Mathematical analysis of simple behavioral epidemic models. *Mathematical biosciences*, *375*, 109250.

LeJeune, L., Ghaffarzadegan, N., Childs, L. M., & Saucedo, O. (2025). Formulating human risk response in epidemic models: exogenous vs endogenous approaches. *European Journal of Operational Research*.

Levin, A. T., Hanage, W. P., Owusu-Boaitey, N., Cochran, K. B., Walsh, S. P., & Meyerowitz-Katz, G. (2020). Assessing the age specificity of infection fatality rates for COVID-19: systematic review, meta-analysis, and public policy implications. *European journal of epidemiology*, *35*(12), 1123-1138.

Li, W., Wang, Q., Liu, Y., Small, M. L., & Gao, J. (2022). A spatiotemporal decay model of human mobility when facing large-scale crises. *Proceedings of the National Academy of Sciences*, *119*(33), e2203042119.

Lim, T. Y., Xu, R., Ruktanonchai, N., Saucedo, O., Childs, L. M., Jalali, M. S., Rahmandad, H., & Ghaffarzadegan, N. (2023). Why Similar Policies Resulted In Different COVID-19 Outcomes: How Responsiveness And Culture Influenced Mortality Rates: Study examines why similar policies resulted in different COVID-19 outcomes in using data from more than 100 countries. *Health Affairs*, *42*(12), 1637-1646.

Lipsitch, M., & Dean, N. E. (2020). Understanding COVID-19 vaccine efficacy. *Science*, *370*(6518), 763-765.

Liu, H., Wang, J., Liu, J., Ge, Y., Wang, X., Zhang, C., Cleary, E., Ruktanonchai, N. W., Ruktanonchai, C. W., & Yao, Y. (2023). Combined and delayed impacts of epidemics and extreme weather on urban mobility recovery. *Sustainable Cities and Society*, 104872.

Mahmud, M. S., Eshun, S., Espinoza, B., & Kadelka, C. (2024). Adaptive human behavior and delays in information availability autonomously modulate epidemic waves. *medRxiv*, 2024.2011. 2023.24317838.

Masters, N. B., Shih, S.-F., Bukoff, A., Akel, K. B., Kobayashi, L. C., Miller, A. L., Harapan, H., Lu, Y., & Wagner, A. L. (2020). Social distancing in response to the novel coronavirus (COVID-19) in the United States. *Plos One*, *15*(9), e0239025.

Matrajt, L., Eaton, J., Leung, T., & Brown, E. R. (2021). Vaccine optimization for COVID-19: Who to vaccinate first? *Science Advances*, *7*(6), eabf1374.

Moore, S., Hill, E. M., Dyson, L., Tildesley, M. J., & Keeling, M. J. (2021). Modelling optimal vaccination strategy for SARS-CoV-2 in the UK. *PLOS Computational Biology*, *17*(5), e1008849.
Mossong, J., Hens, N., Jit, M., Beutels, P., Auranen, K., Mikolajczyk, R., Massari, M., Salmaso, S., Tomba, G. S., & Wallinga, J. (2008). Social contacts and mixing patterns relevant to the spread of infectious diseases. *PLoS medicine*, *5*(3), e74.
Narayan, P. K. (2005). The saving and investment nexus for China: evidence from cointegration tests. *Applied economics*, *37*(17), 1979-1990.
National Academies of Sciences, E., & Medicine. (2020). Framework for equitable allocation of COVID-19 vaccine.
O'Driscoll, M., Ribeiro Dos Santos, G., Wang, L., Cummings, D. A., Azman, A. S., Paireau, J., Fontanet, A., Cauchemez, S., & Salje, H. (2021). Age-specific mortality and immunity patterns of SARS-CoV-2. *Nature*, *590*(7844), 140-145.
Okada, M., Yamanishi, K., & Masuda, N. (2020). Long-tailed distributions of inter-event times as mixtures of exponential distributions. *Royal Society open science*, *7*(2), 191643.
Oraby, T., Tyshenko, M. G., Maldonado, J. C., Vatcheva, K., Elsaadany, S., Alali, W. Q., Longenecker, J. C., & Al-Zoughool, M. (2021). Modeling the effect of lockdown timing as a COVID-19 control measure in countries with differing social contacts. *Scientific reports*, *11*(1), 3354.
Osi, A., & Ghaffarzadegan, N. (2024). Parameter estimation in behavioral epidemic models with endogenous societal risk-response. *PLoS Computational Biology. In-press*.
Pardo-Araujo, M., García-García, D., Alonso, D., & Bartumeus, F. (2023). Epidemic thresholds and human mobility. *Scientific reports*, *13*(1), 11409.
Perra, N. (2021). Non-pharmaceutical interventions during the COVID-19 pandemic: A review. *Phys Rep*, *913*, 1-52. https://doi.org/10.1016/j.physrep.2021.02.001
Pesaran, M. H., Shin, Y., & Smith, R. J. (2001). Bounds testing approaches to the analysis of level relationships. *Journal of applied econometrics*, *16*(3), 289-326.
Prem, K., Cook, A. R., & Jit, M. (2017). Projecting social contact matrices in 152 countries using contact surveys and demographic data. *PLOS Computational Biology*, *13*(9), e1005697.
Rahmandad, H. (2022). Behavioral responses to risk promote vaccinating high-contact individuals first. *System Dynamics Review*, *38*(3), 246-263.
Rahmandad, H., Lim, T. Y., & Sterman, J. (2021). Behavioral dynamics of COVID-19: estimating underreporting, multiple waves, and adherence fatigue across 92 nations. *System Dynamics Review*, *37*(1), 5-31.
Rahmandad, H., & Sterman, J. (2022). Quantifying the COVID-19 endgame: Is a new normal within reach? *System Dynamics Review*, *38*(4), 329-353.
Rahmandad, H., Xu, R., & Ghaffarzadegan, N. (2022a). Enhancing long-term forecasting: Learning from COVID-19 models. *PLoS Comput Biol*, *18*(5), e1010100. https://doi.org/10.1371/journal.pcbi.1010100
Rahmandad, H., Xu, R., & Ghaffarzadegan, N. (2022b). A missing behavioural feedback in COVID-19 models is the key to several puzzles. *BMJ Glob Health*, *7*(10). https://doi.org/10.1136/bmjgh-2022-010463

Reluga, T. C. (2010). Game theory of social distancing in response to an epidemic. *PLOS Computational Biology*, *6*(5), e1000793.
Richmond, B. (1994). System dynamics/systems thinking: Let's just get on with it. *System Dynamics Review*, *10*(2-3), 135-157.
Ruggeri, K., Panin, A., Vdovic, M., Većkalov, B., Abdul-Salaam, N., Achterberg, J., Akil, C., Amatya, J., Amatya, K., & Andersen, T. L. (2022). The globalizability of temporal discounting. *Nature Human Behaviour*, *6*(10), 1386-1397.
Ruktanonchai, C. W., Lai, S., Utazi, C. E., Cunningham, A. D., Koper, P., Rogers, G. E., Ruktanonchai, N. W., Sadilek, A., Woods, D., & Tatem, A. J. (2021). Practical geospatial and sociodemographic predictors of human mobility. *Scientific reports*, *11*(1), 15389. https://www.nature.com/articles/s41598-021-94683-7.pdf
Rumain, B., Schneiderman, M., & Geliebter, A. (2021). Prevalence of COVID-19 in adolescents and youth compared with older adults in states experiencing surges. *Plos One*, *16*(3), e0242587.
Saad-Roy, C. M., & Traulsen, A. (2023). Dynamics in a behavioral–epidemiological model for individual adherence to a nonpharmaceutical intervention. *Proceedings of the National Academy of Sciences*, *120*(44), e2311584120.
Schecter, S. (2021). Geometric singular perturbation theory analysis of an epidemic model with spontaneous human behavioral change. *Journal of Mathematical Biology*, *82*(6), 54.
Shakeel, S. M., Kumar, N. S., Madalli, P. P., Srinivasaiah, R., & Swamy, D. R. (2021). COVID-19 prediction models: A systematic literature review. *Osong public health and research perspectives*, *12*(4), 215.
Shin, Y., Yu, B., & Greenwood-Nimmo, M. (2014). Modelling asymmetric cointegration and dynamic multipliers in a nonlinear ARDL framework. *Festschrift in honor of Peter Schmidt: Econometric methods and applications*, 281-314.
Sims, C. A. (1980). Macroeconomics and reality. *Econometrica: journal of the Econometric Society*, 1-48.
Slovic, P. (1987). Perception of risk. *Science*, *236*(4799), 280-285.
Sterman, J. D. (2000). Business Dynamics: Systems thinking and modeling for a complex world. *MacGraw-Hill Company*.
Suzuki, T., Lubashevsky, I., & Zgonnikov, A. (2018). Complexity of human response delay in intermittent control: The case of virtual stick balancing. *arXiv preprint arXiv:1808.05002*.
U.S. Department of Commerce, B. o. t. C. (2022). Population Estimates Program 2022 and 2020 Decennial Census. https://www.ers.usda.gov/data-products/county-level-data-sets/county-level-data-sets-download-data/
van Heusden, K., Stewart, G. E., Otto, S. P., & Dumont, G. A. (2023). Effective pandemic policy design through feedback does not need accurate predictions. *PLOS Global Public Health*, *3*(2), e0000955.
Verelst, F., Willem, L., & Beutels, P. (2016). Behavioural change models for infectious disease transmission: a systematic review (2010–2015). *Journal of The Royal Society Interface*, *13*(125), 20160820. https://doi.org/10.1098/rsif.2016.0820

Warren, M. S., & Skillman, S. W. (2020). Mobility changes in response to COVID-19. *arXiv preprint arXiv:2003.14228*.

Wei, Z., & Zhuang, J. (2023). On the adoption of nonpharmaceutical interventions during the pandemic: An evolutionary game model. *Risk Analysis*, *43*(11), 2298-2311.

WHO. (2000). *The world health report 2000: health systems: improving performance*. World Health Organization.

Wibral, M., Pampu, N., Priesemann, V., Siebenhühner, F., Seiwert, H., Lindner, M., Lizier, J. T., & Vicente, R. (2013). Measuring information-transfer delays. *Plos One*, *8*(2), e55809.

Wrigley-Field, E., Kiang, M. V., Riley, A. R., Barbieri, M., Chen, Y.-H., Duchowny, K. A., Matthay, E. C., Van Riper, D., Jegathesan, K., & Bibbins-Domingo, K. (2021). Geographically targeted COVID-19 vaccination is more equitable and averts more deaths than age-based thresholds alone. *Science Advances*, *7*(40), eabj2099.

Xi, W., Pei, T., Liu, Q., Song, C., Liu, Y., Chen, X., Ma, J., & Zhang, Z. (2020). Quantifying the time-lag effects of human mobility on the COVID-19 transmission: a multi-city study in China. *Ieee Access*, *8*, 216752-216761.

Xu, R., Rahmandad, H., Gupta, M., DiGennaro, C., Ghaffarzadegan, N., Amini, H., & Jalali, M. S. (2021). Weather, air pollution, and SARS-CoV-2 transmission: a global analysis. *The Lancet Planetary Health*, *5*(10), e671-e680.

Xu, W.-J., Zhong, C.-Y., Ye, H.-F., Chen, R.-D., Qiu, T., Ren, F., & Zhong, L.-X. (2020). Coupled effects of epidemic information and risk awareness on contagion. *arXiv preprint arXiv:2009.05327*.

Zhang, G., Osi, A., Ghaffarzadegan, N., Rahmandad, H., & Xu, R. (2025). Identifying delayed human response to external risks: an econometric analysis of mobility change during a pandemic. *BMC Medical Research Methodology*, *25*(1), 244.

Zhang, X., Scarabel, F., Murty, K., & Wu, J. (2023). Renewal equations for delayed population behaviour adaptation coupled with disease transmission dynamics: A mechanism for multiple waves of emerging infections. *Mathematical biosciences*, *365*, 109068.

Zhang, Z., Jalali, M. S., & Ghaffarzadegan, N. (2025). Behavioral Dynamics of Epidemic Trajectories and Vaccination Strategies: A Simulation-Based Analysis. *Journal of Artificial Societies and Social Simulation*, *28*(1).